2022

Induction of Antibiotic Activity Against Methicillin-Resistant Staphylococcus Aureus in Small Molecules Through Zinc Activation

Rachel Michaela Andrews
University Of Alabama At Birmingham

INDUCTION OF ANTIBIOTIC ACTIVITY AGAINST METHICILLIN-RESISTANT *STAPHYLOCOCCUS AUREUS* IN SMALL MOLECULES THROUGH ZINC ACTIVATION

by

RACHEL MICHAELA ANDREWS

OLAF KUTSCH, COMMITTEE CHAIR
SUSAN BIRKET
JUAN CALIX
TERJE DOKLAND
MICHAEL GRAY

A DISSERTATION

Submitted to the graduate faculty of The University of Alabama at Birmingham,
in partial fulfillment of the requirements for the degree of
Doctor of Philosophy

BIRMINGHAM, ALABAMA

2022

INDUCTION OF ANTIBIOTIC ACTIVITY AGAINST METHICILLIN-RESISTANT *STAPHYLOCOCCUS AUREUS* IN SMALL MOLECULES THROUGH ZINC ACTIVATION

RACHEL MICHAELA ANDREWS

GRADUATE BIOMEDCAL SCIENCES - MICROBIOLOGY

ABSTRACT

Methicillin-resistant Staphylococcus aureus (MRSA) is a serious human pathogen with a staggering potential for multi-drug resistance. Because of this, the Centers for Disease Control and Prevention and the World Health Organization monitor the spread of MRSA and encourage antibiotic development efforts targeting this pathogen. Despite this, few antibiotics have been developed and brought to market in recent decades. To continue treating infections caused by this organism, we must identify novel antibiotic molecules with different mechanisms of action from known antibiotics. Bacterial copper-dependent inhibitors (CDIs), molecules that become antibacterial in the presence of copper (Cu), have been studied as a novel class of antibiotics. However, CDIs are notoriously toxic due to the inherent and self-potentiating toxicity of Cu itself. Recently, zinc (Zn), though previously understood to be an essential micronutrient, can become antibacterial under certain conditions, but unlike Cu, Zn does not redox cycle and produce reactive oxygen species of its own accord. Based on this, we sought to activate antibacterial action in small molecules with Zn rather than Cu in the following studies.

In the first study, we demonstrate Zn-activated antibiotics are readily identifiable in characterized chemical space against MRSA using a Zn-dependent screening approach, and we characterize the most promising of these hits, the sunscreen ingredient avobenzone (AVB), as an anti-staphylococcal Zn-activated metallo-antibiotic. In the

second study, we expand upon Zn-activated metallo-antibiotics by exploring the metal specificity of metal-binding and antibacterial classes of privileged structures to show Zn-dependent antibiotics, like other drugs, can be optimized for a specific activity with a structure activity relationship study (SAR). Here we demonstrate metal specificity of 8-hydroxyquinolines and benzimidazoles is dependent on specific R-group modifications. Ultimately, our data establish Zn-dependent antibiotics as their own class of antibiotics with potential for development pipeline that mirrors those already in use for antibiotic development.

Keywords: *Staphylococcus aureus*, antibiotic discovery, zinc, avobenzone, 8-hydroxyquinolines, benzimidazoles

ACKNOWLEDGEMENTS

First, I would like to thank my mentor, Dr. Olaf Kutsch, for taking me on as a student, giving me space to continue a project I believed in, and offering your expertise. I would also like to thank my committee members, Drs. Birket, Calix, Dokland, and Gray, for all the insight that has guided this project and their support, especially in these final months. A special thank you to Dr. Gray for your added hand in my mentorship in the final leg of my graduate career.

Next, a thank you to my lab members, past and present. Your consistent encouragement is much appreciated. You all were there for me on the days when I most needed the support. For those that I trained or mentored, it has been an honor and one of the highlights of my graduate career to watch you grow and become independent thinkers. To all my other GBS friends, thank you for your support, philosophical debates, and all the other ridiculous moments you included me in.

I would especially like to thank my friends and family. To my dad, Wayne, you were the one who taught me education is freedom. I am here because of your consistent sacrifices in the name of my education and wellbeing, and I cannot express how thankful I am for that. I would like to thank my younger brother, Grayson, for his absolute faith in me. I hope I can live up to the person you believe me to be. Thank you to my adoptive mom Terri for opening her home and heart to me these last ten years. I never expected meeting your son would mean I would gain a second family, so thank you. Another thank you to my friend and lab mate Sophia for being the friend I needed exactly when I needed

her. I'm so glad we met. To Cameron and Ash, you are the lifelong best friends I always wished for. Thank you for the countless game nights, late night rubber band fights, karaoke car rides, jerry-rigged instruments, and Sun Day Fun Days, but most importantly, thank you for offering your kindness, support, and love. Ash, you showed me how to unabashedly seek joy, and Cameron, you taught me to take pride in the little steps and to see myself as valuable. When I falter, you two are always there. Finally, a huge thank you to my partner, Jesse. You have been my home for the past ten years. You've been there when the dark thoughts are too much to handle on my own, and in my brightest memories, you're always there. I truly would not have made it this far without your belief in me.

TABLE OF CONTENTS

Page

LIST OF TABLES

Tables *Page*

REPURPOSING SUNSCREEN AS AN ANTIBIOTIC: ZINC-ACTIVATED AVOBENZONE INHIBITS METHICILLIN-RESISTANT *STAPHYLOCOCCUS AUREUS*

MODULATING METALLO-ANTIBIOTIC ACTIVITY: A STRUCTURE ACTIVITY RELATIONSHIP STUDY

LIST OF FIGURES

Figures *Page*

REPURPOSING SUNSCREEN AS AN ANTIBIOTIC: ZINC-ACTIVATED AVOBENZONE INHIBITS METHICILLIN-RESISTANT *STAPHYLOCOCCUS AUREUS*

MODULATING METALLO-ANTIBIOTIC ACTIVITY: A STRUCTURE ACTIVITY RELATIONSHIP STUDY

INTRODUCTION

History and Epidemiology of Methicillin-Resistant Staphylococcus aureus

The bacterium *Staphylococcus aureus* is a Gram-positive facultative anaerobe known for causing disease in humans and animals. While primarily responsible for skin and soft tissue infections (SSTIs) [1], *S. aureus* can also cause more severe disease. This includes localized diseases, such as pneumonia, osteomyelitis, and necrotizing fasciitis, and invasive bloodstream infections (BSIs) [2] that can lead to endocarditis, sepsis, and toxic shock syndrome [3-5]. Furthermore, *S. aureus* readily colonizes and forms biofilms on medical devices, leading to nosocomial infections that complicate treatment [6]. Severe *S. aureus* infections also more predominately affect individuals with underlying conditions, such as immunocompromised individuals with human immunodeficiency virus (HIV) or diabetes [7, 8]. According to the World Health Organization (WHO) and the Centers for Disease Control (CDC), BSIs in particular are associated with higher rates of comorbidity and poorer patient outcomes [9, 10]. Of the 68 countries that reported BSI data to the WHO for the 2020 GLASS surveillance report, 91% reported at least one BSI caused by *S. aureus*. According to the report, *S. aureus* caused 115,622 BSIs worldwide during the reporting period, representing approximately 22.2% of the total reported. This is likely an underestimate as the report only included cases that led to a hospital stay [10]. Generally, clearance of an *S. aureus* infection requires treatment with antibiotics [9, 11].

Unfortunately, *S. aureus* readily generates resistance to antibiotics, the most common of which is methicillin-resistant *S. aureus* (MRSA). Methicillin, a semi-

synthetic β-lactam antibiotic with higher affinity for bacterial penicillin binding protein (PBP) than its chemical analog penicillin [12, 13], was first introduced into the clinic in 1960, and a methicillin-resistant clone was identified only a year later in the United Kingdom [14]. At the time it was hypothesized this was a result of the clinical use of methicillin to treat infections, but recent evidence suggests methicillin resistance first evolved in environmental S. aureus strains infecting European hedgehogs before spreading to clinical strains [15]. Following the initial isolation of a MRSA strain, MRSA spread across the globe. By 1967, Australia recorded its first ever case of MRSA in Sydney [16], and the first outbreak of MRSA in the United States (US) was reported in 1968 in Boston City Hospital [17]. Over the next 30 years, MRSA became endemic to multiple large US cities [18].

However, MRSA was primarily relegated to hospital settings. If a MRSA strain did spread into the surrounding community, it remained limited to the family units of an individual who contracted a MRSA infection while in the hospital [19]. This pattern changed drastically in the late 1990s. Reports began circulating that MRSA strains were being isolated from otherwise healthy individuals in 1999 and that these strains were genetically distinct from those causing nosocomial infections [3, 20, 21]. The first case of a MRSA infection in an otherwise healthy individual was reported in 1999 in a pediatric patient from the University of Chicago Children's Hospital [22]. The same year, a retroactive study of MRSA isolates in a San Francisco jailed population showed that 15 MRSA infections occurred in healthy individuals rather than individuals with underlying conditions between 1996 and 1999 [21]. Another study confirmed this same trend in Los Angeles prisons between 1997 – 2002 [23]. The divergence in phenotype, genetic

lineage, and epidemiology among MRSA isolates led to a classification of MRSA strains as either hospital-acquired (HA-MRSA) or community-acquired (CA-MRSA) [18]. A CA-MRSA strain called USA300 went on to become an epidemic strain in the US, gaining notoriety as a "superbug" when the professional American football team, the St. Louis Rams, were affected by an outbreak of CA-MRSA among its players and staff in 2003 [24]. MRSA is now endemic Western countries. The CDC began including MRSA in their action plan to combat healthcare-associated infections in 2008 [25], and the CDC listed MRSA a serious public health threat in its 2013 Antimicrobial Resistance Report [26]. While cases of HA-MRSA have decreased in the last decade due to the implementation of preventative measures in hospitals, MRSA caused nearly 323,700 hospitalized infections in the US in just 2017, representing an economic burden of $1.7 billion [9]. At the time of writing in 2022, the CDC still categorizes MRSA as a serious public health concern.

Horizontal Gene Transfer of Antimicrobial Resistance and Virulence in S. aureus

Antibiotic resistance is directly linked to infection severity and treatment failure [27-31]. Of these resistant organisms, *S. aureus* is the primary cause of nosocomial infections in wealthy countries [10, 32], and evidence suggests that antibiotic resistance *S. aureus* is a growing problem in non-Western countries that have greater barriers to medical care [10]. Despite its clonal lineage, *S. aureus* is adept at gaining a diverse array of accessory genes, such as antimicrobial resistance genes (ARGs) and virulence determinants, with each strain having a different configuration of determinants that ultimately shape infection dynamics and treatment regimens [3]. Furthermore, mobile

genetic elements (MGEs) represent the primary source of diversity of S. aureus strains. MGEs are regions of DNA that can be mobilized from one bacterial cell and transferred to another cell, a process known as horizontal gene transfer (HGT), and they come in a variety of forms. In *S. aureus*, MGEs can include prophages, phage-related chromosomal islands (PRCIs) known as S. aureus pathogenicity islands (SaPIs), conjugative and non-conjugative plasmids, transposons, and chromosomal cassettes [33, 34]. Approximately 15 – 20% of the S. aureus genome is dedicated to MGEs [34]. In many cases, MGEs can encode virulence genes, ARGs, or both. Thus, the presence of absence of certain MGEs are crucial for determining the antibiotic sensitivity and virulence phenotypes of *S. aureus* isolates [34].

Lysogenic bacteriophages are the primary drivers of genetic diversity in S. aureus and commonly encode virulence genes [35, 36]. Prophages form when a lysogenic phage infects a bacterial cell and the phage genome integrates into the host chromosome at a phage-specific integration site, becoming quiescent [34]. The infected cell is known as a lysogen. Under certain environmental conditions, such as those that induce the bacterial SOS response, the prophage will reactivate, enter the lytic cycle, and produce mature virions capable of infecting other cells upon release from the lysed host cell [34, 37]. The most well-characterized prophages of *S. aureus* are Φ11 and 80α due to their high transducing efficiency [38, 39]. Both Φ11 and 80α are lysogenic phages from the *Siphoviridae* family that, like other members of their family, have a double-stranded DNA (dsDNA) genome and a proteinaceous capsid composed of an icosahedral head, a long, non-contractile tile, and tail fibers that bind to the unique wall teichoic acids (WTAs) linked to the peptidoglycan cell wall of *S. aureus* [35, 40, 41]. Upon transport of

the genome into a host cell, the phage genomes integrate into the host chromosome at the insertion site using a sequence-specific integrase. Phages from this family that infect *S. aureus* are divided into six clades through polymorphisms in *int*, the gene encoding the integrase [42]. The phage genomes are divided into six discrete modules: the 1) lysogeny, 2) replication, 3) packaging, 4) head, 5) tail, and 6) lysis modules. Accessory genes are generally encoded within the lysogenic or lytic modules, and certain virulence gene tend to be associated with a specific clade of lysogenic *S. aureus* phages [35].

Multiple prophages are responsible for encoding immunomodulatory toxins that affect the type and severity of an S. aureus infection. The phage ΦPVL, a member of Sa2int, includes *lukSF* [43], the genes encoding the pore-forming toxin Panton-Valentine leucocidin (PVL) that induces necrosis in human neutrophils [44-47]. PVL is partially responsible for the emergence of USA300 and is common among CA-MRSA strains [3]. PVL-positive isolates have been associated with necrotizing pneumonia, a severe *S. aureus* infection that can be fatal within 48 hours [48, 49]. In contrast, Sa1int phages, will encode exfoliative toxins that lead to skin conditions like impetigo and staphylococcal scalded-skin syndrome [35, 50-53]. Meanwhile, Sa3int phages are responsible for encoding the immune evasion cluster (IEC) found in 96% of human nasal isolates [35, 54].

IEC includes several genes, including *chp*, *scn*, and *sak* [55]. Chemotaxis inhibitory protein (CHIPS) [56], the product of *chp*, binds to the C5a receptor and formyl peptide receptor 1 of neutrophils and monocytes, thereby inhibiting chemotaxis in these cells by preventing their interactions with their cognate chemoattractants [57, 58]. Staphylokinase (Sak) encoded by *sak* is a plasminogen activator the converts

plasminogen to the serine protease plasmin that degrades fibrin from blood clots [59-61]. Sak was also shown to prevent opsonization by phagocytes by cleaving immunoglobulins and C3b deposited on the cell surface [61]. In 2013, Kwiecnski *et. al.* showed expression of Sak by *S. aureus* promotes infection establishment by increasing skin penetration but reduced severe, disseminated disease in mice [62]. This may be due the fact that the integration of Sa3int phage genomes interrupt the gene encoding β-hemolysin, *hlb*, and inactivating it [56]. β-hemolysin is well known for its hemolytic activity [63], but it was also shown in 2013 to be cytotoxic against human keratinocytes, suggesting a role in colonization and disseminated disease [64]. Lastly, *scn* encodes staphylococcal complement inhibitor (Scn) [56]. As its name suggests, Scn inhibits complement, but unlike Sak, Scn stabilizes C3 convertase to prevent new deposition of the opsonin C3b. This in turn greatly decreases phagocytosis by neutrophils [65]. Taken together, strains encoding IEC may be more specialized for colonization, while strains that instead produce a functional copy of β-hemolysin are better suited for disseminated disease [42, 66].

While prophages themselves can encode virulence factors, they also contribute to the mobilization of host DNA by a variety of mechanisms. First, prophages can perform generalized transduction once reactivated. In the process of replicating the phage genome with host machinery and packaging of the replicated DNA into the capsid head, host DNA can be packaged instead of the phage genome, resulting in a heterogenous population of viral particles composed of infectious virions and transducing particles, the latter of which can transfer the host DNA to another bacterial cell [34]. In *S. aureus*, it is estimated that approximately 1.5% of the host genome can be transferred through this

process, including plasmid DNA [34, 67-70]. For example, 80α can transfer the plasmid-encoded gene *blaZ*, or penicillinase, within USA300[71]. It has also been noted that smaller types of chromosomal cassettes, such as Staphylococcal Chromosomal Cassette mec (SCCmec) types I and IV that encode β-lactam resistance, can be transferred with transducing particles as they are within the size limit of the capsid head [72, 73]. Interestingly, recipient cells must already possess a plasmid encoding the *bla* operon that encodes β-lactamase and its transcriptional regulators BlaI and BlaR [74]. SCCmec I and IV do not encode the regulatory genes *mecIR*, and it is proposed that BlaI and BlaR act in trans to regulate β-lactam resistance encoded by these cassettes [75], hinting at the interplay between divergent MGEs.

Specialized forms of transduction also contribute to host DNA transfer. Autotransduction occurs when populations of phage-susceptible cells release transducing particles that transduce lysogens resistant to the phage [69]. Lateral transduction is the most recent recognized form of transduction. Identified in *S. aureus* in 2018, lateral transduction is the result of a time delay in the expression of the phage excisionase during phage genome replication. This results in large regions of the bacterial chromosome being replicated and nonspecifically packaged into capsid head. The process also relies on a specific head packaging mechanism called headful packing where a *pac* phage cleaves the DNA being packaged after a certain length rather than at a specific cleavage site, like what is seen in cos phages. Remarkably, lateral transduction could potentially mobilize almost the entire chromosome of the *S. aureus* strain RF22 because of the chromosomal spacing of integrated *pac* phages. While this process was studied in the well-characterized phage Φ11, the authors note pathogens have a larger proportion of

prophages compared to non-pathogenic species and imply this process could play an outsized role in the transfer of ARGs [67, 76].

In some cases, dedicated MGEs can co-opt prophages for their dissemination. This is the case for *S. aureus* pathogenicity islands (SaPIs) in *S. aureus*. SaPIs are regions of chromosomally integrated DNA with conserved gene modules originating from a phage that have lost their structural genes required for forming a capsid. Furthermore, SaPIs do not have the ability to regulate their own replication and excision from the chromosome. As such, a helper phage is required to induce SaPI replication and to generate structural components [77]. SaPIs can include several different ARGs and virulence genes. As an example, SaPI1 is a 15 kb island that includes *tst*, the gene encoding the superantigen toxic shock syndrome toxin-1 [78, 79]. SaPI1 includes its own integrase that is responsible for its integration the host chromosome when phage are not being actively being generating in the recipient cell [78]. Mobilization requires the helper phage 80α to be induced and expression of phage-encoded dUTPase. Due to a 40 amino acid stretch, dUTPase binds to the repressor of SaPI1 replication and excision and de-represses the system. Once the SaPI1 region is induced and replicated, proteins from SaPI1 bind to the phage scaffolding protein and alter capsid formation of 80α. This results in capsid heads that are too small to package the full phage genome and will therefore selectively package SaPI1 replicons [77] The host cell will then lyse, releasing infectious 80α virions and transducing particles housing SaPI1. Various SaPI types have been identified in S. aureus, each requiring a different helper phage and packaging mechanism. Regardless, SaPIs, and PRCIs from other Gram-positive organisms, encode accessory genes that can affect the resistance phenotype of the expressing strain [77].

Plasmids represent one of the primary methods for *S. aureus* strains to gain multi-drug resistance. *S. aureus* plasmids are generally categorized based on their method of replication, either rolling-circle replication (RCR) or theta-type (θ-type) replication [80]. RCR plasmids tend to be smaller (less than 8 kb) and are generally non-conjugative as they rarely carry the suite of genes necessary for forming a type IV secretion system (T4SS) or relaxase components for self-replication and mobilization. As a result, RCR plasmids will only carry one resistance determinant [80]. However, RCR plasmids can confer resistance to multiple classes of antibiotics. Tetracycline, chloramphenicol, and aminoglycoside resistance have all been recorded with various plasmids from this group [81-84]. Θ-type plasmids, on the other hand, are typically much larger than RCR plasmids with conjugative elements that can transfer the plasmid to another cell. As such, θ-type plasmids, which encode multiple resistance determinants and play a major role in the establishment of multi-drug resistant populations of *S. aureus* [80]. The most well-studied family of θ-type plasmids is typified by pSK41. This plasmid confers resistance to multiple aminoglycosides, quaternary ammonia compounds, and the antiseptic ethidium bromide. The genes responsible for these resistances are *aacA-aphD* and *aaD* for aminoglycosides resistance [85, 86], and *qacC*, which provides cross-resistance to quaternary ammonia compounds and antiseptics [87-89]. Importantly, conjugative plasmids may also transport non-conjugative plasmids. In order for conjugation to occur, the plasmid in question must be linearized. A site-specific relaxase encoded by the plasmid nicks the plasmid at the *oriT*, the DNA sequence recognized by the relaxase, and generates a double-stranded break in the DNA [80]. A 2015 study found that if the *oriT* of a non-conjugative plasmid is similar enough to that of a conjugative plasmid, the non-

conjugative plasmid could be mobilized along with the conjugative plasmid [90, 91]. In addition, an RCR plasmid encoding β-lactamase was shown to be mobilized through transduction with the phages 80α and ΦJB in USA300 [71], indicating interplay between co-housed plasmids and phages can increase the host range, and therefore antimicrobial resistance, of plasmids.

Genomic islands and chromosomal islands, large regions of chromosomally integrated DNA, are especially important in the drug resistance profile of *S. aureus*. The most well-characterized of these islands in S. aureus is the Staphylococcal Chromosomal Cassette mec (SCCmec) that is responsible for the methicillin resistance displayed by MRSA strains [92]. Despite the global prevalence of MRSA, the exact determinant of methicillin resistance in *S. aureus* was not discovered until 1986, 25 years after MRSA was first reported. An approximately 30 kilobase (kb) region of accessory DNA was identified within an *S. aureus* strain that conferred resistance to β-lactam antibiotics when transformed into *Escherichia coli*. This region of DNA was termed the *mec* element [93]. The next year, a Japanese group sequenced the gene responsible for methicillin resistance and termed it *mecA* [94]. It was determined *mecA* encoded an alternative PBP with a lower affinity for β-lactam antibiotics, bypassing the activity of β-lactams like methicillin [95]. We now understand the *mec* gene is part of a much larger MGE, SCCmec, 14 types of which have been since been described [96].

SCCmec is a 20 – 40 kb, depending on the type, region of DNA integrated near the origin of replication of the *S. aureus* chromosome and is organized into three regions: 1) the ccr gene complex, 2) the mec gene complex, and 3) the joining (J) regions [97]. The *ccr* gene complex sits at the 5’ end of the cassette and contains two site-specific

recombinases, a combination of either *ccrA*, *ccrB*, or *ccrC*, that are responsible for the accurate excision and integration of SCCmec at the chromosomal insertion site *attB* [98]. The *mec* gene complex follows the *ccr* gene complex and is responsible for encoding resistance to methicillin and other β-lactam antibiotics. Two different allotypes of the *mec* gene provide this resistance [92, 97]. The genes *mecA* and *mecC* all encode the alternative PBP called PBP2a [94, 99]. Interestingly, an SCCmec-like was identified in *Macrococcus caseolyticus* that encoded the gene *mecB*, rather than *mecA* or *mecC*, for methicillin resistance [100]. This region can also encode regulatory genes that alter the expression of the *mec* gene. These include *mecI*, which encodes a transcriptional repressor of *mec* [101], and *mecR1* encoding a β-lactam-sensing metalloproteinase hypothesized to degrade MecI when β-lactam antibiotics are present [102]. The J regions are split into three segments, J1, J2, and J3, based on where they localize in the cassette. J1 sits upstream of the *ccr* gene complex. J2 lies between the *ccr* and *mec* complexes, and J3 borders the 3' end of the *mec* complex. These J regions can also incorporate other accessory DNA segments, including transposon and plasmid sequences that encode antimicrobial and heavy metal resistance genes. The exact combination of the major components of SCCmec is used to divide the various cassettes into different types [97].

The resistance and virulence profile of an *S. aureus* strain is ultimately determined by the sum total of all the MGEs it encodes. Therefore, the disease phenotype and epidemiology of a strain can be predicted by examining the MGEs of that strain. As, an example, the most common CA-MRSA strain type by pulsed field gel electrophoresis is USA300 [3, 103-105]. A clonal complex 8 MRSA strain originally isolated from the wrist abscess of a 36 year-old white male with a history of intravenous drug use in Los

Angeles in 2000, USA300 became the dominant strain type during the CA-MRSA epidemic in the US [106]. This strain has a number of virulence determinants that led to its predominance among heathy individuals. First and foremost, USA300 encodes SCCmec IV, making it methicillin resistant. Unlike most HA-MRSA strains, USA300 includes the prophage ΦSA2usa that encodes the Panton-Valentine leucocidin (PVL), which may encourage disseminated disease. In this vein, a second prophage, ΦSA3usa, encodes *sak* and *chp*, providing another set of virulence genes associated with increased rates of colonization [106]. Additionally, USA300 gained the arginine catabolic mobile element (ACME) [106]. ACME is a 30.9 kb genomic island incorporated at the *attB* integration site at the 3' end of SCCmec IV [106]. It is thought to have been obtained from the skin commensal Staphylococcus epidermidis through HGT [107]. ACME encodes the arginine deaminase pathway that ultimately converts arginine to ammonia, carbon dioxide, and water. This protects *S. aureus* from inhibition by nitric oxide produced by neutrophils and provides a fitness advantage compared to a strain lacking ACME [108, 109]. Importantly, ACME improves the survival of USA300 on the skin and is likely the primary driver of its spread among healthy individuals [110, 111]. Furthermore, USA300 gained two enterotoxins, *sek2* and *seq2*, through its acquisition of SaPI5 [106]. These genes encode superantigens that bind to major histocompatibility complex class II molecules and elicit an excessive release of cytokines from activated T cells [106]. Lastly, USA300 encodes three plasmids: pUSA01, pUSA02, and pUSA03. The first two plasmids, pUSA01 and pUSA02, are small plasmids less than 5 kb in size [106]. While less is understood about pUSA01, pUSA02 encodes *tetK*, providing resistance to tetracyclines. Meanwhile, pUSA03 is a 37 kb conjugative plasmid that

confers resistance to macrolides, lincosamides, and streptogramin B through the gene *ermC* and resistance to muripirocin through *ileS* [106]. Taken together, these MGEs result in a difficult-to-treat strain that is both multi-drug resistant and well-equipped for colonization and survival on the skin, ultimately explaining its prevalence in healthy populations.

It remains unclear when and how HGT occurs during the course of an infection. Phage induction has been demonstrated during antibiotic stress in vitro, suggesting increased rates of HGT may occur during treatment [112-114]. Additionally, a 2013 study published in Nature demonstrated that mice treated with ciprofloxacin, ampicillin, or ampicillin and ciprofloxacin resulted in gut microbiota phage genomes containing larger proportions of bacterial genes encoding functions related to the antibiotic treatment in mice. The authors contend this increased connectivity between phage and the microbiota during antibiotic treatment is due to increased phage integration and a broader host range for phages to infect [115]. Other studies suggest biofilms are a likely location for HGT[116]. Studies have also found higher rates of rates conjugation and increased numbers of released virions in biofilms relative to planktonic cultures [117].

Another concern is how far a given MGE, and therefore ARGs, can spread among bacterial species. The lysogenic phages of *S. aureus* are trophic for the unique WTAs embedded in the cell wall of *S. aureus* [40]. Given this, transduction is likely limited to certain Gram-positive species that possess WTAs with a similar structure to those of *S. aureus*. DNA transferred through HGT would also need to be able to escape the RM systems encoded by *S. aureus*. Despite these limitations, certain MGEs primarily associated with *S. aureus* have been documented in other species. SaPI, the genetic

carrier of the toxin gene *tst*, has been reported in *Listeria monocytogenes* [38]. *S. aureus* has also gained MGEs from other species. ACME, having been received from *Staphylococcus epidermidis* [107], is a prime example of how acquisition of foreign DNA can drastically affect the life cycle of an organism, and the transposon Tn1546 from vancomycin-resistant enterococci gave rise vancomycin resistance in MRSA [118]. As such, HGT generates a complicated network of ARGs between various bacterial species, many of which have a profound impact on the treatment of infectious diseases like *S. aureus*.

Antibiotic Discovery

Antibiotic screening was first introduced in 1904 by Paul Ehrlich. Ehrlich, who began by studying bacteria-staining dyes, hypothesized that since synthetic stains could bind and differentiate between bacteria, a small molecule capable of a killing a specific bacterial species could also be synthesized, a theoretical molecule he termed the magic bullet. He instituted a successful but labor-intensive approach to identify purely synthetic antibiotics effective against *Treponema pallidum*, the causative agent of syphilis, in rabbits. This process involved synthesizing multiple compound series where a single molecular backbone was slightly altered with a myriad of different R groups, resulting in a suite of structurally related analogs. Analogs would then be administered to rabbits infected with *T. pallidum* to test for efficacy [119]. By 1909, Ehrlich's group identified compound 606, an organoarsenic compound, that could be used to treat syphilis and was marketed under the name Salvarsan [120]. His method later identified the sulfanilamide, quinoline, and oxazolidinone classes of antibiotics, of which the latter two are still in use

today. His method also led to the discovery of specific drugs, including metronidazole, isoniazid, and ethambutol [120].

However, the screening platform responsible for the discovery of most of the known classes of antibiotics would not be developed until after the discovery of penicillin in 1928 by the Scottish physician Sir Alexander Fleming [121]. Unlike the antibiotics synthesized by the Ehrlich group, penicillin is natural product made by some molds of the genus *Penicillium*, and as such demonstrated antibiotics could be identified from antibiotic-producing organisms [121]. Selman Waksman, a microbiologist and biochemist, took advantage of this to develop a simplified antibiotic screening platform that did not require extensive synthetic chemistry, what is now known as the Waksman platform [122]. Instead of generating a library of modified chemical scaffolds, Waksman isolated a collection of culturable soil bacteria and tested them against a lawn of a target organism. Antibiotics could then be isolated from strains generating a zone of inhibition, the first of which was streptomycin [123]. The Waksman platform was an immense success and ushered in the Golden Age of Antibiotic Discovery (1940s – 1970s). This period saw the discovery and clinical introduction of most of the major antibiotic classes in use today, including the macrolides, rifamycins, and aminoglycosides [122, 124].

However, the Waksman platform began to fall out of use starting in the 1970s when screens were returning known antibiotics rather than novel molecules. *Actinomycetes*, the group of soil bacteria used in the Waksman platform, were considered to have been fully mined of all potential antibiotics after three decades of screening [124]. To compensate, the field shifted to innovative techniques to identify new antimicrobials and bacterial targets. Combinatorial chemistry was used to synthesize

large compound libraries and robotic platforms capable of rapidly screening thousands of compounds against a target organism laid the foundation for the advent of high throughput drug screening in the current era. Meanwhile, big data methods, such as genomics, transcriptomics, and proteomics, enabled identification of alternative targeting strategies [125]. These targets could then be purified and screened against to identify molecules capable of inhibiting those specific targets. This in turn caused a shift from whole-cell screening to readily adaptable protein target screening [124].

Despite numerous innovations in drug screening, only two new antibiotics, daptomycin and bedaquiline, have been introduced since the fall of the Waksman platform. Of the two drugs, only bedaquiline was identified after the Waksman platform became obsolete. Daptomycin was actually identified using the Waksman platform in 1986 but wasn't introduced clinically until years later [122]. Concerningly, resistance has already been reported for both drugs since their clinical introduction [126, 127]. By the early 2000s, researchers were raising alarms over the dearth of novel antimicrobials. Multiple reports, including those from the pharmaceutical industry, indicated screening efforts failed to discover new antibiotics, and reduced profit margins incentivized pharmaceutical companies to abandon or reduce their antibiotic screening divisions [128-131]. Furthermore, health organizations like the CDC release antimicrobial resistance surveillance reports detailing the need for novel antibiotics to be developed that can counteract more difficult-to-treat infections [9].

One potential reason for the scarcity of new antibiotics identified by high throughput screens (HTS) is the adoption of Lipinski's Rule of Five in library assembly. Lipinksi's rules were first introduced in 2001 and defined chemical properties associated

with improved bioavailability when administered orally. Specifically, Lipinski set limitations on the hydrophobicity, mass, number of chiral centers, and hydrogen binding partners of compounds [132]. Many iterations of Lipinski's Rule of Five have been generated over the years and tailored for particular purposes, but the majority follow the same basic principles laid out by Lipinski. These principles were incorporated by companies generating compound libraries for HTS, such that most libraries available for purchase are based on Lipinski's rules to some degree [122]. While this strategy improved hit discovery for drug categories like neurotropic and anticancer therapeutics, the same was not true for antibiotics. In fact, known antibiotics notoriously break Lipinski's Rule of Five. Antibiotics, especially those synthesized by other organisms, are generally large, synthetically challenging, and complicated structures [130]. As a result, screening of natural products, or molecules synthesized by biological organisms, gained prominence as their molecular characteristics better matched those of known antibiotics [133, 134]. One approach was to identify other groups of bacteria that could potentially produce antibiotics by culturing previously unculturable bacteria using a device called Ichip that allows for culturing of soil and water bacteria in their own environment. In theory, other phylogenetic groups of bacteria could possess a different suite of untapped antimicrobials compared to Actinomycetes, which could in turn be used to resurrect the Waksman platform. Encouragingly, this method identified teixobactin, a promising non-ribosomally synthesized antibiotic that interrupts peptidoglycan synthesis and did not generate resistance in vitro over a 30-day period [135]. Teixobactin is proof that shifting to screening of natural products could uncover new antibiotics.

The majority of antibiotics currently in use target one of five major pathways: 1) cell envelope integrity, 2) DNA replication, 3) transcription, 4) translation, and 5) folic acid metabolism. All of these pathways are essential for basic survival while also being specific for bacterial products over mammalian systems [122]. However, resistance has been documented for each one of these antibiotic mechanisms [122]. In order to counteract the antimicrobial crisis, we must identify new drugs with a wider array of mechanisms of action. Alternative options for antibiotic discovery were proposed in the early 2000s at the start of the crisis. Rather than developing entirely new screening techniques, focus shifted to identifying inhibitors of targets utilized throughout the course of an infection using existing HTS platforms. One of the more common methods is to seek inhibitors of virulence mechanisms that would ultimately allow a more robust and effective immune response to the pathogen. For instance, one successful screening attempt against *M. tuberculosis* identified inhibitors of cytolytic toxin export by screening a small molecule library against infected lung fibroblasts, rather than identifying a direct inhibitor of *M. tuberculosis*. If a molecule was ineffective, *M. tuberculosis* would be able to release the toxin ESX-1, killing the fibroblasts, whereas those capable of inhibiting the transport of ESX-1 would result in cultures containing viable M. tuberculosis and fibroblasts [136]. Similarly, multiple screening efforts have been made to identify inhibitors of quorum sensing and biofilm formation and dispersal against multiple bacterial species [137-139]. Further, a rational design effort produced a hapten structurally reminiscent of a quorum sensing molecule used by *S. aureus* that, when applied in a mouse model, induced protective monoclonal antibodies against the native quorum sensing inducer and ultimately prevented abscess formation by S. aureus [140].

An additional benefit of screening for virulence inhibition is that it reintroduces biological context, namely an infection, that is lost by protein target screening that became a staple of pharmaceutical screening techniques. Evidence clearly demonstrates targeting of virulence mechanisms is an effective means of antibiotic discovery, and the variety of potential targets bodes well for potentially generating a large pool of effective molecules to draw upon for development, future discovery, and rational design studies.

New antimicrobials are desperately needed to counteract the growing prevalence of antimicrobial resistance. To do so, we must adopt new and refine old screening strategies. HTS forms the backbone of industrial screening, and, while it has not proven particularly fruitful in unearthing novel antibiotics in the past, will be necessary for rapid screening and for new approaches to be adopted by the organizations with the greatest number of resources. A return to whole-cell screening and the introduction of infection-based methods will facilitate discovery of virulence-reducing antibiotics. Furthermore, HTS platforms may become more successful at identifying antibiotics outright by specializing library design, not for oral bioavailability, but for the express purpose of antibiotic discovery by including natural products and complicated structures that deviate from Lipinski's Rule of Five. Ultimately though, the primary source of innovation has been the shift to new drug targets. The success of future antibiotic discovery will likely hinge on developing methods to efficiently identify these kinds of activities.

Nutritional Immunity as Inspiration for Antibiotics

With the knowledge that future antibiotic development will require identifying new modes of inhibition, one way to gain inspiration for alternative bacterial targeting

strategies is to look to the innate immune system. The innate immune system, especially phagocytes like macrophages and neutrophils, has evolved a series of varied and broadly applicable methods of targeting and killing invading bacteria. These methods include degradation enzymes (lysozyme, granzyme B, serine proteases) [141-143], low pH [144], reactive oxygen species (ROS)[145, 146], and controlled shifts in metal availability [147-149]. This last method is known as nutritional immunity.

Historically, nutritional immunity refers to actions taken by the innate immune system to restrict a pathogen's access to nutritional metals and the mechanisms utilized by a pathogen to compete for those metals. Iron (Fe) is at the forefront of this struggle. Fe is a *d*-block transition metal and is the most abundant transition metal on the planet. Importantly, Fe is necessary for all life on Earth. As such, all organisms have developed methods to acquire or retain sufficient quantities to sustain life [150, 151]. In humans, heme bound to hemoglobin makes up the largest store of Fe [152]. In the event of erythrocyte damage, heme-binding proteins, like hemopexin, will scavenge the released heme, and free serum Fe is bound to the Fe transport protein transferrin [153-155]. Humans also encode the Fe storage proteins lactoferrin and ferritin, the latter of which can store over 4000 atoms of Fe in case of Fe depletion [156-158]. These proteins also play a role in impeding the uptake of Fe by bacterial pathogens during an infection [148].

However, Fe is also an essential nutrient for bacteria, especially during infection when the host sequesters Fe, and it has long been known that clinical Fe supplementation in patients with an infection exacerbates the infection [159]. Given this, bacteria encode multiple Fe scavenging and uptake systems. Siderophores are a prime example of this molecular arms race. Siderophores, small non-ribosomally synthesized chelating

peptides, are synthesized and released by many different bacteria. These molecules have high affinities for Fe, allowing bacteria to scavenge Fe from the environment and compete with each other for survival [160]. In the case of an infection, siderophores scavenge host Fe from tissues and make it available to the pathogen [148]. To combat this, mammalian hosts also export siderocalins, dedicated siderophore-binding proteins that sequester siderophores away from the invading bacteria [161, 162]. In turn, some pathogens also encode stealth siderophores, modified forms of an existing siderophore, to bypass sequestration by siderocalins [163, 164]. In addition, many pathogens will encode hemolytic toxins. *S. aureus* encodes three hemolytic toxins, α-toxin, γ-toxin and δ-toxin, that either form pores in or solubilize erythrocyte membranes, making the largest store of host Fe available for scavenging [165].

Competition for Fe is a complicated but well characterized interwoven network of pathogen and host proteins and small molecules. Similar networks are also seen for the nutritional transition metals manganese (Mn) and zinc (Zn) [148]. Several siderophore-like molecules, now termed metallophores, are released by certain species to assist in Zn uptake and are necessary for bacterial fitness during an infection [166-170]. *S. aureus* encodes the *cnt* operon that is responsible for the synthesis and an export of the Zn-binding metallophore staphylopine [171, 172]. Additionally, pathogens commonly encode dedicated Mn and Zn uptake operons, and the expression of these operons is necessary for virulence [148]. *E. coli* encodes ZupT and the ZnuABC system for Zn uptake [173, 174]. Similar systems are found in other gram-negative bacteria [175-179]. Meanwhile, gram-positive organisms, like *Streptococcus pneumoniae*, encode the similar but unrelated *adc* operon for this purpose [180, 181].

One host molecule that plays a major role in controlling available Mn and Zn levels during infection is the immune protein calprotectin. Calprotectin is a heterodimeric protein composed of S100 A8 and S100 A9 released by neutrophils at the site of infection [182-184]. As its name suggests, calprotectin was originally studied for its ability to bind to and sequester calcium ions away from pathogens [185]. More recent studies have also shown calprotectin also acts as a sink for Mn and Zn to limit a pathogen's access to the metals [186-189]. This activity by calprotectin has also been shown to be protective against abscesses formed by *S. aureus* in mice [190], highlighting a pathogen's need for these metals for both survival and pathogenesis *in vivo*.

While nutritional immunity primarily focuses on the sequestration of essential metals away from pathogens during an infection by the host immune system, the innate immune system also makes use of toxic metals to directly damage pathogens. Phagocytic innate immune cells, specifically neutrophils and macrophages, will perform a process called the copper burst [148]. Phagocytic cells will actively transport copper (Cu) into the phagosomes and phagolysosomes containing an engulfed pathogen using a dedicated Cu efflux pump [148]. In humans, this high affinity pump is called ATP7A and is an integral membrane protein responsible for transporting Cu ions from the host cell cytoplasm into the phagosome [191]. Once in the phagosome, Cu undergoes redox cycling through the Fenton and Haber Weiss reactions, resulting in reactive oxygen species (ROS) that damage the pathogen's membranes and surface proteins [192]. If Cu penetrates the bacterial plasma membrane, it can also degrade iron-sulfur (Fe-S) clusters necessary for oxidative phosphorylation and branched chain amino acid synthesis [193-196] and mis-metalate proteins with a metal cofactor due to its high affinity for metal-binding moieties,

thereby inactivating them [197]. Cu can also mediate direct damage to proteins by catalyzing disulfide bond formation between neighboring cysteines or preventing the formation of native disulfide bonds required for protein function or maturation [192]. As such, pathogenic bacteria commonly encode Cu-resistance machinery. *S. aureus* encodes, at minimum, the *copAZ* operon regulated by the Cu-binding transcription factor CsoR [198, 199]. CopA is a P1B-type ATPase responsible for Cu export out of the cell. CopZ acts as a Cu chaperone that chelates individual Cu ions to prevent further damage by the metal and transports it to CopA for export [200]. However, different strains of *S. aureus* will encode extra Cu resistance machinery, such as the Cu exporters CopB and CopX, and other bacterial pathogens will encode Cu detoxification machinery in concert with export systems. Some strains of S. aureus also encode the Cu-chelating lipoprotein CopL partially responsible hyper-resistance to Cu [201]. Other mechanisms responsible for managing and detoxifying ROS can be encoded for further resistance to the downstream effectors of Cu toxicity, such as catalase and multicopper oxidases [202-204].

Given the importance of Cu toxicity in the functioning of the innate immune system, Cu could potentially be exploited for medicinal benefit. One study found that Cu alloy fixtures can significantly reduce bacterial load on high touch surfaces in hospitals, leading some hospitals to install Cu fixtures to reduce transmission of nosocomial infections [205]. As far as potential therapies are concerned, Cu chelators have primarily been implemented in the treatment of Wilson's disease, a genetic disorder that results in excessive Cu accumulation [206]. In this case, Cu chelators are employed to remove excess Cu from tissues and promote its excretion. Subsequent Zn supplementation counteracts future Cu absorption [207]. As of the time of writing, this is the only Cu

chelation treatment with Food and Drug Administration (FDA) approval. However, certain Cu chelators, particularly 8-hydroxyquinolines (8HQ) and thiosemicarbazones (TSC), have been studied as potential treatments for neurological conditions with dysregulated metal concentrations due to their ability to cross the blood brain barrier [208]. These motifs have also been studied for their anticancer properties. TSCs precomplexed with Cu can induce apoptosis in leukemic cells through ROS generation [209], and glyoxal-bis(N4-methylthiosemicarbazone) (GTSM), is capable of inhibiting cancer cell growth when complexed with Cu [210]. Meanwhile, clioquinol (CIQ) and PBT2, two different 8HQ analogs, are proposed treatments for Huntington's disease [211, 212], and PBT2 has entered phase II clinical trial for the treatment of Alzheimer's disease [213].

Encouragingly, recent studies also document Cu-dependent antibacterial activity of certain small molecule classes against *M. tuberculosis*, *Mycoplamsa* spp., *Ureaplamsa* spp. and *S. aureus* [214-225]. A screening effort published in Antimicrobial Agents and Chemotherapy demonstrated high throughput screens could identify molecules capable of inhibiting both replicating and non-replicating *M. tuberculosis* specifically in the presence of Cu. This screen identified GTSM and the related molecule diacetylbis(N(4)-methyl-3-thiosemicarbazone (ATSM) as Cu-dependent inhibitors of M. tuberculosis [224]. An additional Cu-dependent screening effort against MRSA was also successful at identifying Cu-dependent inhibitors (CDIs) [216], indicating this strategy could be broadly applicable to multiple pathogenic bacteria. Importantly, the implementation of Cu-dependent screening improved the hit rate of the resulting screens. In both cases, a library was screened twice in parallel, once with Cu and once without, such that hit

compounds could be classified as independent or Cu-dependent. As screens excluding Cu would only result in independent hits, the inclusion of Cu as a screening condition allowed for identification of CDIs in addition to the independent hits that theoretically would have been identified by a standard screen. Thus, Cu-dependent screening improved the efficiency of hit identification in antibacterial screening [216].

A later combinatorial chemistry study discovered a specific chemical motif, termed the NNSN motif, of pyrazolyl thioureas and carbothiamides was responsible for the Cu-dependent antibacterial activity against *S. aureus* and *E. coli* [218]. Interestingly, this NNSN motif is also incorporated into GTSM, and previous studies with GTSM suggested this motif was essential for the Cu-dependency of GTSM as well [224]. As expected of Cu chelators, the sulfur and nitrogen atoms of the NNSN motif are necessary for these molecules to bind to Cu [218]. Since these studies, a Bayesian machine learning approach was developed for the purpose of identifying Cu-dependent clusters based on a molecule's two-dimensional structure. This approach identified several sulfur-containing molecular classes as potential CDIs [217], potentially suggesting Cu binding is an important factor in Cu-dependent antibiotic activity.

Another cluster, the pyrazolopyrimidinones, or the PZPs, was also shown to inhibit MRSA [214]. Unlike other CDIs whose activities remain unknown, the mechanism of Cu-dependent killing of the PZPs was determined to be Cu ionophore activity where the PZPs would shield the Cu ions from detection by the Cu resistance regulon of *S. aureus*, resulting in a toxic intracellular accumulation of Cu [214]. One important result of this toxicity is ATP depletion. Cu export is the most direct method of counteracting Cu toxicity in *S. aureus*, a process performed by ATPases [200, 201]. By

depleting the cell's ATP pool, Cu export is shut down and hampers the primary method that could ensure *S. aureus* survival to the treatment. The PZPs then make promising lead candidates for future development due to the ability of the PZPs with Cu to both exert toxicity and counteract potential resistance mechanisms [214]. Similarly, another CDI, APT-6K, shows promise for combination therapy against MRSA. While a CDI in its own right, APT-6K synergizes with ampicillin at sub-inhibitory concentrations, and this synergy results in reduced ampicillin resistance in clinical multidrug-resistant MRSA isolates [215]. CDIs could therefore potentially be implemented clinically for various purposes, either as a stand-alone antibiotic or to make otherwise unfeasible therapeutic options viable again.

Despite numerous studies demonstrating the efficacy of CDIs against a wide range of pathogens, the therapeutic implementation of CDIs may be limited. Eukaryotic toxicity of Cu chelating compounds is well documented. TSCs, of which GTSM is an example, have long been studied for their anticancer properties in the presence of Cu [209]. Due to their overlapping effects against eukaryotic cells, TSCs, which make up the bulk of characterized CDIs to date, are likely poor candidates for antibiotic development. Additionally, APT-6K is the only characterized CDI with a favorable therapeutic index against human cell lines [215]. Multiple studies suggest the anticancer properties of TSCs complexed with Cu are due to ROS generation through Fenton chemistry perpetuated by Cu, resulting in widespread and nonspecific damage of cellular components [192, 209]. By generating this self-potentiating and uncontrolled toxicity, Cu itself may pose the greatest challenge to metallo-antibiotic development.

Zinc in Biology

Another potential avenue for metallo-antibiotic development is to search for Zn-dependent molecules in place of CDIs. Like Cu, Zn is a *d*-block transition metal with high affinity for metal-binding moieties. However, Zn is unique from Cu due to its filled *d*-orbitals. This reduces the inherent reactivity of Zn and renders Zn redox inert [226]. Zn is also the second most abundant transition metal behind Fe [227]. Potentially as a result of both its availability and increased stability, Zn is traditionally considered an essential micronutrient. Approximately 5% of known bacterial proteomes are composed of Zn-binding proteins, and this expands to 10% of eukaryotic proteomes due to the presence of Zn finger motif transcription factors [228, 229].

Zn performs many biological functions. As previously suggested, Zn plays a major role in eukaryotic transcription regulation through transcription factors with Zn finger motifs [226, 228]. Zn is also incorporated as a cofactor in many different enzymes where it primarily carries out non-redox catalysis [230]. Zn metalloenzymes are abundant. All six major Enzyme Commission Classes contain at least one enzyme with Zn as a cofactor [230]. Interestingly, Zn, while itself unable to redox cycle, still participates catalytically in some oxidoreductases by working in concert with redox-active cofactors and shifting between coordination geometries within the active site [231]. Of the known Zn metalloenzymes, 66% of them are hydrolases, where Zn catalyzes the hydrolytic cleavage of the substrate by coordinating with a water molecule and the substrate [230]. Hydrolases are a broad class of enzymes that take part in major biological processes [232], from nucleotide excision repair [233] to antibiotic resistance [234, 235], and therefore Zn is a central component to these important processes.

Zn can also act as structural cofactor to provide stability to enzymes and large macromolecular complexes and to facilitate protein binding [226, 236]. For instance, *E. coli* DNA-dependent RNA polymerase (RNAP) coordinates with two different Zn ions in the β' subunit. Both Zn ions performs structural functions. The first helps to compact the β' subunit for RNAP complex formation, while the second ion facilitates RNAP binding to secondary proteins for transcription initiation, elongation, and termination [237-239]. Depending on the species, certain ribosomal proteins also bind to Zn, and the loss of Zn from these proteins commonly results in reduced translation efficiency [240-244]. Furthermore, Zn was shown to mediate the complexation of a human protein hormone to one of its receptors [245]. Lastly, eukaryotic Zn finger proteins, which bind Zn between an α-helix and two or three β-sheets, are a major family of proteins that utilize Zn to bind to DNA, RNA, and other biological molecules for their function [226]. Based on the available human protein sequences as of 2006, Zn finger motifs make up approximately 40% all human Zn-binding proteins. Most of the Zn finger protein are transcription factors, where Zn is used to bind to the major groove of the DNA template [228]. As such, Zn plays a major role in gene regulation in humans.

Despite Zn's role as an essential nutrient across biology, Zn can become toxic at high concentrations. The exact mechanism Zn toxicity has not yet been defined, but unlike Cu, Zn does not directly contribute to ROS generation [226]. Instead, Zn toxicity is thought to be caused by the affinity of Zn for metal-binding moieties in proteins [246]. The affinity of a divalent *d*-block transition metal for metal-binding motifs is defined by the Irving-Williams Series (Mn < Fe < Co < Ni << Cu > Zn), where metals with the highest atomic number have the greatest affinity for these motifs. The exception to this

trend is the relation between Cu and Zn. While Zn is further to the right on the periodic table relative to Cu, Cu has the highest affinity metal-binding moieties due to additional stabilization by the Jahn-Teller Effect [247]. It is hypothesized that the greater affinity of Zn results in mismetalation of key proteins, where structural or catalytic metals lower on the Irving-Williams Series are either removed or replaced by Zn, thereby inactivating those proteins [246]. Previous work showed high physiological concentrations of Zn and other metals can degrade solvent accessible Fe-S clusters of an *E. coli* dehydratase, leading to its inactivation [248], and Zn has long been known to be an inhibitor of aconitase, an Fe-S cluster protein of tricarboxylic acid cycle [249]. Additionally, Zn was shown to inhibit Fe-S cluster biogenesis in *E. coli* by binding to the Fe transfer protein IscA [250]. Finally, high extracellular Zn concentrations inhibit Mn uptake in *S. pneumoniae* by irreversibly binding to the Mn-binding protein PsaA. This in turn prevents proper metalation of its primary superoxide dismutase, SodA, required for detoxification of hydrogen peroxide produced as a byproduct of its metabolism [227].

Previous models of nutritional immunity only considered Zn as nutrient, leading to a paradigm where host Zn pools are restricted and sequestered from pathogens through methods like calprotectin. However, recent work revealed the innate immune system also utilizes Zn intoxication to counteract pathogens similarly to Cu [148]. Atomic force spectroscopy showed macrophages infected with mycobacteria had higher levels of Zn compared to uninfected controls [251], and *M. tuberculosis* requires Zn exporters to survive within host macrophages [252]. In concert with this, macrophages infected with *M. tuberculosis* will express metallothioneins, small metal-binding peptides used to regulate labile metal concentrations, potentially suggesting Zn intoxication is part of a

coordinated process to inhibit phagocytized M. tuberculosis [252]. Additionally, *Streptococcus pyogenes* requires Zn export machinery to survive inside neutrophils such that mutants without functional Zn export machinery are readily cleared by neutrophils [253]. Furthermore, Zn deficiency leads to a broad increase in susceptibility to infections [254-256]. This evidence leads to a new model of nutritional immunity where extracellular Zn is sequestered by innate immune cells to prevent pathogen's access to Zn, and phagocytized pathogens are poisoned through Zn intoxication where Zn concentrations can be more readily controlled. In total, this demonstrates Zn can act as an effective antimicrobial, so much so that dedicated cellular processes evolved to utilize Zn intoxication for this purpose. A such, Zn, if its antimicrobial properties could be harnessed in a manner similar to that of Cu, may offer another avenue for antibiotic discovery.

Opportunities for Advancement of Zinc-Activated Antibiotics

Despite the clear evidence of Zn as an antimicrobial metal, few efforts have been made to take advantage of this property therapeutically. Only two antimicrobials have been given FDA-approval that require Zn for their action. The first is bacitracin, a cyclic polypeptide antibiotic purified from a *Bacillus* species that was isolated from a wound infection in the 1940s [257]. Its mechanism of action was not elucidated until 1970s when it was shown that bacitracin inhibits peptidoglycan synthesis by preventing the dephosphorylation of undecaprenol pyrophosphate to the lipid carrier undecaprenol phosphate [258, 259]. Unfortunately, bacitracin is largely relegated to use on the skin due to nephrotoxicity [260]. As such, it is a common component of first aid antibacterial

ointments. Zn pyrithione is the second Zn-activated antimicrobial drug. Zn pyrithione possesses antifungal activity and is commonly found in over-the-counter anti-dandruff shampoos. However, its mechanism of action is not entirely clear, and there is evidence to suggest that while it is used as a precomplexed Zn salt, Zn itself may not be required for this action, with one study indicating Zn is displaced by Cu once penetrating the target organism [261].

Yet bacitracin is a clear indication that Zn-activated antibiotics can be developed and clinically introduced. Doing so in the modern age of drug discovery will require the development of a Zn-activated antibiotic discovery pipeline, from hit identification to in vivo studies, that can be easily adopted by agencies with the resources needed for their development. Ideally, this pipeline would make use of technological advances utilized by pharmaceutical companies, namely HTS, as this would likely reduce the cost of adopting this method. Given that industrial antibiotic screening has largely not been successful in the last few decades [122], Zn-activated antibiotics will also likely need to be readily identifiable within the available chemical space to justify their development. Furthermore, Zn-activated antibiotics should be chemically modifiable to maximize their on-target effects while minimizing off-target effects through structure activity relationship (SAR) studies. Lastly, different clusters of Zn-activated antibiotics would preferably possess separate and unique modes of action compared to bacitracin, as multiple bacitracin resistance mechanisms have been documented.

This study seeks to identify and characterize proof-of-concept Zn-activated antibiotics to demonstrate their potential for antibiotic development, with the above features taken into consideration. Previously, our research group developed an HTS

protocol to identify CDIs from drug screening libraries against multiple bacterial species [216]. This method led to the discovery and characterization of several classes of CDIs, including the TSCs and PZPs, as inhibitors of MRSA [214, 218]. Importantly, this screening method is a simple and readily adaptable whole-cell screening platform that more closely considers bacterial metabolism compared to standard antibiotics screening protocols. By modifying this platform for Zn-dependent antibiotic discovery, we demonstrate Zn-activated antibiotics are efficiently and accurately identified from a bioactive library containing molecules with biological actions, including FDA-approved drugs. We find consideration of physiological Zn concentrations greatly increases the efficiency of hit identification using this method, allowing for the identification of the UV-A filter and sunscreen component avobenzone (AVB) as a potent Zn-activated inhibitor of MRSA. AVB complexed with Zn (AVB-Zn) is effective against a panel of multi-drug resistant clinical MRSA isolates with no toxicity observed against human immune cells and could be developed as cream that improved mouse survival in a MRSA wound infection model. AVB-Zn then is a model for Zn-dependent antibiotic development against a significant bacterial threat with high rates of clinical resistance.

Additionally, this work establishes Zn-activated antibiotics are modifiable, an essential feature for drug development. This study focuses on two groups of privileged structures within drug discovery that were found to be Zn-activated inhibitors of *S. aureus*, the 8HQs and the benzimidazoles (BZIs), as they are easily modifiable chemically. By modifying specific R-groups, we can modulate the metal requirements and requirements of either the 8HQs or the BZIs. We find halogenated 8HQs have the highest potency against *S. aureus*, while BZI metal specificity is readily adjusted by R-

group modifications. This results in pools of BZI analogs with combined Cu and Zn specificity and others with solely Zn dependency for their action against S. aureus. Therefore, Zn-dependent antibiotics could be rationally designed for specifically Zn dependency over Cu specificity and a broader host range. Taken in total, this work establishes Zn-activated antibiotics as a viable avenue for future antibiotic discovery.

REPURPOSING SUNSCREEN AS AN ANTIBIOTIC: ZINC-ACTIVATED AVOBENZONE INHIBITS METHICILLIN-RESISTANT *STAPHYLOCOCCUS AUREUS*

by

RACHEL M. ANDREWS, GRETCHEN E. BOLLAR, A. SOPHIA GIATTINA, ALEX G. DALECKI, JOHN R. WALLACE JR., LEAH FRANTZ, KAYLA ESCHLIMAN, OBDULIA COVARRUBIAS-ZAMBRANO, JOHNATHAN D. KEITH, ALEXANDRA DUVERGER, FREDERIC WAGNER, FRANK WOLSCHENDORF, STEFAN H. BOSSMANN, SUSAN E. BIRKET, AND OLAF KUTSCH

Submitted to *Metallomics*

Format adapted for dissertation

ABSTRACT

Methicillin-resistant *Staphylococcus aureus* (MRSA) is a major healthcare concern with associated healthcare costs reaching over $1 billion in a single year in the United States. Antibiotic resistance in *S. aureus* is now observed against last line of defense antibiotics, such as vancomycin, linezolid, and daptomycin. Unfortunately, high throughput drug discovery approaches to identify new antibiotics effective against MRSA have not resulted in much tangible success over the last decades. Previously, we demonstrated the feasibility of an alternative drug discovery approach, the identification of metallo-antibiotics, compounds that gain antibacterial activity only after binding to a transition metal ion and as such are unlikely to be detected in standard drug screens. We now report avobenzone, the primary active ingredient of most sunscreens, can be activated by zinc to become a potent antibacterial compound against MRSA. Zinc-activated avobenzone (AVB-Zn) potently inhibited a series of clinical MRSA isolates (MIC: 0.62 – 2.5 μM), with no signs of pre-existing resistance. AVB-Zn was also active against clinical MRSA isolates that were resistant against the commonly used zinc-salt antibiotic bacitracin. We found AVB-Zn exerted no cytotoxicity on human cell lines and primary cells. Lastly, we demonstrate AVB-Zn can be deployed therapeutically as lotion preparations, which showed efficacy in a mouse wound model of MRSA infection. AVB-Zn thus demonstrates Zn-activated metallo-antibiotics are a promising avenue for future drug discovery.

INTRODUCTION

As a result of the worldwide rise of antibiotic-resistant bacteria and the simultaneous decline in antibiotic drug discovery, antibiotic-resistant pathogens represent an imminent global health emergency [1]. The increased incidence of infections with antibiotic-resistant bacteria results in longer hospital stays, increased treatment costs, and higher numbers of patients succumbing to bacterial infections. In 2019, the six primary pathogens for which patient death was associated with antibacterial resistance were *Escherichia coli, Klebsiella pneumoniae, Streptococcus pneumoniae, Acinetobacter baumannii, Pseudomonas aeruginosa* and *Staphylococcus aureus*. Together, drug resistant forms of these bacteria were responsible for roughly 900 000 deaths worldwide with a total of approximately 3.5 million deaths attributable to antimicrobial resistance. Methicillin-resistant *S. aureus* (MRSA) alone caused more than 100 000 deaths in 2019 and is considered especially problematic [1].

Despite the ongoing antimicrobial resistance crisis, antibiotic development has largely stalled. Only two new antibiotic classes have been discovered since the 1970s, and of the few antibiotics brought to market, the majority were initially identified during the Golden Age of antibiotic discovery (1940 – 1970) but were not approved for clinical use until the 21st century [2-4]. Since the fall of the Waksman platform that fueled the Golden Age, modern high throughput screening attempts have focused on identifying inhibitors of known protein targets, such as DNA gyrase, but have eliminated whole-cell screening methods that take bacterial permeability and metabolism into account [4]. Attempts to chemically modify scaffolds of synthetic or natural antibiotics to improve potency, increase the activity spectrum, and overcome mechanisms of drug resistance

have governed antibiotic drug discovery for the last few decades [5]. However, the repeated introduction of only slightly modified drugs (e.g. β-lactams), chemical entities for which bacteria had already developed resistance mechanisms, provided only temporary relief [5]. Other approaches, such as the use of bacteriophages, polymers, and engineered nanoparticles have certainly shown promise, but the clinical feasibility of these therapy candidates for standard clinical use remains to be proven [6, 7]. Taken together, these approaches led to a decades-long antibacterial innovation gap, resulting in few novel antibiotics.

Another avenue of antibiotic drug discovery is the identification and advancement of metal-dependent inhibitors, small molecule inhibitors that only exert their activity in the presence of a transition metal. These efforts have primarily focused on copper (Cu)-dependent inhibitors on the premise that the inherent antibacterial and self-potentiating redox cycling of Cu could be focused against a target organism [8-17]. Indeed, this very property has been harnessed by innate immune cells where Cu is actively imported into phagosomes to damage engulfed pathogens [18]. Unfortunately, the nonspecific cytotoxic activity of these inhibitors, which seems to be related to the redox activity of Cu, also targets eukaryotic cells and can be cytotoxic [19].

However, recent evidence suggests zinc (Zn), a *d*-block transition metal commonly regarded as an essential micronutrient with no redox activity [20], can act as an antimicrobial. Neutrophils and macrophages were shown to employ Zn similarly to Cu against phagocytized *Streptococcus pyogenes* [21, 22] and mycobacteria [23, 24] respectively. Zn can also activate chemical compounds to become antibacterial. Bacitracin, a common antibiotic in first-aid ointments, is primarily active in the presence

of Zn [25], and PBT2, a compound in clinical trials for the treatment of Alzheimer's and Huntington's disease [26, 27], was shown to be an effective inhibitor of multiple bacterial species when combined with high concentrations of Zn [28, 29]. Despite this, no dedicated screening effort, to our knowledge, has been employed to identify other Zn-activated antimicrobials.

Here we demonstrate that drug screens designed to discover Zn-activated inhibitors efficiently identify new antibiotics. Using a proof-of-concept Zn-dependent screening approach, we show Zn is highly efficient at activating previously unknown metal-dependent inhibitors against MRSA from a library of FDA-approved drugs and bioactive molecules. Using this method, we identified avobenzone (AVB), an active ingredient in sunscreens, as a potent and effective Zn-activated inhibitor of MRSA. We also found Zn-activated AVB (AVB-Zn) is effective at inhibiting multi-drug resistant MRSA isolates at concentrations with no apparent eukaryotic toxicity. Finally, we show AVB-Zn could be developed as a therapeutic lotion using a murine wound infection model of MRSA.

METHODS

Bacterial strains and culture conditions.

All *S. aureus* strains utilized in this study were routinely cultured in Mueller-Hinton (MH; Oxoid) medium at 37°C shaking at 180 rpm prior to transfer into experiment-specific media. Apart from clinical isolates, all strains used in this study were purchased from ATCC. The clinical multi-drug resistant MRSA isolates were de-identified and obtained from the UAB Laboratory Medicine. Resistance profiles of each

isolate were also characterized by and obtained from the UAB Laboratory Medicine. For the mouse experiments, USA300-LAC was cultured in Luria-Bertani (LB; Sigma-Aldrich) broth.

Antibiotics, compounds, and reagents.

The bioactives screening library was purchased from Selleckchem. Avobenzone was purchased from Selleckchem and Sigma. All compounds were reconstituted to 10 mM concentration in 100% anhydrous dimethyl sulfoxide (DMSO; Fisher Chemical), aliquoted, and stored at -80°C for long-term storage. Antibiotics were dissolved in double-distilled water (ddH_2O), sterile filtered with 0.2 µm nylon filters (Fisher Scientific) and stored as 10 mg/mL aliquots at -80°C. Copper sulfate salts and zinc sulfate heptahydrate salts were purchased from Sigma. Metal stock solutions were stored as 100 mM aliquots in ddH_2O at 4°C following sterile filtration with 0.2 µm nylon filters. The metabolic indicator dye resazurin (Sigma) was stored at 800 µg/mL in ddH_2O at 4°C following sterile vacuum filtration with a 0.2 µm nylon filter.

Zn-dependent antibiotic screening and analysis.

Zn-dependent screening of the 1582-compound bioactives screening library (Selleckchem) was performed against USA300-LAC. Prior to screening, the compound library was diluted to 800 µM in 100% anhydrous DMSO (Fisher Chemical) in 96-well round-bottom plastic plates (Fisher Scientific) using a Beckman Coulter FX^p robotic platform. The dilution plates were then covered with adhesive aluminum film (Thermo Scientific) and stored at -80°C. To reduce variability across screening days, high density

USA300-LAC seed stocks were used to generate the inoculum for the screen. Briefly, USA300-LAC was cultured to mid-exponential phase in MH medium, washed twice with 1x RPMI-1640 (Corning) to remove residual MH medium, and normalized to an optical density at 600 nm (OD_{600}) of five in 1x RPMI 1640 supplemented with 15% glycerol (Fisher Chemical) for cryoprotection. The cells were aliquoted then stored at -80°C for future use.

To perform the screen, a seed stock was thawed, briefly centrifuged to remove the medium, and normalized to an inoculum OD_{600} of 0.01 in 1x RPMI-1640, allowing a 30-minute rest period in the medium. Dilution plates were thawed, and compounds were screened at 10 µM in 1x RPMI-1640 with and without either 25 µM $CuSO_4$ or 25 µM $ZnSO_4 \cdot 7H_2O$ using the Beckman Coulter FX^p robotic platform. Resazurin was added to the medium at a final concentration of 10 µg/mL as a surrogate marker of bacterial growth. All screening plates were incubated at 37°C + 5% CO_2 for 12 hours and metabolic conversion of resazurin to the fluorescent product resorufin (ex. 530 nm, em. 590 nm) was determined using a Biotek™ Cytation 3 plate reader. Measurements were background subtracted and normalized as percent growth of the negative control wells on the same plate. Hit compounds were defined as compounds that reduced the growth of USA300-LAC by at least 50% relative to the vehicle-treated controls. Hit compounds were subdivided into inactive, metal-dependent, metal-inverse, or metal-independent categories by comparing the percent growth for a given compound without a metal to that of the same compound with a metal.

Determination of minimal inhibitory concentration.

The minimal inhibitory concentration (MIC) of the tested compounds was determined using challenge assays as previously described [13, 14]. Briefly, each strain was cultured to mid-exponential phase in MH medium, as determined by OD_{600} measurement. Cultures were then washed twice in the chemically defined treatment medium, 1x RPMI-1640, to remove residual MH medium. *S. aureus* cultures were normalized and treated at an OD_{600} of 0.005 (5 million CFUs/mL) in 1x RPMI-1640. Each strain was treated with compounds that were serially titrated 1:2 in the assay medium in 96-well flat-bottom plastic plates with or without either 25 µM $CuSO_4$ or 25 µM $ZnSO_4$. Compound-untreated samples for each metal condition were used as negative controls. *S. aureus* strains were treated for 18 – 20 hours at 37°C with 5% CO_2. Following the treatment period, bacterial growth was determined by measuring the absorbance of each well at 600 nm using a Biotek™ Cytation 3 plate reader. Measurements were then background adjusted and normalized to either the untreated control or the metal only control. The minimal inhibitory concentration (MIC) was defined as the minimal compound concentration that reduced the growth of the strain to 10% or less than that of the untreated control.

Binding constant determination.

Binding constants were determined using UV/Vis-absorption spectroscopy by titrating AVB with Cu(I), Cu(II), and Zn(II). Briefly, 1 mM AVB in 100% anhydrous DMSO was titrated in HEPES (4-(2-hydroxyethyl)-1-piperazineethanesulfonic acid) buffer (pH = 7.2 - 7.4) with 800 µM CuBr, $CuSO_4$, or $ZnSO_4$ at the following

concentrations: 0 µM, 25 µM, 50 µM, 75 µM, 100 µM, and 150 µM. Once the gradient of solutions was prepared, full spectrum UV/Vis-absorption spectroscopy was performed to detect characteristic spectral changes that occur as a consequence of metal cation binding. Binding constants were calculated by importing the spectra of individual titrations with each metal into the UV 1:1 Bindfit program (http://app.supramolecular.org/bindfit/).

Eukaryotic toxicity assays.

Jurkat T cells were originally purchased from the ATCC and cultured at 37°C with 5% CO_2 in 1x RPMI-1640 supplemented with 10% heat-inactivated fetal bovine serum (Cytiva, HyClone™), 100 U/mL penicillin, 100 µg/mL streptomycin, and 2 mM L-glutamine (HyClone™, GE). Peripheral blood mononuclear cells (PBMCs) were isolated from commercially obtained buffy coats. Cell numbers and viability in the presence or absence of drug or metals were assessed using a Guava EasyCyte flow cytometer (GUAVA easyCyte™ BGR HT (Luminex)). This flow cytometer uses a capillary-based analytical system combined with a precision pump and provides precise absolute cell counts without the need of using reference beads. Each cell line was tested against serial 1:2 titrations of a given compound starting at 30 µM to 0.04 µM with and without 15 µM $ZnSO_4$ or $CuSO_4$. Cells were seeded at a standard density of 100,000 cells/well in 96-well flat-bottom plastic plates at 37°C + 5% CO_2 for 24 hours then assessed for viability using forward and side scatter gating (FSC/SSC).

Lotion preparation and modified Kirby-Bauer diffusion assays.

Antibiotic lotions were formulated by using a commercially available polyethylene glycol (PEG)-based lotion (CeraVe, CVS) as a base. To ensure thorough mixing of the lotion and additives, the lotion was mixed with 30% (v/v) Tween-80 (Sigma-Aldrich) in sterile ddH_2O to form an inert base lotion composed of CeraVe lotion + 3% (v/v) Tween-80. Zn-containing lotions were made by mixing this base lotion with 1.5 M $ZnSO_4$ dissolved in sterile ddH_2O for a final concentration of 10 mM $ZnSO_4$. An equal volume of sterile ddH_2O was added to lotions lacking Zn. AVB (Sigma) or bacitracin (Sigma) dissolved in 100% anhydrous DMSO were added to the control and Zn-containing lotions for a final concentration of 25 mM and 10 mM respectively. The vehicle lotion was generated by adding an equivalent volume of 100% DMSO and sterile ddH_2O as used in the compound and Zn-containing lotions respectively. Each component was thoroughly incorporated into the base lotion by vortexing for one minute, and lotions were stored at 4°C in the dark for up to two weeks. The antibacterial activity of each lotion was assessed using a modified Kirby-Bauer disc diffusion assay. Briefly, MH agar plates with identical indentations in the agar were inoculated with 2 million cells(cm^{-2}) of USA300-LAC. Lotions were dispensed into each indentation using a standard volume of 100 µL using sterile Leuer lock syringes (Fisher Scientific) and 22-gauge needles (PrecisionGlide™, BD). The plates were inverted and incubated for 18 – 20 hours at 37°C. Zones of inhibition were measured and compared to that of the vehicle control for each treatment.

Murine wound model.

For use in *in vivo* wound experiments, USA300-LAC was grown overnight in LB broth (Sigma-Aldrich) at 37°C with 250 rpm shaking. Bacterial cultures were washed and resuspended to 10^4 CFUs/mL in sterile phosphate-buffered saline (PBS; ThermoFisher Scientific). Commercially available sterile gauze was trimmed to 6 mm square dressings and incubated with bacterial culture at room temperature for 10 min prior to use. Mouse surgical methods were adapted from the wound model of Brandenburg, *et al*. [30]. On study day 0, 5 – 6 month-old C57BL/6 mice bred and maintained in-house were anaesthetized via intraperitoneal injection with 85.5 mg/kg ketamine hydrochloride (Vedco Inc.) and 12.5 mg/kg xylazine (MWI) in cocktail. The cranial thoracodorsal region was shaved and prepared for surgery using 70% ethanol (ThermoFisher Scientific) and topical analgesic (Burn Jel; Water-Jel Technologies LLC) for pain control. A silicon O-ring (McMaster-Carr) was attached to the skin via four to six 5-0 interrupted nylon sutures and secured with tissue adhesive (GLUture; Zoetis Inc.). A 6 mm diameter wound was created within the ring using a biopsy punch. Bacteria-laden dressings were applied to the wound, allowed to incubate, and removed four hours later.

Each mouse was housed individually and monitored following the procedure until fully ambulatory. On day 1 post-infection, treatment was initiated with 100 µL of either vehicle control lotion, AVB lotion, AVB-Zn lotion, or commercially available bacitracin ointment (Bacitraycin Plus; First Aid Research Corp.) applied to the wound surface via sterile syringe. Treatments were applied daily through study day 7, <2 hours prior to the start of the facility dark cycle. On study day 8, mice were euthanized via intraperitoneal injection of 200 µL pentobarbital sodium (390 mg/mL; Vortech). Throughout the study,

mice were monitored for signs of distress (severe weight loss, prolonged lethargy) and euthanized when necessary, under the advisory of UAB veterinary staff. All animal experiments at UAB were conducted in accordance with UAB Institutional Animal Care and Use Committee (IACUC) approved protocols. Animals were bred and housed in standard cages with a 12-hour light/dark cycle at 71 – 75°F with ad libitum access to food and water. Experimental groups were composed of even numbers of males and females.

Mouse survival was assessed on each day during the experiment. Significance in mouse survival between groups was determined using a log rank test for trend. On day 8 of the study, swabs of the wounds of the sacrificed mice were performed with sterile cotton swabs. CFUs were enumerated by inoculating mannitol salt agar plates with the swabs and incubating the plates overnight at 37°C. Mean CFUs were calculated for each treatment group, and significance was determined using a Kruskal-Wallis test.

RESULTS

Identification of Zn-activated antibiotics against MRSA.

To determine whether Zn, as the only *d*-block transition metal without innate redox activity [31], has the capacity to activate otherwise inactive compounds to exert antibacterial activity, we screened a library of 1582 FDA-approved drugs and compounds with known bioactivities in the presence or absence of Zn. The screen was performed against the well-described MRSA strain USA300-LAC in the chemically defined medium 1x RPMI-1640. Given that Cu-complexed compounds are the primary focus of current antibacterial metallodrug research [10, 13, 14, 17], we performed a parallel screen using Cu to directly compare the efficacy of Zn and Cu to promote antibacterial activation of

compounds. Each compound was tested for antibacterial activity without a metal, with 25 µM $ZnSO_4$, or with 25 µM $CuSO_4$. Growth after overnight incubation at 37°C was determined by measuring resorufin fluorescence, the product of the metabolic indicator dye resazurin (Figure 1A). Compounds that reduced the growth of USA300-LAC by 50% or more were classified as hits.

The screen identified 143 hits out of a total 1582 compounds for a hit rate of approximately 9%. Of the compounds identified, 78 compounds (4.9%) were classified as independent and subsequently inhibited staphylococcal growth independent of a metal (Figure 1B – C; lower left quadrant). As expected, this category included antibiotics known to target *S. aureus* (42), such as the rifamycin class and antiseptics (8) (Supplemental Figure 1A – B), while narrow spectrum antibiotics targeting other organisms were exclusively classified as inactive (Supplemental Figure 1C – D). Importantly, we were able to accurately identify bacitracin, a common cyclic polypeptide antibiotic used in first-aid ointments that requires Zn for its activity [32, 33], as Zn-dependent (Supplemental Figure 2A upper left quadrant; Supplemental Figure 2B, upper right quadrant). This highlights both the accuracy of Zn-dependent screening and the need to include metals as antibiotic screening conditions to recognize successful antibiotic molecules whose activities would otherwise be overlooked.

Screening with physiologically relevant concentrations of both Zn and Cu nearly doubled the hit rate of the screen as a whole. Zn activation was displayed in 49 (3.1%) of the otherwise inert compounds (Figure 1B), and antibacterial Cu activation was seen for 37 of the compounds (2.3%) (Figure 1C). While some compounds were activated by both Cu and Zn (25), compounds solely activated by Zn (24) within the screen predominated

over compounds with Cu-specific activation (12). Zn was thus an efficient activating component for metallo-antibiotics. This would suggest the inherent redox potential of a metal like Cu is not necessarily required to induce the metallo-antibiotic activity of small chemical molecules, thereby broadening the possible modes of action a metallo-antibiotic could possess. Zn-activated compounds could act as Zn ionophores and cause mismetallation of essential enzymes by the intracellular release of Zn, as has been previously described [28, 29]. Alternatively, compounds could directly coordinate with Zn, thereby altering the compound conformation to a form active against a specific target, or Zn-activated molecules may simply possess increased membrane permeability. Regardless of the mechanism, it is evident that consideration of physiological Zn concentrations during the drug screening process can expand the chemical space of discoverable active compounds.

Figure 1

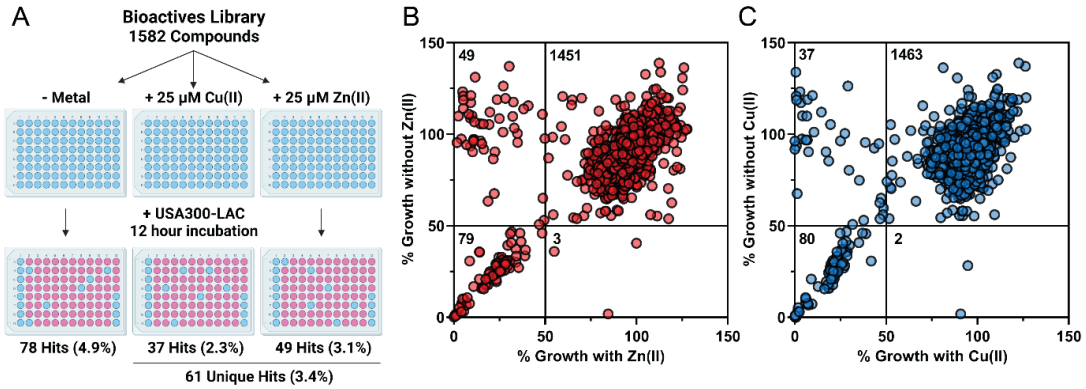

Figure 1 Metal-dependent screening identifies metal-activated antibiotics against MRSA.

(A) The bioactives library from Selleckchem was screened in 1x RPMI-1640 with and without 25 µM $CuSO_4$ or 25 µM $ZnSO_4$ against the MRSA strain USA300-LAC. Growth was measured indirectly by the conversion of the metabolic dye, resazurin, to the fluorescent product resorufin (ex/em 530/590 nm) after overnight incubation at 37°C with 5% CO_2. Compounds that reduced the growth of USA300-LAC by at least 50% were declared as hits. This screen outline was generated using BioRender.com. (B) Compounds were classified into various activity groups by graphing the percent growth of USA300-LAC in the presence of each compound with a metal to that without the same metal. Inactive compounds are displayed in the upper right quadrant, while independent compounds plot to the lower left quadrant. The upper left quadrant represent metal-dependent hits, and inverse hits are shown in the lower right quadrant. Zn-dependent screening identified 49 Zn-dependent hits, 79 independent hits, and three Zn-inverse hits. (C) Cu-dependent screening identified 37 Cu-dependent hits, 80 independent hits, and two Cu-inverse hits.

Supplemental Figure 1

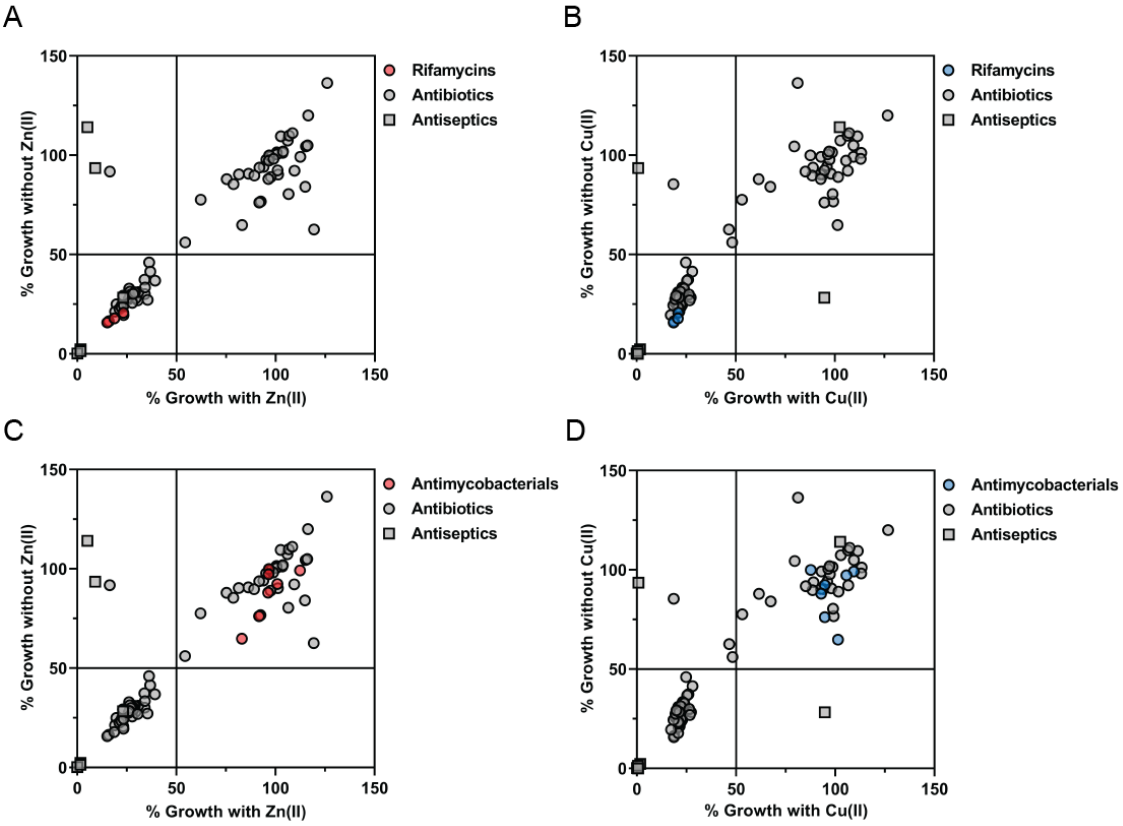

Supplemental Figure 1 Screen results of internal antibiotic controls.
The Zn and Cu screening results for all the antibiotics and antiseptics included in the bioactives library were plotted to confirm their expected activity against MRSA. Members of the rifamycin antibiotic class (4) were independently active against USA300-LAC regardless of Zn (A) or Cu (B). Meanwhile, narrow spectrum antibiotics specific for mycobacteria (7) were classified as inactive irrespective of metal condition (C, D).

Supplemental Figure 2

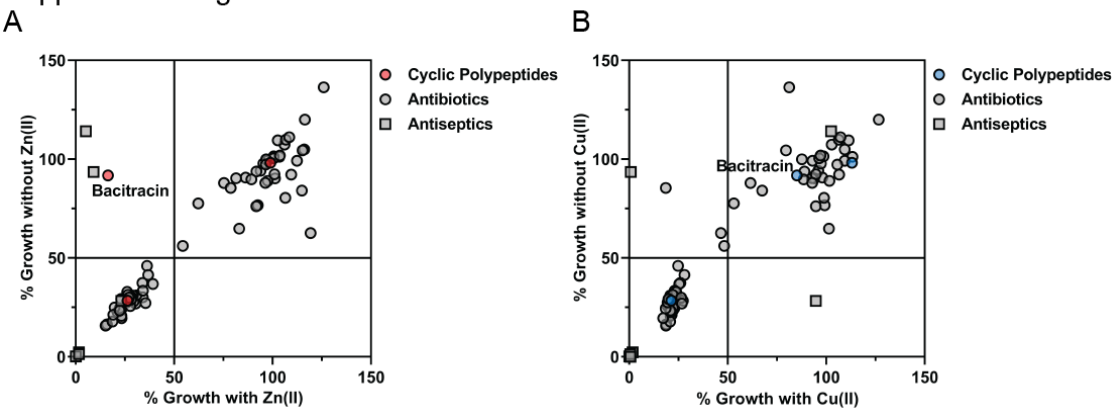

Supplemental Figure 2 Screen results of bacitracin.
The metal-dependent screening activities of cyclic polypeptide antibiotics are highlighted among the full spectrum of antibiotics and antiseptics screened with Zn (A) and Cu (B). Metal-dependent screening correctly identified the Zn-specific cyclic polypeptide bacitracin as possessing Zn-dependent activity but not independent or Cu-dependent action against USA300-LAC.

Avobenzone is a potent Zn-activated metallo-antibiotic against MRSA.

While the drug screen identified a series of FDA-approved drugs as Zn-activated compounds against MRSA, most are known to have notable or serious side effects, such as cancer agents (e.g. ponatinib, tamoxifen, toremifene citrate) or antifungals (e.g. clotrimazole, bifonazole, tioconazole), and would thus not warrant further exploration. An exception to this is avobenzone, which was identified as being activated by both Zn and Cu. Avobenzone (AVB), or 1-(4-*tert*-butylphenyl)-3-(4-methoxyphenyl)propane-1,3-dione, is an FDA-approved UV-A filter and a common active ingredient in commercial sunscreens and beauty products [34]. It is composed of a central 1,3-diketone group connecting two 2,4-substituted phenyl rings with a methoxy and a tert-butyl substituent (Figure 2A).

Given that ketone groups are known to coordinate with transition metals [35-38], we hypothesized AVB would form a complex with Zn to inhibit *S. aureus*. We first confirmed AVB complexed with Cu and Zn (Table 1). UV/vis spectroscopy binding studies demonstrated that Zn(II) (K_D = 5.9 µM) and Cu(II) (K_D = 4.4 µM), but not Cu(I), efficiently bound to AVB, confirming the existence of an AVB-Zn and AVB-Cu complex specific to their divalent form. While these constants fall short of the binding activity of high-affinity metal chelators, such as TPEN (N,N,N′,N′-tetrakis(2-pyridinylmethyl)-1,2-ethanediamine) or EDTA (2,2',2",2"'-(Ethane-1,2-diyldinitrilo)tetraacetic acid), for which K_Ds are reported in the picomolar to femtomolar range [39], the K_Ds are similar to those we determined for bacitracin. Bacitracin also had similar affinities for Zn(II) (K_D = 5.7 µM) and Cu(II) (K_D = 1.4 µM) as AVB. Thus, AVB has a similar affinity for Zn as a Zn-binding, FDA-approved antibiotic.

Having demonstrated AVB complexes with divalent Zn and Cu, we next determined the minimal inhibitory concentration (MIC), or the lowest concentration causing 90% inhibition of bacterial growth, of AVB against MRSA. For this purpose, challenge assays of AVB in the presence and absence of Zn or Cu were performed against USA300-LAC, and inhibition was determined by normalizing A_{600} measurements, a marker of bacterial growth, to that of the compound-untreated control of each metal condition. In line with the screening results for AVB, AVB alone exerted no antibacterial activity against USA300-LAC but gained antibacterial activity in the presence of a metal, with AVB-Cu effective at inhibiting the growth of USA300-LAC at 2.5 μM (Figure 2C). However, AVB-Zn was the most potent of these combinations, with an MIC of 1.25 μM against USA300-LAC. In contrast, the MIC of bacitracin-Zn (5 μM) was four-fold higher than that of AVB-Zn (Figure 2D), underscoring the potential of AVB-Zn as an antibiotic treatment.

We next tested whether clinical multidrug-resistant MRSA isolates [40, 41] possessed pre-existing resistance mechanisms against AVB-Zn (Figure 2E). None of the five tested isolates showed any signs of pre-existing resistance to AVB-Zn relative to USA300-LAC, with the MICs ranging from 0.6 – 2.5 μM depending on the isolate. While this panel only includes a limited number of strains, the resistance profiles of these strains cover most major antibiotic classes in clinical use, implying AVB-Zn has an alternative mechanism of action than most antibiotics currently in use (Supplemental Table 1).

This finding was particularly interesting given that four out of five of these clinical isolates possessed resistance to bacitracin-Zn. CI-4 and CI-5 (MIC = 10 μM)

were partially resistant to bacitracin-Zn relative to USA300-LAC, while CI-2 and CI-3 were fully resistant to the complex in our system (Figure 2F). While resistance to Zn-activated compounds can develop, these findings suggest that these resistance mechanisms do not necessarily provide cross-resistance to other Zn-activated compounds, further indicating Zn activation does not induce a single mode of action.

Figure 2

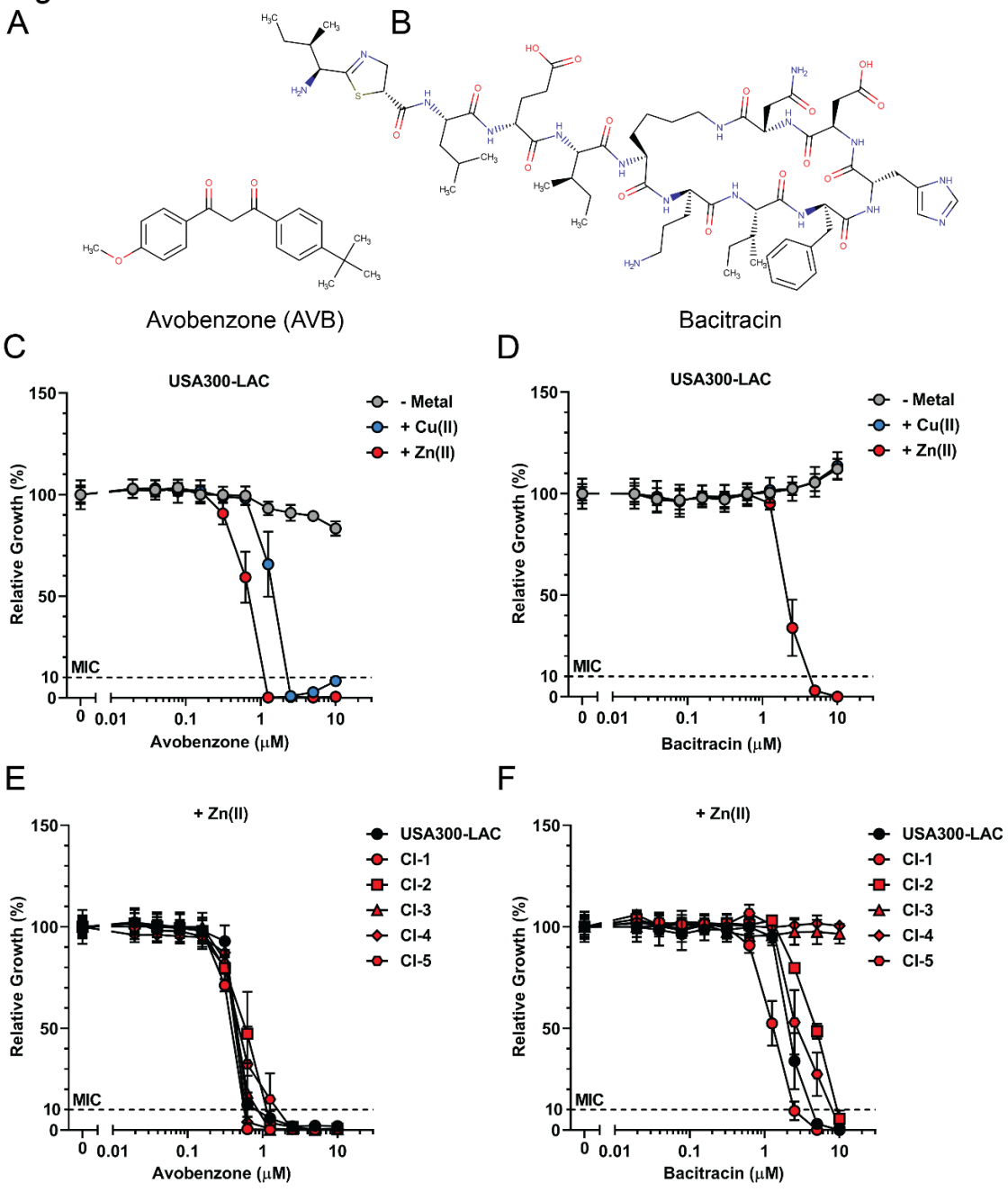

Figure 2 Metal-specific anti-staphylococcal activities of AVB and bacitracin. (A) Chemical structure of avobenzone. (B) Chemical structure of bacitracin. The minimal inhibitory concentrations (MIC) of AVB (C) and bacitracin (D) were determined against USA300-LAC under multiple metal conditions by titrating each compound in 1x RPMI-1640 with and without either 25 μM $CuSO_4$ or 25 μM $ZnSO_4$. Growth was determined after 20 hours of incubation at 37°C using A_{600} measurements as a readout. Percent growth was calculated by normalizing the A_{600} measurements relative to that of the compound-untreated control of each metal condition. Data represent the mean ± SEM (n

= 3 biological replicates, 3 technical replicates each). The sensitivity of the multidrug-resistant MRSA isolates, CI-1 – 5, to (E) AVB-Zn and (F) bacitracin-Zn were compared to USA300-LAC using dose-response curves described above (C and D) with 25 µM $ZnSO_4$. Data represent the mean ± SEM (n = 3 biological replicates, 3 technical replicates each).

	Avobenzone		Bacitracin	
Metal	K_A (M^{-1})	K_D (µM)	K_A (M^{-1})	K_D (µM)
Cu(I)	6900	144.93	9299	107.54
Cu(II)	225 759	4.43	738 223	1.35
Zn(II)	168 982	5.92	172 757	5.79

Table 1 Metal binding kinetics of AVB and bacitracin.
Association constants (K_A) and dissociation constants (K_D) of AVB and bacitracin with CuBr, $CuSO_4$, and $ZnSO_4$ were determined using UV/vis spectroscopy. AVB and bacitracin were titrated against a constant metal concentration in a HEPES buffer (pH 7.2 – 7.4). K_A and K_D were calculated by importing the resulting spectra into the Bindfit program (http://app.supramolecular.org/bindfit/).

Drug Target	Antibiotic Class	Antibiotic Formulation	CI-1	CI-2	CI-3	CI-4	CI-5
Peptidoglycan Synthesis	β-Lactam	Amoxicillin + Clavulanic Acid	R	R	R	R	R
		Ampicillin + Sulbactam	R	R	R	R	R
		Ampicillin	R	R	R	R	R
		Penicillin	R	R	R	R	R
	Glycopeptide	Vancomycin	S	S	S	S	S
	Cephalosporin	Ceftriaxone	R	R	R	R	R
Cell Membrane	Cyclic Lipopeptide	Daptomycin	S	S	S	S	S
DNA Gyrase	Fluoroquinolone	Ciprofloxacin	S	R	S	S	R
		Levofloxacin	S	R	S	S	R
		Ofloxacin	R	R	R	R	R
Translation - 50S Subunit	Lincomycin	Clindamycin	R	R	S	S	R
	Macrolide	Erythromycin	R	R	R	R	R
Translation - 30S Subunit	Aminoglycoside	Gentamicin	S	S	S	S	S
	Tetracycline	Tetracycline	R	S	S	S	S
Folic Acid Metabolism	Sulfonamide	Sulfamethoxazole + Trimethoprim	S	S	S	S	S

Supplemental Table 1 Resistance profiles of multi-drug resistant MRSA isolates.

The resistance profiles of each multidrug-resistant MRSA isolate were determined by the UAB Laboratory Medicine. Profiles are clustered by antibiotic target then chemical class. R represents resistant, and S indicates sensitive.

Minimal Zn requirements of AVB.

Drug screening conditions are usually designed to maximize hit discovery and, in this case, were performed at a slightly higher Zn concentration than what is commonly found in human serum [42, 43] to encourage compound interaction with Zn. While a screening concentration of 25 µM Zn may be physiologically relevant under some conditions, we wanted to determine the minimum effective concentrations of AVB and Zn required for maximal AVB-Zn activity against MRSA. To test this, we performed dose matrices against USA300-LAC by titrating Zn against AVB and measured bacterial growth using A_{600} measurements as a readout following overnight incubation. As expected of a metal-binding compound, the potency of the AVB-Zn complex increased by increasing the concentration of either component (Figure 3A). AVB required as little as 0.16 µM Zn to reach an MIC of 10 µM AVB against USA300-LAC. This resulted in maximal potency (0.62 µM AVB) with just 15 µM Zn, falling within the 10 – 20 µM range of human serum Zn [42, 43]. In contrast, bacitracin required at least 15 µM Zn to reach an MIC of 10 µM (Figure 3B). As such, AVB-Zn far exceeds the efficacy of the FDA-approved antibiotic bacitracin with the same Zn concentration.

Figure 3

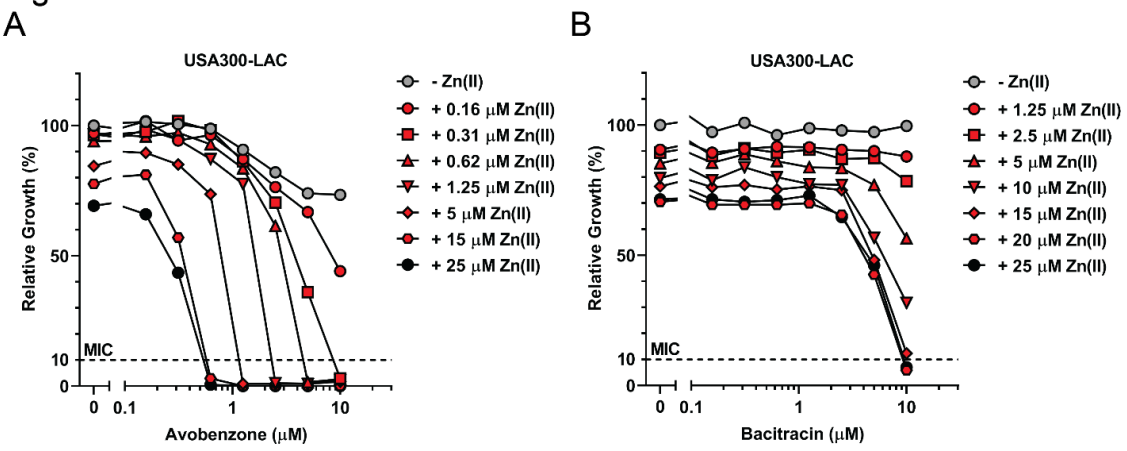

Figure 3 Minimal Zn requirements of AVB and bacitracin.
(A) AVB and (B) bacitracin were serially titrated against serial titrations of $ZnSO_4$ in 1x RPMI-1640 to determine the minimum concentration of Zn required to achieve the lowest minimal inhibitory concentration (MIC) of each compound against USA300-LAC. Bacterial growth was measured using endpoint A_{600} measurements after 20 hours of incubation at 37°C. Growth was normalized as a percent of the growth of the untreated control. Data are representative of three separate experiments. Individual Zn concentrations that did not result in major changes in bacterial growth are not presented for clarity.

AVB-Zn is not toxic to eukaryotic cells.

We next sought to determine the toxicity of AVB-Zn against eukaryotic cells in our system by performing challenge assays of AVB, AVB-Zn, and AVB-Cu against human Jurkat T cells and patient-derived peripheral blood mononuclear cells (PBMCs) from three healthy donors. Cell viability and proliferation were measured after 24 hours of treatment using flow cytometric analysis. Cell viability was defined as the percentage of cells in a forward scatter/side scatter-based viability gate, and cell number was defined as the absolute number of cells within this gate. The latter analysis can detect inhibitory effects to cell proliferation that do not result in cell death and may be the most sensitive means to detect toxic drug effects.

In contrast to the potent antibacterial activity of AVB-Zn against *S. aureus*, AVB, AVB-Cu, and AVB-Zn displayed minimal cytotoxicity against both cell types tested (Figure 4). Minor toxicity for all forms of AVB against Jurkat T cells was observed only at the highest concentrations and resulted in less than a 20% reduction in cell viability (Figure 4A). As with viability, Jurkat proliferation was only affected at the highest concentration of AVB tested (Figure 4B). Encouragingly, cell viability (Figure 4C) and proliferation (Figure 4D) of PBMCs were unaffected by any of the treatments after 24 hours. AVB-Zn, then, is a promising candidate for antibiotic development due to its potent antibacterial action with minimal toxic effects against human cells.

Figure 4

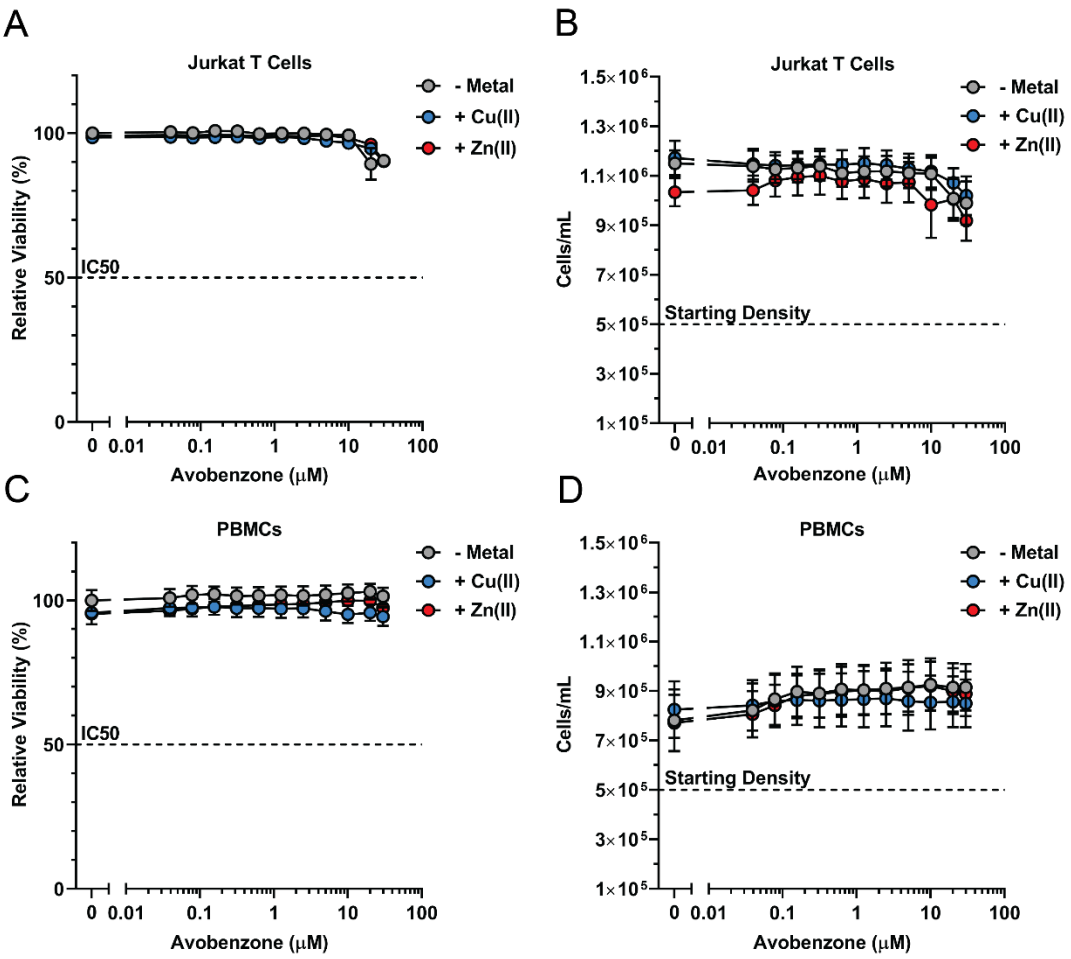

Figure 4 AVB toxicity against Jurkat T cells and healthy donor PBMCs. Jurkat T cells (A, B) and healthy donor peripheral blood mononuclear cells (C, D) were treated for 24 hours with serial 1:2 titrations of avobenzone by itself or with either 15 μM $ZnSO_4$ or 15 μM $CuSO_4$. Absolute cell viability (A, C) was then determined by flow cytometry as the percentage of cells within a life-gate as determined by forward scatter/side-scatter analysis. Absolute cell numbers (B, D), within the same life-gate, were also determined using flow cytometry to assess potential effects on cell proliferation. For all experiments, data represent the mean ± SEM (n = 3 biological replicates, 3 technical replicates each).

AVB-Zn efficacy in a murine wound infection model.

Our data suggest AVB-Zn shows promise as a repurposed antibiotic. To this end, we wanted to test if AVB-Zn is effective at inhibiting *S. aureus in vivo*. *S. aureus* commonly causes skin and soft-tissue infections, and AVB currently has FDA approval for use on the skin. Because of this, we chose to test AVB-Zn in a murine wound infection model using PEG-based lotion treatment preparations.

First, we prepared and tested the *in vitro* efficacy of lotion-based treatments of AVB-Zn against USA300-LAC using a modified Kirby-Bauer disc diffusion assay. Briefly, an inert base lotion composed of a commercial PEG-based lotion and 3% (v/v) Tween-80 was mixed with components of each treatment to make the various treatment lotions. MH agar plates with 100 µL volume indentations were inoculated with USA300-LAC, and the indentations were filled with each treatment lotion. Zones of inhibition were measured following overnight incubation (Supplemental Figure 3A).

Using this method, we compared the efficacy of four different lotion preparations: a vehicle control, Zn alone, bacitracin-Zn, and AVB-Zn, to inhibit the growth of USA300-LAC. These results were compared to a commercially available bacitracin-Zn first-aid ointment. No inhibitory effect was observed against USA300-LAC with the vehicle control and Zn control lotions (Supplemental Figure 3B). However, both the bacitracin-Zn and AVB-Zn lotions generated zones of inhibition. Interestingly, the commercial bacitracin-Zn ointment did not noticeably inhibit USA300-LAC growth, indicating the size of the zones of inhibition are likely due to limitations in the rate of diffusion in this system.

Once efficacious lotion treatments were established, we tested the preparations in an *S. aureus* wound infection mouse model to determine the *in vivo* efficacy of AVB-Zn. These results were also compared to the efficacy of the commercial bacitracin-Zn ointment. Briefly, the cranial thoracodorsal region of each C57BL/6 mouse was shaved and cleaned for surgery. A silicon O-ring was secured to the shaved area and a biopsy punch was used to create a 6 mm wound within each O-ring. A 6 mm dressing coated with USA300-LAC was then applied to the wound. The wound dressing model is a modification of a previously established model for the study of delayed wound healing caused by *Pseudomonas aeruginosa* biofilms [30]. Given the dimension of the punch biopsy, the ensuing infection would be considered equivalent to a deep tissue infection. Treatment began 24 hours post-application of the bacteria and was re-applied once a day for one week. Mouse survival was monitored over the course of the study, and colony forming units (CFUs) were enumerated from wound swabs upon sacrifice (Figure 5A).

While there was no significant difference in CFUs isolated from the wounds of each treatment group (Supplemental Figure 4), we did observe a significant difference in trend ($p = 0.0173$) in mouse survival over the course of the experiment. Of the mice treated with just a vehicle control cream ($n = 10$), 4 mice (40%) died or were euthanized due to signs of insurmountable disease within the first 72 hours (Figure 5B). In the group of mice treated with the commercial bacitracin preparation ($n = 5$) one mouse (20%) died after 48 hours, while no mice from the AVB-Zn treatment group died ($n = 5$). Interestingly, there was also no death observed in the group of mice treated with AVB lotion lacking Zn ($n = 5$), which suggests AVB may locally coordinate with Zn and become activated to exert its antibacterial effect. Though additional studies, especially in

systemic infection models, are required to optimize the AVB-Zn concentrations needed therapeutically, these *in vivo* data support our *in vitro* results that AVB-Zn protects against insurmountable MRSA infection similarly to a known antibiotic.

Supplemental Figure 3

A

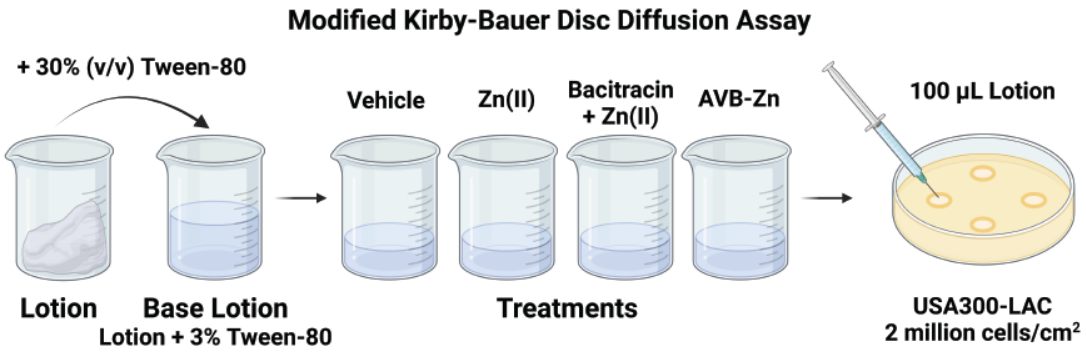

B

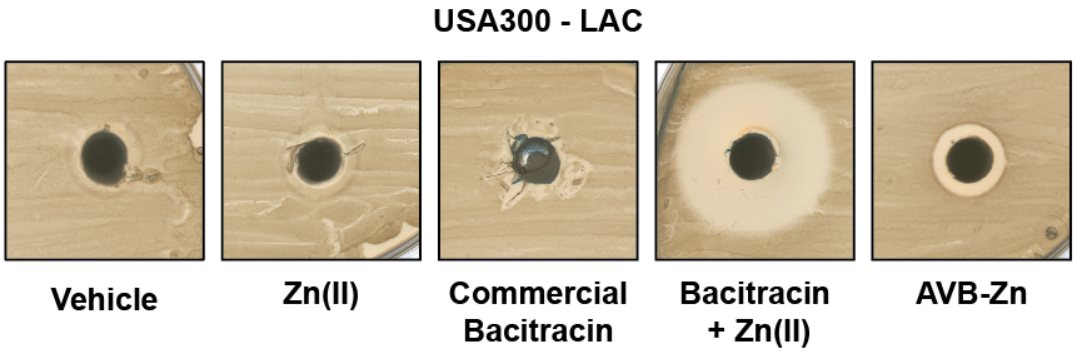

Supplemental Figure 3 *In vitro* lotion efficacy.
(A) Treatment lotions were prepared by initially mixing a commercial polyethylene glycol-based lotion with 30% Tween-80 to form an inert but loose base lotion. The base lotion was then mixed with the treatment components to form four treatment lotions: a vehicle control, 10 mM $ZnSO_4$, 10 mM bacitracin with 10 mM $ZnSO_4$, and 25 mM avobenzone with 10 mM $ZnSO_4$ (AVB-Zn). A modified version of the Kirby-Bauer disc diffusion assay was utilized to determine lotion efficacy against USA300-LAC. Lotions were dispensed into indentations of MH agar plates inoculated with $2x10^6$ cells(cm^{-2}) using sterile Leuer-lock syringes and 22-gauge needles. Plates were incubated inverted for 20 hours at 37°C, and zones of inhibition for each treatment were assessed. The protocol schematic for the lotion preparation and modified Kirby-Bauer disc diffusion protocol was created using BioRender.com. (B) Of the tested lotions, only the bacitracin-Zn and the AVB-Zn lotions inhibited the growth of USA300-LAC.

Supplemental Figure 4

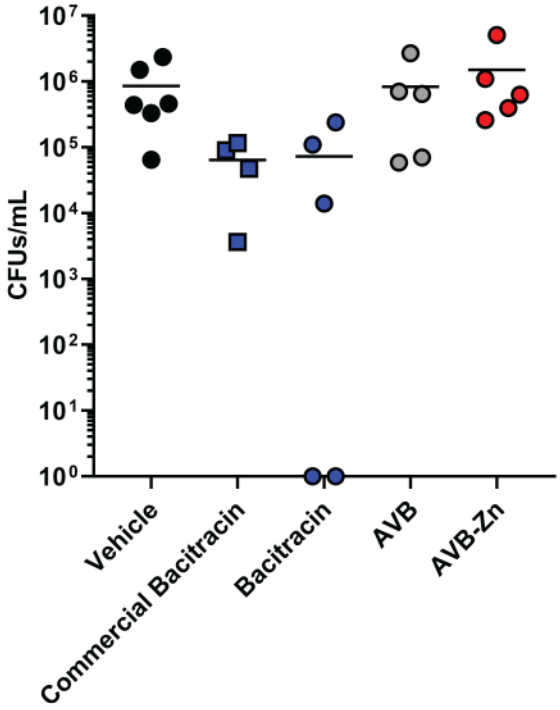

Supplemental Figure 4 CFU isolation from murine model.
Colony forming units (CFUs) were isolated from the wounds of surviving mice at the end of the treatment period using sterile swabs and cells were cultured on mannitol salt agar plates overnight at 37°C. Means were calculated for each treatment condition, and significance was determined using a Kruskal-Wallis test.

Figure 5

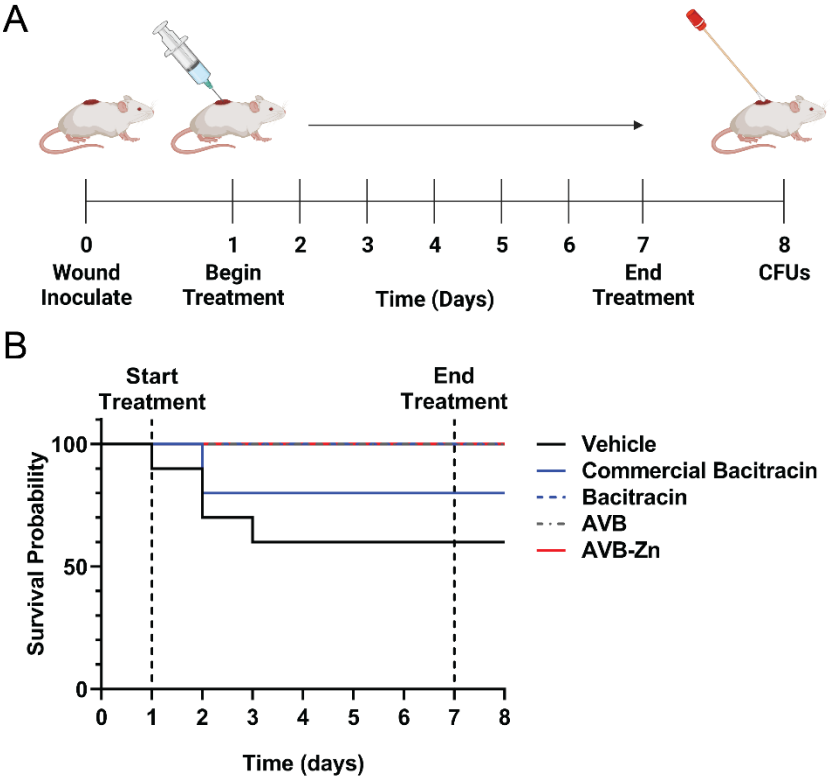

Figure 5 AVB-Zn efficacy in a murine wound infection model.
(A) To determine the antibacterial efficacy of these cream preparations we used a wound model of *S. aureus* infection in C57BL/6 mice that simulates a soft tissue infection using USA300-LAC. Lotion treatment began 24 hours post-application of the bacteria and continued through day 7. Treatments included a vehicle control (n = 10), a commercially available bacitracin-Zn ointment (n = 5), bacitracin-Zn lotion (n = 5), avobenzone (AVB, n = 5), and avobenzone-Zn (AVB-Zn, n = 5). The *in vivo* antibacterial effect of each treatment was determined by measuring USA300-LAC colony forming units (CFUs) isolated from the wounds and mouse survival. Animals that showed signs of severe distress were euthanized. The schematic for the mouse model was created using BioRender.com. (B) Survival was assessed each day over the course of the experiment, and significance between treatment groups were compared using a log rank test for trend ($p = 0.0173$).

DISCUSSION

Through our proof-of-concept screen, we have demonstrated Zn is highly effective at inducing antibacterial activities in small molecules. Consideration of Zn within our screening protocol expanded the pool of identified hits by 3.1%, from 78 hits to 127 hits. This enabled the discovery that AVB, a UV-A filter with FDA-approval for use on the skin, is uniquely positioned to be repurposed as a Zn-activated antibiotic against MRSA. We found AVB requires submicromolar concentrations of Zn for activation and is equally effective at inhibiting multi-drug resistant MRSA isolates as a lab-adjusted MRSA strain *in vitro* when combined with Zn. Furthermore, AVB-Zn displayed minimal cytotoxic effects *in vitro* and was effective at preventing mortality when applied as a lotion in a mouse wound model of MRSA infection. This discovery from a small compound library emphasizes the largely unexplored potential of Zn-activated compounds as antibacterial agents.

Our discovery of AVB-Zn is not the first report to show Zn-activated compounds can have antibacterial activity. Bacitracin-Zn was described in 1945 [32] and was later shown to sequester and prevent the dephosphorylation of undecaprenol pyrophosphate (UPP) to undecaprenol phosphate (UP), a lipid carrier required for peptidoglycan synthesis [33, 44]. More recently, PBT2, a Zn ionophore antibiotic with an 8-hydroxyquinoline backbone, was shown to kill erythromycin-resistant group A *Streptococcus*, MRSA, and vancomycin-resistant *Enterococcus* and to reverse antibiotic resistance when combined with Zn [45]. However, our results indicate AVB-Zn operates using a different mechanism of action than the two compounds listed above. Clinical MRSA isolates with full resistance to bacitracin-Zn in our system were still susceptible to

inhibition by AVB-Zn. While it is unclear by which mechanism these isolates gained bacitracin-Zn resistance, the two known bacitracin resistance mechanisms in *S. aureus* are the *bacA* gene and the two-component system BceRS. The *bacA* gene confers resistance by encoding a UPP phosphatase that dephosphorylates UPP to UP [46-48] The second mechanism involves transport and sensing of bacitracin and other polypeptide antibiotics using the BceRS two-component system [49, 50] with homologous systems found in gram-positive bacteria like *Bacillus subtilis* and *Streptococcus mutans* [51, 52] Given that both systems are specific for either the activity or chemical structure of bacitracin, AVB-Zn is unlikely to inhibit *S. aureus* in the same manner as bacitracin. Furthermore, we found AVB-Zn requires submicromolar concentrations of Zn to inhibit *S. aureus*. This contrasts with PBT2, whose ionophore activity requires 400 – 600 μM Zn to cause Zn intoxication [45]. Because of this, we surmise the AVB-Zn complex itself possesses antibacterial activity that may have a single cell target separate from that of bacitracin. Future studies will be required to fully elucidate this mechanism.

Up to this point, antibiotic discovery efforts for metallodrugs have focused on Cu-compound complexes, as Cu by itself is a potent antibacterial agent [8, 9, 15], but their inherent toxicity to eukaryotic cells has hampered their development beyond the early research stage [19]. This study provides another avenue for metallodrug identification and development. Zn-dependent screening revealed AVB-Zn to be a potent antibiotic against MRSA that circumvents the challenge plaguing Cu-based antibiotics: toxicity. We demonstrated AVB, regardless of the metal complex being tested, possesses very little toxicity against both tumor and healthy donor human blood cells. Furthermore, AVB-Zn improved mouse survival in a MRSA wound infection model. Given that only a

small number of compounds were screened in this study, the ready identification of such a promising molecule bodes well for larger and more expensive screening efforts.

Unfortunately, drug screens that could capitalize on Zn-activated antibiotics are usually performed in a rich medium of no physiological relevance that only acts as a rich, nutritional resource to optimize bacterial growth rather than considering the metabolic requirements of the target organism in the human body. These media are not defined and do not consider physiologically relevant transition metal concentrations. It is established that variation between different media and even between lots of a single medium will affect drug discovery [53]. This variation is exemplified by MH broth where Zn concentrations can range between 0.2 – 1.3 μg/ml, the equivalent of 3 – 18 μM. These differences have biological and analytical consequences. Differences in Zn concentrations between commercial MH lots even affect the classification of the antimicrobial susceptibility of metallo-β-lactamase-harboring bacteria [53]. As most drug screening conditions used to explore the currently available chemical space do not consider the presence of physiologically relevant concentrations of Zn, our results suggest that re-exploration of available chemical compound libraries for antibacterial Zn-activated metallodrugs could be a promising avenue forward to overcome the current shortage of effective antibiotics.

ACKNOWLEDGEMENTS

Parts of this work were funded by R01AI121364 (OK, SHB, KE). RMA was funded in part by the AMC21 Scholarship from the UAB School of Medicine. We would also like to thank Dr. William Benjamin, Jr. (UAB) for supplying the clinical isolates

utilized in this study and Drs. Cameron L. Crawford and Melissa S. McDaniel (UAB) for their valuable insight.

REFERENCES

1. Murray CJL, Ikuta KS, Sharara F *et al.* Global burden of bacterial antimicrobial resistance in 2019: a systematic analysis. *The Lancet* 2022;**399**(10325):629-55. doi: https://doi.org/10.1016/S0140-6736(21)02724-0

2. Brown ED, Wright GD. Antibacterial drug discovery in the resistance era. *Nature* 2016;**529**(7586):336-43. doi: 10.1038/nature17042

3. Lewis K. Antibiotics: Recover the lost art of drug discovery. *Nature* 2012;**485**(7399):439-40. doi: 10.1038/485439a

4. Lewis K. Platforms for antibiotic discovery. *Nature Reviews Drug Discovery* 2013;**12**(5):371-87. doi: 10.1038/nrd3975

5. Silver LL. Challenges of antibacterial discovery. *Clin Microbiol Rev* 2011;**24**(1):71-109. doi: 10.1128/cmr.00030-10

6. Eskenazi A, Lood C, Wubbolts J *et al.* Combination of pre-adapted bacteriophage therapy and antibiotics for treatment of fracture-related infection due to pandrug-resistant Klebsiella pneumoniae. *Nat Commun* 2022;**13**(1):302. doi: 10.1038/s41467-021-27656-z

7. Gao W, Zhang L. Nanomaterials arising amid antibiotic resistance. *Nat Rev Microbiol* 2021;**19**(1):5-6. doi: 10.1038/s41579-020-00469-5

8. Dalecki AG, Crawford CL, Wolschendorf F. Chapter Six - Copper and Antibiotics: Discovery, Modes of Action, and Opportunities for Medicinal Applications. In: Poole RKs (ed). *Advances in Microbial Physiology*: Academic Press, 2017, 193-260

9. Lemire JA, Harrison JJ, Turner RJ. Antimicrobial activity of metals: mechanisms, molecular targets and applications. *Nature Reviews Microbiology* 2013;**11**(6):371-84. doi: 10.1038/nrmicro3028

10. Dalecki AG, Malalasekera AP, Schaaf K *et al.* Combinatorial phenotypic screen uncovers unrecognized family of extended thiourea inhibitors with copper-dependent anti-staphylococcal activity. *Metallomics* 2016;**8**(4):412-21. doi: 10.1039/c6mt00003g

11. Dalecki AG, Zorn KM, Clark AM *et al.* High-throughput screening and Bayesian machine learning for copper-dependent inhibitors of Staphylococcus aureus†. *Metallomics* 2019;**11**(3):696-706. doi: 10.1039/c8mt00342d

12. Dalecki Alex G, Haeili M, Shah S *et al.* Disulfiram and Copper Ions Kill Mycobacterium tuberculosis in a Synergistic Manner. *Antimicrobial Agents and Chemotherapy* 2015;**59**(8):4835-44. doi: 10.1128/AAC.00692-15

13. Crawford CL, Dalecki AG, Narmore WT *et al.* Pyrazolopyrimidinones, a novel class of copper-dependent bactericidal antibiotics against multi-drug resistant S. aureus†. *Metallomics* 2019;**11**(4):784-98. doi: 10.1039/c8mt00316e

14. Crawford CL, Dalecki AG, Perez MD *et al.* A copper-dependent compound restores ampicillin sensitivity in multidrug-resistant Staphylococcus aureus. *Scientific Reports* 2020;**10**(1):8955. doi: 10.1038/s41598-020-65978-y

15. Speer A, Shrestha TB, Bossmann SH *et al.* Copper-boosting compounds: a novel concept for antimycobacterial drug discovery. *Antimicrob Agents Chemother* 2013;**57**(2):1089-91. doi: 10.1128/aac.01781-12

16. Totten AH, Crawford CL, Dalecki AG *et al.* Differential Susceptibility of Mycoplasma and Ureaplasma Species to Compound-Enhanced Copper Toxicity. *Frontiers in Microbiology* 2019;**10**

17. Festa Richard A, Helsel Marian E, Franz Katherine J *et al.* Exploiting Innate Immune Cell Activation of a Copper-Dependent Antimicrobial Agent during Infection. *Chemistry & Biology* 2014;**21**(8):977-87. doi: https://doi.org/10.1016/j.chembiol.2014.06.009

18. Hood MI, Skaar EP. Nutritional immunity: transition metals at the pathogen–host interface. *Nature Reviews Microbiology* 2012;**10**(8):525-37. doi: 10.1038/nrmicro2836

19. Santini C, Pellei M, Gandin V *et al.* Advances in Copper Complexes as Anticancer Agents. *Chemical Reviews* 2014;**114**(1):815-62. doi: 10.1021/cr400135x

20. Cunha TA, Vermeulen-Serpa KM, Grilo EC *et al.* Association between zinc and body composition: An integrative review. *Journal of Trace Elements in Medicine and Biology* 2022;**71**:126940. doi: https://doi.org/10.1016/j.jtemb.2022.126940

21. Ong C-lY, Gillen CM, Barnett TC *et al.* An Antimicrobial Role for Zinc in Innate Immune Defense Against Group A Streptococcus. *The Journal of Infectious Diseases* 2014;**209**(10):1500-8. doi: 10.1093/infdis/jiu053

22. Ong C-lY, Walker MJ, McEwan AG. Zinc disrupts central carbon metabolism and capsule biosynthesis in *Streptococcus pyogenes*. *Scientific Reports* 2015;**5**:10799. doi: 10.1038/srep10799

23. Botella H, Peyron P, Levillain F *et al.* Mycobacterial P1-Type ATPases Mediate Resistance to Zinc Poisoning in Human Macrophages. *Cell Host & Microbe* 2011;**10**(3):248-59. doi: https://doi.org/10.1016/j.chom.2011.08.006

24. Wagner D, Maser J, Lai B *et al.* Elemental Analysis of *Mycobacterium avium*, *Mycobacterium tuberculosis*, and *Mycobacterium smegmatis*-Containing Phagosomes Indicates Pathogen-Induced Microenvironments within the Host Cell's Endosomal System. *The Journal of Immunology* 2005;**174**(3):1491

25. Ming LJ, Epperson JD. Metal binding and structure-activity relationship of the metalloantibiotic peptide bacitracin. *J Inorg Biochem* 2002;**91**(1):46-58. doi: 10.1016/s0162-0134(02)00464-6

26. Investigators HSGRH. Safety, tolerability, and efficacy of PBT2 in Huntington's disease: a phase 2, randomised, double-blind, placebo-controlled trial. *The Lancet Neurology* 2015;**14**(1):39-47. doi: https://doi.org/10.1016/S1474-4422(14)70262-5

27. Lannfelt L, Blennow K, Zetterberg H *et al.* Safety, efficacy, and biomarker findings of PBT2 in targeting Aβ as a modifying therapy for Alzheimer's disease: a phase IIa, double-blind, randomised, placebo-controlled trial. *The Lancet Neurology* 2008;**7**(9):779-86. doi: https://doi.org/10.1016/S1474-4422(08)70167-4

28. Brazel EB, Tan A, Neville SL *et al.* Dysregulation of Streptococcus pneumoniae zinc homeostasis breaks ampicillin resistance in a pneumonia infection model. *Cell Rep* 2022;**38**(2):110202. doi: 10.1016/j.celrep.2021.110202

29. De Oliveira DMP, Forde BM, Phan MD *et al.* Rescuing Tetracycline Class Antibiotics for the Treatment of Multidrug-Resistant Acinetobacter baumannii Pulmonary Infection. *mBio* 2022:e0351721. doi: 10.1128/mbio.03517-21

30. Brandenburg KS, Calderon DF, Kierski PR *et al.* Novel murine model for delayed wound healing using a biological wound dressing with Pseudomonas aeruginosa biofilms. *Microb Pathog* 2018;**122**:30-8. doi: 10.1016/j.micpath.2018.05.043

31. Maret W. The redox biology of redox-inert zinc ions. *Free Radical Biology and Medicine* 2019;**134**:311-26. doi: https://doi.org/10.1016/j.freeradbiomed.2019.01.006

32. Johnson BA, Anker H, Meleney FL. Bacitracin: A New Antibiotic Produced by a Member of the B. Subtilis Group. *Science* 1945;**102**(2650):376-7. doi: 10.1126/science.102.2650.376

33. Stone KJ, Strominger JL. Mechanism of Action of Bacitracin: Complexation with Metal Ion and C55-Isoprenyl Pyrophosphate. *Proceedings of the National Academy of Sciences* 1971;**68**(12):3223-7. doi: 10.1073/pnas.68.12.3223

34. Kockler J, Robertson S, Oelgemöller M *et al.* Chapter Three - Butyl Methoxy Dibenzoylmethane. In: Brittain HGs (ed). *Profiles of Drug Substances, Excipients and Related Methodology*: Academic Press, 2013, 87-111

35. Huang YH, Gladysz JA. Aldehyde and ketone ligands in organometallic complexes and catalysis. *Journal of Chemical Education* 1988;**65**(4):298. doi: 10.1021/ed065p298

36. Burlov AS, Vlasenko VG, Chal'tsev BV *et al.* Metal Complexes of Aroyl(acyl)benzoylhydrazones of Aromatic Aldehydes and Ketones: Coordination Modes and Properties. *Russian Journal of Coordination Chemistry* 2021;**47**(7):439-72. doi: 10.1134/S1070328421070010

37. Arnaud-Neu F, Collins EM, Deasy M *et al.* Synthesis, x-ray crystal structures, and cation-binding properties of alkyl calixaryl esters and ketones, a new family of

macrocyclic molecular receptors. *Journal of the American Chemical Society* 1989;**111**(23):8681-91. doi: 10.1021/ja00205a018

38. Gruet K, Crabtree RH, Lee D-H *et al.* Two-Point Cooperative Binding of Ketones by a Metal and by a Neighboring Pendant NH Group. *Organometallics* 2000;**19**(11):2228-32. doi: 10.1021/om000115b

39. Radford RJ, Lippard SJ. Chelators for investigating zinc metalloneurochemistry. *Curr Opin Chem Biol* 2013;**17**(2):129-36. doi: 10.1016/j.cbpa.2013.01.009

40. Crawford CL, Dalecki AG, Perez MD *et al.* A copper-dependent compound restores ampicillin sensitivity in multidrug-resistant Staphylococcus aureus. *Sci Rep* 2020;**10**(1):8955. doi: 10.1038/s41598-020-65978-y

41. Crawford CL, Dalecki AG, Narmore WT *et al.* Pyrazolopyrimidinones, a novel class of copper-dependent bactericidal antibiotics against multi-drug resistant S. aureus. *Metallomics* 2019;**11**(4):784-98. doi: 10.1039/c8mt00316e

42. Giroux EL, Durieux M, Schechter PJ. A study of zinc distribution in human serum. *Bioinorganic Chemistry* 1976;**5**(3):211-8. doi: https://doi.org/10.1016/S0006-3061(00)82019-0

43. Folin M, Contiero E, Maria Vaselli G. Zinc content of normal human serum and its correlation with some hematic parameters. *Biometals* 1994;**7**(1):75-9. doi: 10.1007/BF00205198

44. Ming L-J, Epperson JD. Metal binding and structure–activity relationship of the metalloantibiotic peptide bacitracin. *Journal of Inorganic Biochemistry* 2002;**91**(1):46-58. doi: https://doi.org/10.1016/S0162-0134(02)00464-6

45. Bohlmann L, De Oliveira DMP, El-Deeb IM *et al.* Chemical Synergy between Ionophore PBT2 and Zinc Reverses Antibiotic Resistance. *mBio* 2018;**9**(6). doi: 10.1128/mBio.02391-18

46. Chalker AF, Ingraham KA, Lunsford RD *et al.* The bacA gene, which determines bacitracin susceptibility in Streptococcus pneumoniae and Staphylococcus aureus, is also required for virulenceThe GenBank accession number for the sequence reported in this paper is AF228662. *Microbiology* 2000;**146**(7):1547-53. doi: https://doi.org/10.1099/00221287-146-7-1547

47. Cain BD, Norton PJ, Eubanks W *et al.* Amplification of the bacA gene confers bacitracin resistance to Escherichia coli. *Journal of Bacteriology* 1993;**175**(12):3784-9. doi: 10.1128/jb.175.12.3784-3789.1993

48. Ghachi ME, Bouhss A, Blanot D *et al.* The bacA Gene of Escherichia coli Encodes an Undecaprenyl Pyrophosphate Phosphatase Activity*. *Journal of Biological Chemistry* 2004;**279**(29):30106-13. doi: https://doi.org/10.1074/jbc.M401701200

49. Yoshida Y, Matsuo M, Oogai Y *et al.* Bacitracin sensing and resistance in Staphylococcus aureus. *FEMS Microbiology Letters* 2011;**320**(1):33-9. doi: 10.1111/j.1574-6968.2011.02291.x

50. Hiron A, Falord M, Valle J *et al.* Bacitracin and nisin resistance in Staphylococcus aureus: a novel pathway involving the BraS/BraR two-component system (SA2417/SA2418) and both the BraD/BraE and VraD/VraE ABC transporters. *Molecular Microbiology* 2011;**81**(3):602-22. doi: https://doi.org/10.1111/j.1365-2958.2011.07735.x

51. Ouyang J, Tian XL, Versey J *et al.* The BceABRS four-component system regulates the bacitracin-induced cell envelope stress response in Streptococcus mutans. *Antimicrob Agents Chemother* 2010;**54**(9):3895-906. doi: 10.1128/aac.01802-09

52. Bernard R, Guiseppi A, Chippaux M *et al.* Resistance to Bacitracin in Bacillus subtilis: Unexpected Requirement of the BceAB ABC Transporter in the Control of Expression of Its Own Structural Genes. *Journal of Bacteriology* 2007;**189**(23):8636-42. doi: 10.1128/JB.01132-07

53. Bilinskaya A, Buckheit Douglas J, Gnoinski M *et al.* Variability in Zinc Concentration among Mueller-Hinton Broth Brands: Impact on Antimicrobial Susceptibility Testing of Metallo-β-Lactamase-Producing Enterobacteriaceae. *Journal of Clinical Microbiology* 2020;**58**(12):e02019-20. doi: 10.1128/JCM.02019-20

MODULATING METALLO-ANTIBIOTIC ACTIVITY: A STRUCTURE ACTIVITY RELATIONSHIP STUDY

by

RACHEL M. ANDREWS, A. SOPHIA GIATTINA, FRANK WOLSCHENDORF, STEFAN H. BOSSMANN, AND OLAF KUTSCH

In preparation for *Metallomics*

Format adapted for dissertation

ABSTRACT

Antimicrobial resistance is increasing in prevalence among bacterial pathogens, reducing the number of effective treatments for bacterial infections, yet antibiotic development has stalled despite advancements in drug screening technology. Novel approaches to bacterial targeting strategies are sorely needed to counteract the growing threat of antimicrobial resistance. One avenue for development is metallo-antibiotics, or small molecules that become inhibitory in the presence of a transition metal. Previously, our lab uncovered copper-dependent inhibitors of *Mycobacterium tuberculosis* and *Staphylococcus aureus*, and using a Zn-dependent screening approach, we identified the avobenzone as potent Zn-dependent inhibitor of methicillin-resistant *S. aureus*. However, further development of metal-antibiotics will require potential lead structures to be readily optimized for desirable characteristics. Here, we perform a structure activity relationship study to demonstrate R-group modifications of two classes of privileged structures with documented metal-binding capability and antibacterial activity, the 8-hydroxyquinolines (8HQs) and the benzimidazoles (BZIs), result in differential metal-dependent antibacterial activity. We show the addition of halogens to the 8HQ core structure leads to induction of Zn-dependency at the exclusion of Cu dependency, indicating metal dependency can selected for through rational drug design. Furthermore, we show modifications to both the 8HQs and the BZIs can minimize the amount of metal required for activation. In total, our data reveals metallo-antibiotics across classes can be optimized using a combinatorial chemistry and therefore lays the foundation for further metallo-antibiotic development.

INTRODUCTION

Staphylococcus aureus is a serious human and animal pathogen capable of causing localized skin and soft tissue infections to more serious and debilitating infections, such as bloodstream infections, osteomyelitis, and toxic shock syndrome [1]. Treatment of *S. aureus* infections is complicated by the presence of methicillin-resistant strains (MRSA) that are resistant to β-lactam antibiotics, and multidrug resistant forms of MRSA are not uncommon in the clinic. In 2017 in the United States alone, MRSA caused over 300,000 hospitalized infections and resulted in over 10,000 deaths. The total cost of MRSA infections during this period is estimated to be $1.7 billion [2], and the World Health Organization documented an increasing prevalence of these difficult-to-treat strains among developing countries where healthcare may be limited [3].

The prevalence of antibiotic resistance has grown in recent decades, reducing our pharmaceutical arsenal available for the treatment of infectious diseases. Concurrently, antibiotic development has stalled due to a drought of novel antibiotic molecules identified by established drug screening methods, both modern and historical [4], and dwindling profits in the pharmaceutical industry [5-8]. In order to counteract the growing threat of antimicrobial resistance, new antibiotic molecules must be uncovered. Several ventures towards this end have been attempted. Nichols *et. al.* pioneered a new method to culture previously unculturable bacteria in their native environment [9] in an attempt to resurrect the Waksman platform, the premier method for antibiotic screening responsible for identifying most known antibiotics to date [4]. This method ultimately identified the promising and novel natural antibiotic teixobactin, a molecule against which resistance could not be generated [10, 11]. Other attempts include screening for molecules that

reduce bacterial virulence by inhibiting toxin export or biofilm formation [5], the development of antimicrobial nanoparticles [12], and phage therapy [13]. Despite these efforts, no new antibiotic therapy has been given FDA approval since the introduction of the antimycobacterial bedaquiline in 2010 [4].

Another avenue for antibiotic discovery is the burgeoning field of metallo-antibiotics. Metallo-antibiotics are small molecules that gain antibacterial activity in the presence of a transition metal. Most studies in this field focus on copper-dependent inhibitors (CDIs), molecules that become antibacterial when combined with copper (Cu), as Cu has long been known for its naturally occurring antibacterial actions [14]. This led to the discovery of the thiosemicarbazones (TSCs) [15-17] and pyrazolopyrimidinones (PZPs) as CDIs [18]. It has also been noted that certain 8-hydroxyquinolines (8HQ) possess metal-dependent antibacterial action [19, 20]. Recently, we discovered zinc (Zn) can also activate antibacterial activity in otherwise inactive small molecules similarly to Cu by screening a small library of bioactive molecules. From this screen, we identified avobenzone (AVB), a UV-A filter common in sunscreens [21], as possessing both Cu and Zn-dependent inhibitory activity against MRSA (in press). While AVB appears to be a promising candidate for drug repurposing, the combined metal-dependent activities of AVB may pose a challenge to its future development as both activities will need to be defined. This challenge is of broader consequence to metallo-antibiotics as a whole. For instance, the PZPs are also activated by transition metals other than just Cu [18]. Future development of metallo-antibiotics will thus be dependent on being able to modulate the metal dependencies of lead candidates.

Here, we perform a structure activity relationship study (SAR) of classes of privileged structures, or classes of molecules that are readily modified chemically, with documented metal-dependent antibiotic activity to determine if metal-dependency can be manipulated chemically. We show that two classes of privileged structures, the 8HQs and the benzimidazoles (BZIs), are differentially inhibitory against *S. aureus* in combination with various transition metals. We find metal specificity of both the 8HQs and the BZIs are R-group specific, and the metal concentration requirements for the Cu and Zn-dependent activation are modulated in an R-group specific manner. Furthermore, we show Zn dependency can be selected for at the exclusion of Cu dependency and therefore lay a foundation for the rational design of specifically Zn-activated metal-antibiotics.

METHODS

Bacterial strains and culture conditions.

The *S. aureus* strains LAC (FPR3757) and Newman were routinely cultured in the rich medium Mueller-Hinton (MH; Oxoid) broth. Strains were cultured at 37°C while shaking at 180 rpm for aeration and were transferred to the chemically defined medium 1x RPMI-1640 (Corning) for use in assays. Prior to transfer, cultures were washed twice in 1x RPMI-1640 to remove residual MH medium.

Compounds and Reagents.

All 8HQ and BZI analogs were purchased from Chembridge. Avobenzone analogs were either purchased from Chembridge or were synthesized by the Bossmann laboratory at Kansas State University. Compounds were reconstituted in 100% anhydrous

dimethyl sulfoxide (DMSO; Fisher Chemical) at a final concentration of 10 mM unless otherwise prevented due solubility issues. Reconstituted compounds were aliquoted and stored at -80°C for long-term storage. Metal and salt solutions were made by dissolving the salts in double-distilled water (ddH_2O), sterile filtered with 0.2 µm nylon filters (Fisher Scientific), aliquoted, and stored at 4°C. All metals and salts were purchased from Sigma. Metal stock solutions were stored as 100 mM aliquots in ddH_2O at 4°C following sterile filtration with 0.2 µm nylon filters.

Determination of minimal inhibitory concentration.

The minimal inhibitory concentration (MIC) of each chemical analog was tested using challenge assays as previously described [18, 22]. Briefly, *S. aureus* strains were cultured to mid-exponential phase in MH medium, which was determined by measuring the optical density at 600 nm (OD_{600}) of each starter culture. Cultures were normalized and treated at a standard OD_{600} of 0.005 in 1x RPMI-1640. Each strain was treated with compounds that were serially titrated 1:2 in the assay medium in 96-well flat-bottom plastic plates with or without either $CuSO_4$ or $ZnSO_4$. Depending on the assay, the metal concentrations fluctuated between 50 and 15 µM. Compound-untreated samples for each metal condition were used as negative controls. Cultures were treated for 18 – 20 hours at 37°C with 5% CO_2. Growth was determined by measuring the absorbance of each well at 600 nm (A_{600}) using a Biotek™ Cytation 3 plate reader following the treatment period. Readings were background subtracted and normalized to the compound untreated control for each metal condition. We defined the MIC as the lowest concentration which reduced bacterial growth or viability below 10% of the compound untreated control.

Dose Matrices.

Dose matrices were performed in a similar manner to the challenge assays. Strains, culturing methods, starting OD_{600}, and treatment media remain unchanged from the challenge assays. Compounds were serially titrated 1:2 against serial 1:2 titrations of either $CuSO_4$ or $ZnSO_4$ in flat-bottom 96-well plates. Compound concentrations started at 10 µM, while metal concentrations started between 50 µM and 30 µM depending on the experiment. Plates were incubated at 37°C + 5% CO_2 as described above. Relative growth was determined by measuring the A_{600} of each condition, performing background subtraction, and normalizing each condition to that of the untreated control.

RESULTS

Chemical modifications to the structure of AVB eliminate Zn-dependent antibacterial activity.

Previously, we identified AVB as a metallo-antibiotic with potent Zn-dependent inhibitory activity against MRSA (in press). Hypothesizing that Zn dependency can be tuned through chemical modifications for increased potency, we sought to perform a small-scale SAR of AVB analogs, both synthesized and chemically available (Figure 1A). To test this, we challenged the characterized MRSA strain LAC with serial titrations of analog in the presence and absence of a single sub-inhibitory concentration of Zn in the chemically defined medium 1x RPMI-1640 as previously described [18]. Bacterial growth was measured after a 20-hour treatment period, with A_{600} used a surrogate metric of growth, and growth under each condition was normalized as a percent of the analog-untreated control. The minimal inhibitory concentration (MIC) was defined as the lowest

analog concentration that reduced LAC growth by 90%, and the MICs for each concentration were compared to those of the original compound, AVB.

As with AVB, none of the analogs were inhibitory in the absence of Zn (Figure 1B). Because of this, we conclude the core region of AVB composed of the two benzene rings is not innately inhibitory against *S. aureus*. Interestingly, all modifications to AVB resulted in reduced potency of the Zn-dependent action (Figure 1C). All analogs with the exception of AVB-1 lost all Zn-dependency against MRSA within the concentrations tested, and the Zn-dependent activity of AVB-1 was reduced 16-fold relative to AVB. AVB-1 and AVB-3 most closely resemble the original structure. For AVB-1, the trimethyl group is replaced with a hydrogen atom, while the ether group of AVB is replaced with a chlorine atom in in AVB-3. This indicates that loss of either R-group results in reduced potency. Addition of lager, bulkier, or more charged species, as is the case in the remaining analogs, is also detrimental to potency. Ultimately, this may indicate the antibacterial action of Zn- activated AVB (AVB-Zn) is not readily optimized through combinatorial chemistry.

Figure 1

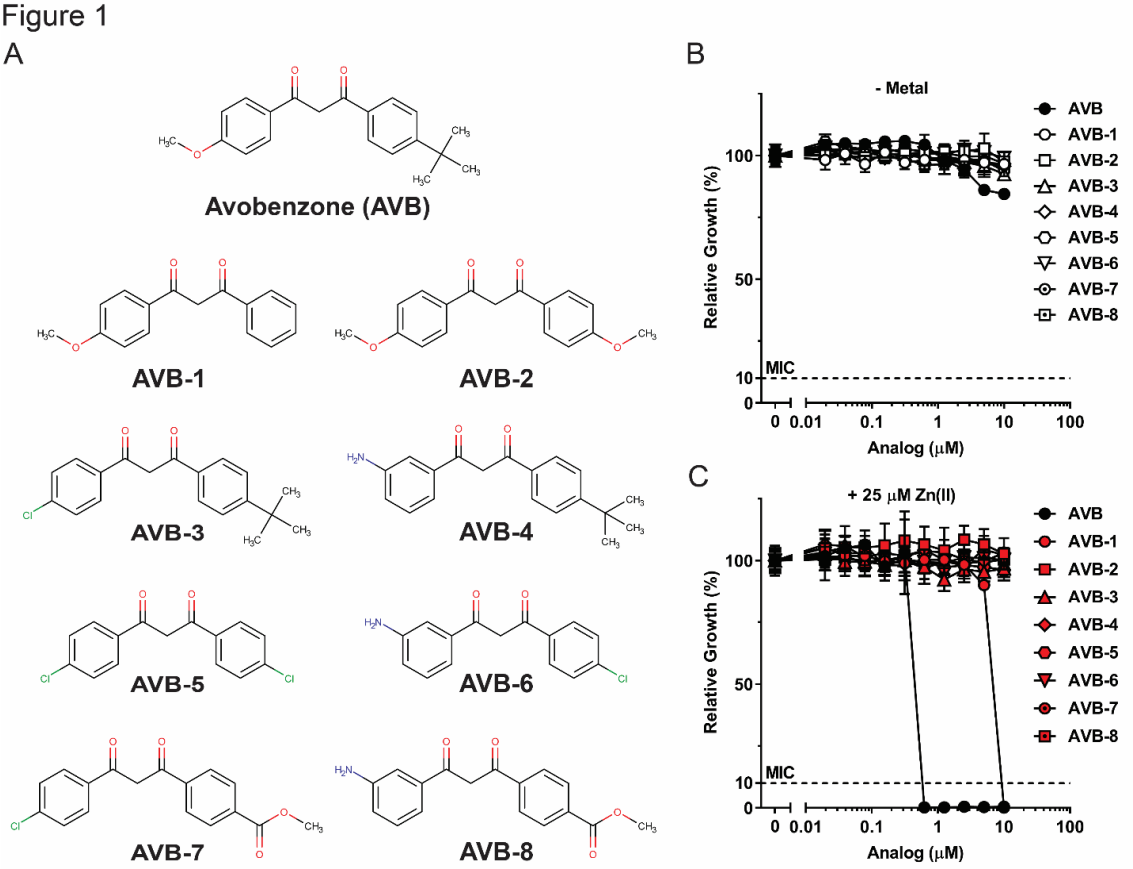

Figure 1 Chemical modifications to avobenzone abolish the zinc-activation of avobenzone.

(A) The two-dimensional structures of avobenzone (AVB) and the AVB derivatives used in this study. Structures were drawn using MarvinSketch by ChemAxon. *S. aureus* LAC was treated with serial titrations of AVB and the AVB derivatives in without a metal (B) and with 25 μM Zn(II) (C) for 20 hours at 37°C. A_{600} readings were used as a marker of cells growth were normalized as a percent of the untreated control for each metal condition. Data represent the mean ± SD (n = 1 biological replicate with 3 technical replicates).

8HQ metal specificity is dependent on R-group modifications.

While we were unable to modify the Zn-dependent action of AVB, other structural backbones with metal-dependent antimicrobial activities may be more amenable to optimization. To test this, we selected a class of privileged structures with known metal-dependent antibacterial or metal-binding capabilities, the 8HQs [23], and assembled a small panel of compounds with an 8HQ backbone (Figure 2A). We chose specific compounds for the 8HQ panel to have a variety of types of R-groups. These include bulky R-groups (broxaldine, BXA), a variety of halogenated analogs (broxyquinoline, BQ; clioquinol, CIQ; and chlorquinaldol, CQ), and nitrogenous R-groups, both neutral (5-amino-8HQ, 5A8HQ) and charged (5-nitro-8HQ, 5N8HQ). We then challenged *S. aureus* with each compound with and without sub-inhibitory concentrations of various transition metals to determine the activity of the compounds with each metal.

Figure 2

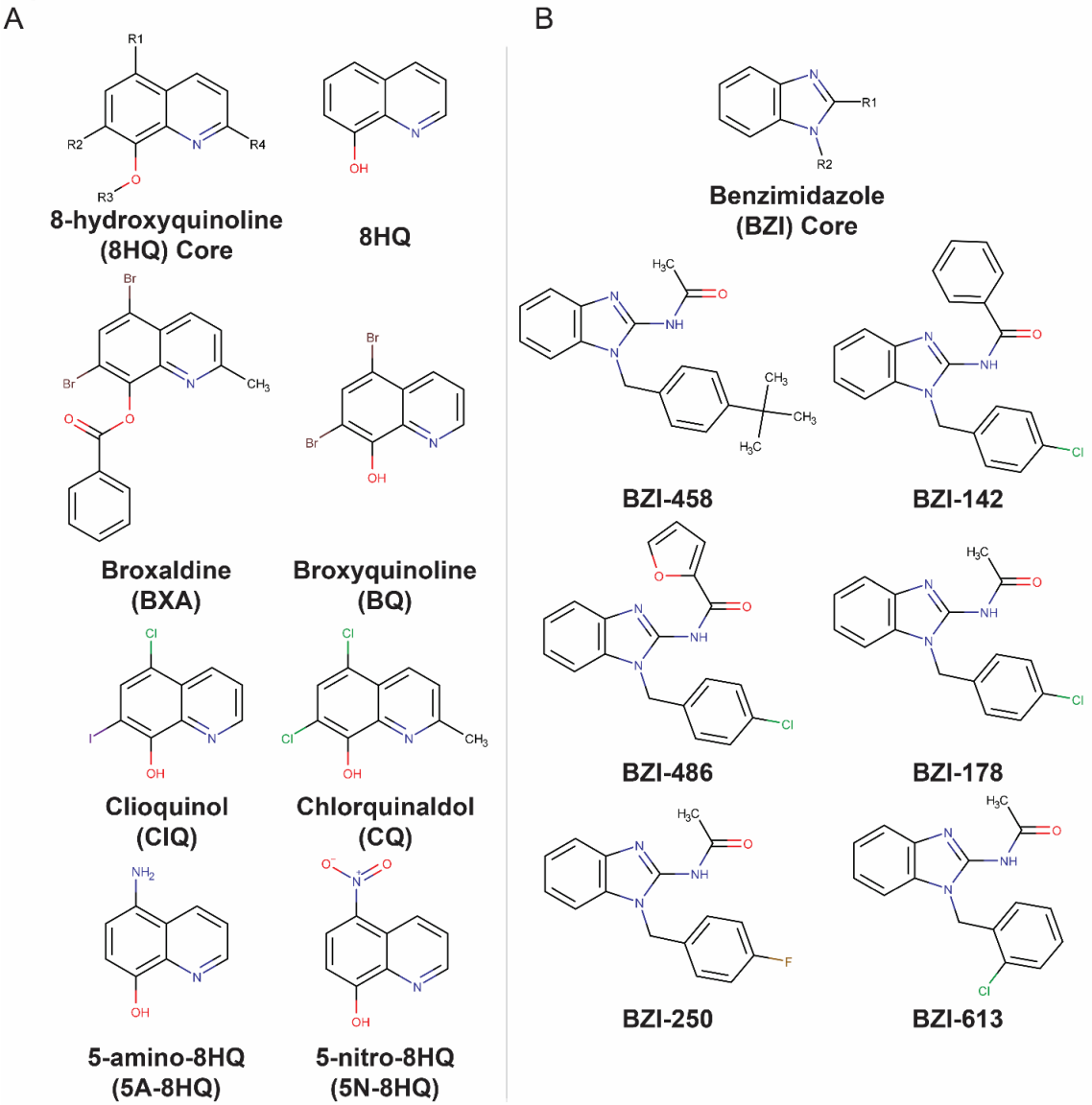

Figure 2 Chemical structures included in the 8-hydroxyquinoline and benzimidazole panels.

The structures depicted in (A) represent the core motif and derivatives of the 8-hydroxyquinoline (8HQ) panel, and (B) represents the core benzimidazole (BZI) motif and the analogs included in the panel. All structures were drawn using MarvinSketch provided by ChemAxon.

Focusing on the 8HQ panel, we challenged LAC with serial titrations of all seven 8HQ compounds individually with and without Cu or Zn. Previously, 8HQ was determined to be a CDI of *Mycobacterium tuberculosis* with no other metal-dependent activity [19]. In keeping with this, we found 8HQ was only inhibitory against *S. aureus* in the presence of Cu (Figure 3A). Interestingly, 8HQ is the only compound in the panel with this pattern of activity. The most potent activity BQ, BXA, CIQ, and CQ (Figure 3B-E) is Zn-dependent, with MICs ranging from 0.16 – 0.31 (μM) with 15 μM Zn. Other than 8HQ, only BXA displays Cu dependency. Meanwhile, 5A-8HQ (Figure 3F) only possesses metal-independent inhibitory activity against *S. aureus*. Lastly, 5N-8HQ (Figure 3G), the only 8HQ molecule with a charged R-group, is inactive against *S. aureus*. These results suggest, contrary to past evidence, that the 8HQ class is more broadly inhibitory with Zn rather than with Cu.

Figure 3

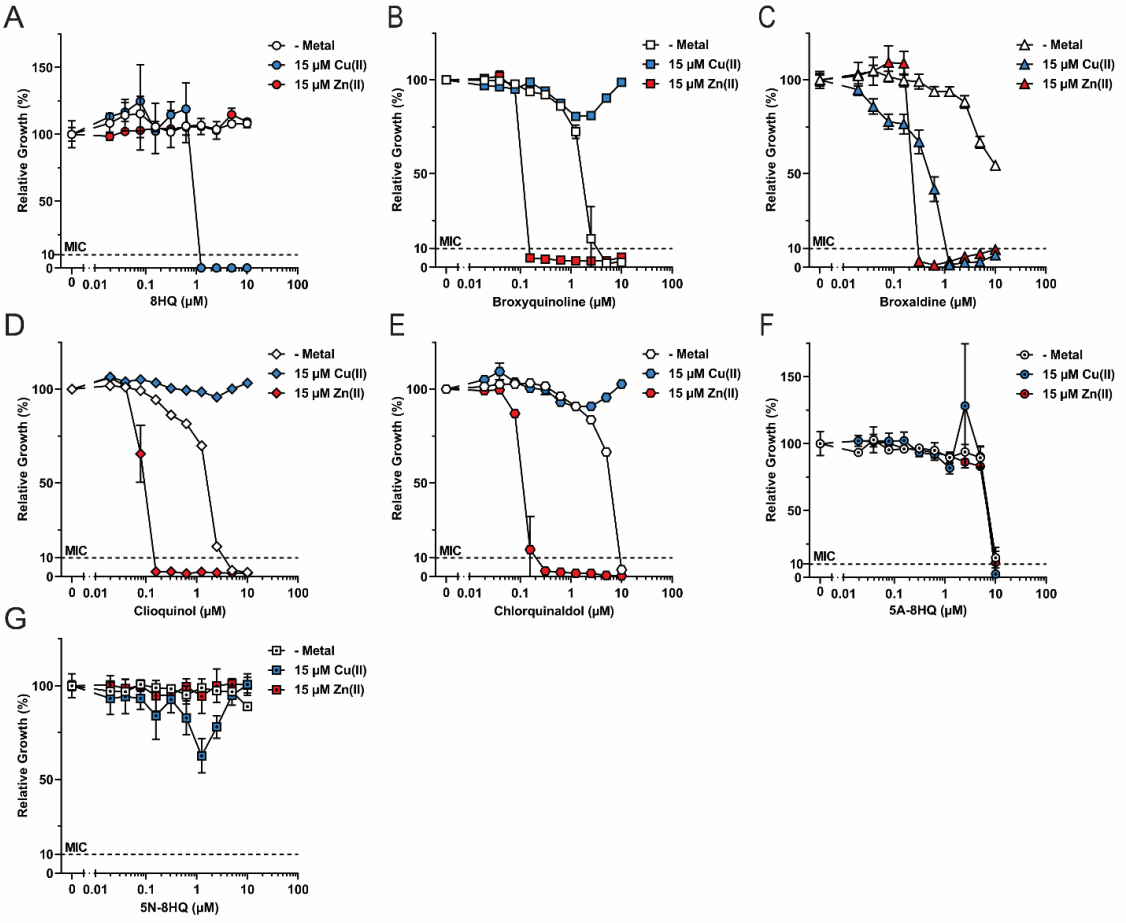

Figure 3 Modifications to the 8-hydroxyquinoline core cause shifts in metal specificity.

S. aureus LAC was exposed to serial titrations of 8-hydroxyquinoline (8HQ) (A), broxyquinoline (B), broxaldine (C) clioquinol (D), chlorquinaldol (E), 5-amino-8HQ (5A-8HQ) (F), and 5-nitro-8HQ (5N-8HQ) (G) in the presence and absence of Cu(II) and Zn(II). Growth was measured after a 20-hour incubation period at 37°C through A600 measurements, and readings were normalized to the untreated control of each metal condition. The minimal inhibitory concentration was defined as the lowest concentration of compound that inhibited the growth of *S. aureus* to at least 10% of the untreated control. The data represent the mean ± SD (n = 1 biological replicate with 3 technical replicates).

It is interesting that just the addition of two halogens off the fifth and seventh carbons of the 8HQ skeleton, as with BQ and CIQ, is sufficient to abolish the Cu dependency displayed by 8HQ and shift the molecules towards Zn dependency. The addition of a hydrophobic group off the first carbon does not appear to alter the activity of these halogenated analogs, nor does the exact type of halogen appear to be of consequence. Rather, the mere presence of a halogen is all that is required to show Zn dependency. Interestingly, BXA, which possesses two bromine atoms and a third bulky side group, exhibits Zn dependency but is unique for also showing Cu dependency. We hypothesize the larger aromatic side chain may be responsible for restoring Cu dependency. Meanwhile the two analogs with nitrogenous R-groups, 5A-8HQ and 5N-8HQ, both lost metal dependency. Nitrogenous R-groups may therefore interfere with metal dependency at this site, though the exact mechanism is unclear. It is also possible the added charge to 5N-8HQ relative to 8HQ results in reduced permeability across the bacterial cell membrane. Regardless, the range of inhibitory activities displayed by the 8HQ compound panel indicates alteration of specific R-groups can lead to variations in both metal dependency and potency. Importantly, this can be done at the exclusion of a metal such that a metallo-antibiotic could be rationally designed to be specific for a given transition metal.

R-group modifications of 8HQs modulate Zn requirements for Zn activation.

Once we established R-group modifications can alter metal specificity, we sought determine whether metallo-antibiotics could be engineered for minimal metal requirements. To do so, we focused on the potent Zn-dependent actions of the four

halogenated 8HQ analogs: BQ, BXA, CIQ, and CQ. We performed dose matrices where a given analog was serially titrated against serial titrations of Zn to determine the minimum concentration of Zn required for inhibition of LAC. LAC was treated with each condition overnight, and relative growth was determined by normalizing A_{600} readings as a percent of the untreated control (Figure 4). Here we found that regardless of analog, inhibition was dose-dependent on both analog and Zn concentrations, suggesting a potential binding interaction. Here we found BQ and CIQ, the most closely related molecules, were nearly identical (Figure 4A, C). Both compounds required as little as 0.31 μM Zn, far less than serum concentrations of Zn, to show clear Zn dependency, and the potency of the analog increased as the Zn concentration increased.

Figure 4

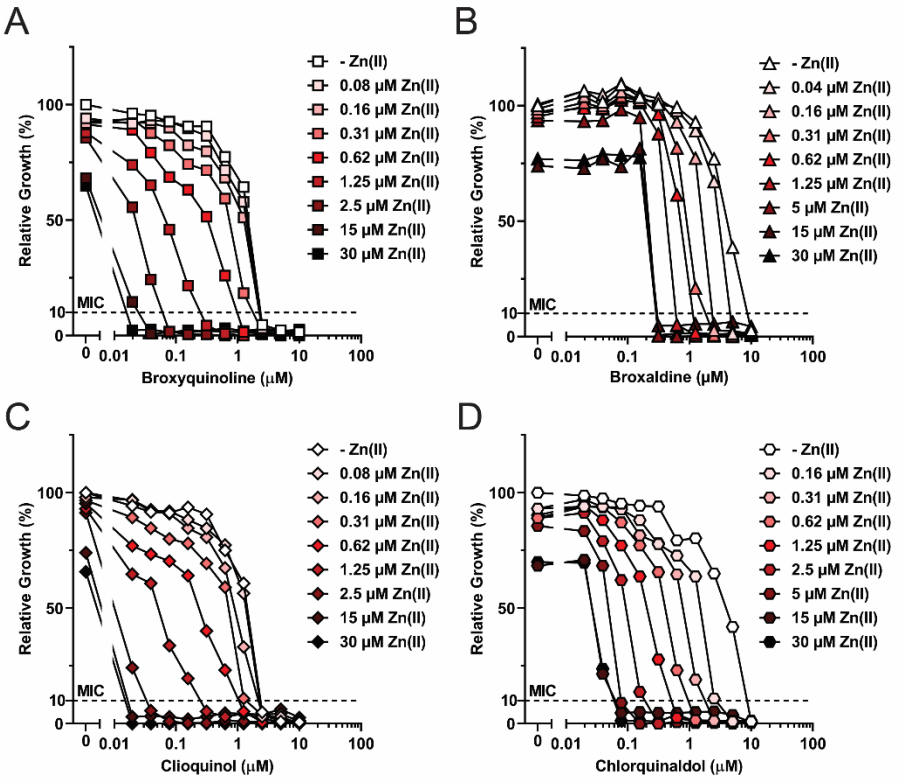

Figure 4 Modifications to the 8-hydroxyquinoline core motif alters the minimum zinc concentration required for activation.

Dose matrices of each compound was performed by serially titrating a compound against serial titrations of Zn(II). *S. aureus* LAC was incubated with each condition for 20 hours at 37°C before A_{600} growth measurements were taken and normalized to the untreated control. Dose matrices are shown for broxyquinoline (A), broxaldine (B), clioquinol (C), and chlorquinaldol (D). Data represents a single biological replicate for each dose matrix.

Additional R-groups outside the 5’ and 7’ halogens appear to have a small effect on the Zn concentration required for Zn-dependent inhibition of *S. aureus*. Both BXA and CQ require less than 100 nM Zn to become more inhibitory than the metal-dependent action of each compound. However, the bulkier BXA has a more limited range of Zn concentrations that affect its potency relative to CQ. Larger R-groups may therefore also alter the range of Zn concentrations resulting in changes in inhibition potency. This is further supported by the broader range of effective Zn concentrations with CQ, though future studies will be required to determine the extent to which R-group size affects Zn requirements. In total, we find members of the 8HQ class of molecules possess differential metal-dependent antibiotic activity and vary in metal requirements needed to become inhibitory against *S. aureus*, demonstrating metallo-antibiotics can be tuned for certain metal specificities and requirements through combinatorial chemistry.

BZI metal specificity is altered by R-groups modifications.

While the 8HQs are modifiable metallo-antibiotics, the same may not be true for other classes of metallo-antibiotics. A previous Cu-dependent screening effort undertaken by our laboratory identified a number of compound clusters with Cu-dependent anti-staphylococcal activity [24]. One of these hit clusters was the BZIs. Like the 8HQs, BZIs are privileged structures and are therefore common structures found in screening libraries [25]. BZIs are also known for binding transition metals [26]. Because of this, we chose to perform another small-scale SAR using the BZI core structure to determine if tuning of metal-antibiotic activity is more broadly applicable across structural classes. The compounds composing the BZI panel were chosen based on a hit compound identified

from our previous screen [24], which we have termed BZI-458. The remaining BZIs were chosen for their aromatic or halogenated R-groups (Figure 2B).

First, we determined the metal specificity of each BZI compound by performing challenge assays against the lab-adjusted *S. aureus* strain Newman with and without various *d*-block transition metals and determining the MIC each BZI compound under each metal condition. The resultant dose-response curves (Figure 5) show each BZI has different inhibitory activity with each metal. None of the BZIs are inhibitory in the absence of a transition metal, and no BZI reduces the growth of *S. aureus* by at least 90% when combined with manganese (Mn). This is not surprising as Mn has the lowest affinity metal binding moieties based on the Irving-Williams Series (Mn < Fe < Co < Ni << Cu > Zn), which describes relative affinity for metal-binding motifs by divalent *d*-block transition metals [27]. The MICs of the BZI panel with each metal condition is shown in Table 1.

Figure 5

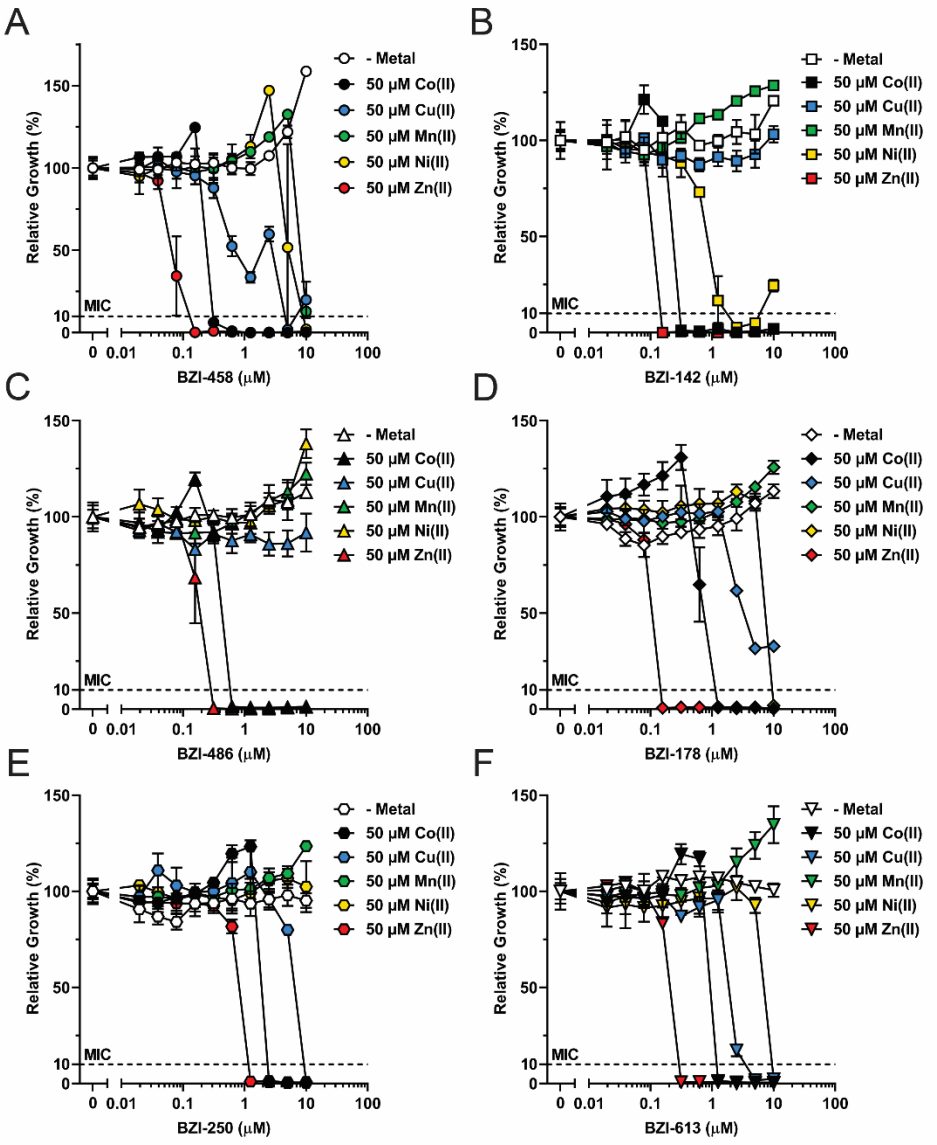

Figure 5 Modifications to the benzimidazole core structure cause shifts in metal specificity.

S. aureus Newman was incubated with serial titrations of BZI-458 (A), BZI-142 (B), BZI-486 (C) BZI-178 (D), BZI-250 (E), and BZI-613 (F) in the presence and absence of the following transition metals: Co(II), Cu(II), Mn(II), Ni(II) and Zn(II). Growth was measured after 20 hours by measuring the A_{600} of each conditions, and readings were normalized to the untreated control of each metal condition. The minimal inhibitory concentration was defined as the lowest concentration of compound that inhibited the growth of *S. aureus* to at least 10% of the untreated control. The data represent the mean ± SD (n = 1 biological replicate with 3 technical replicates).

	MIC (μM)					
Analog	**- Metal**	**Co(II)**	**Cu(II)**	**Mn(II)**	**Ni(II)**	**Zn(II)**
BZI-458	> 10	**0.31**	5	> 10	10	**0.16**
BZI-142	> 10	**0.31**	> 10	> 10	**2.5**	**0.16**
BZI-486	> 10	0.62	> 10	> 10	> 10	0.31
BZI-178	> 10	1.25	> 10	> 10	10	**0.16**
BZI-250	> 10	1.25	10	> 10	> 10	1.25
BZI-613	> 10	1.25	5	> 10	10	0.31

Table 1 The minimal inhibitory concentrations of the benzimidazoles under each metal condition against Newman.
The minimal inhibitory concentration (MIC) is the lowest compound concentration that inhibited the growth of *S. aureus* by at least 90%. Data represents the dose-response curves shown in Figure 5. The values in bold represent the lowest MIC for that metal condition.

Despite being initially identified as CDIs of *S. aureus*, the most potent anti-staphylococcal action for all six BZIs was the Zn-dependent action, and only four of the six BZIs displayed Cu-dependency (Figure 5). All BZIs were inhibitory in the presence of cobalt (Co), though this was always secondary in strength to the Zn-dependent action. Lastly, four of the six BZIs were inhibitory with nickel (Ni), specifically BZI-458, BZI-250, BZI-178, and BZI-613. Importantly, small alterations to the core BZI structure results in BZIs with varying metal dependencies, as is seen with the 8HQs. Additionally, BZIs with an aromatic R1-group lose Cu dependency, again indicating rational drug design could potentially exclude unwanted metal dependencies.

We next performed dose matrices of each BZI serially titrated against either Cu or Zn against Newman to determine the range of metal concentrations resulting in altered BZI potency. BZIs with Cu dependency were titrated against both Cu and Zn, while BZIs that did not inhibit the growth of *S. aureus* with Cu were only titrated against Zn. As expected of metal-binding compounds, the BZIs showed dose-dependence on both the analog and titrated metal. Apart from BZI-458, all the Cu-dependent BZI analogs required 20 µM Cu or more to inhibit *S. aureus* growth. BZI-458 required at least 10 µM Cu (Figure 6A, C, E, G). In contrast, these same analogs only required 0.31 – 1.25 µM Zn for minimum activity (Figure 6B, D, F, H), potentially suggesting a higher binding affinity for Zn over Cu. Generally, the dose matrices for each BZI are reminiscent of each other. The exception is BZI-250, which required more Cu and more Zn to become inhibitory. Additionally, BZI-250 has the largest MIC with Cu and with Zn compared to the remaining BZIs. This is also the only fluorinated BZI, which could indicate the addition of fluorine may interfere with metal binding or inhibitory potential.

Figure 6

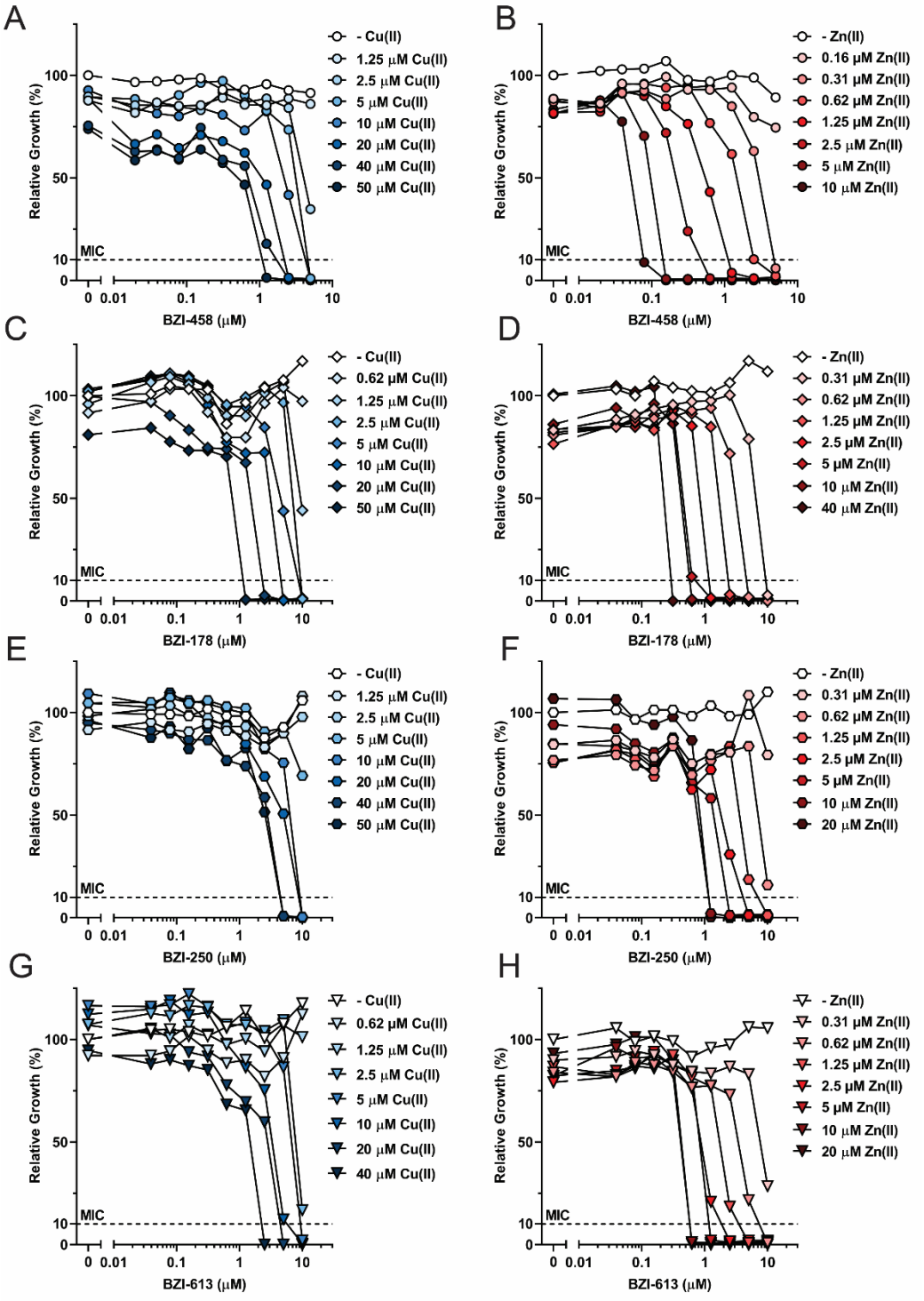
A
- Cu(II)
1.25 μM Cu(II)
2.5 μM Cu(II)
5 μM Cu(II)
10 μM Cu(II)
20 μM Cu(II)
40 μM Cu(II)
50 μM Cu(II)
Relative Growth (%)
MIC
BZI-458 (μM)
B
- Zn(II)
0.16 μM Zn(II)
0.31 μM Zn(II)
0.62 μM Zn(II)
1.25 μM Zn(II)
2.5 μM Zn(II)
5 μM Zn(II)
10 μM Zn(II)
Relative Growth (%)
MIC
BZI-458 (μM)
C
- Cu(II)
0.62 μM Cu(II)
1.25 μM Cu(II)
2.5 μM Cu(II)
5 μM Cu(II)
10 μM Cu(II)
20 μM Cu(II)
50 μM Cu(II)
Relative Growth (%)
MIC
BZI-178 (μM)
D
- Zn(II)
0.31 μM Zn(II)
0.62 μM Zn(II)
1.25 μM Zn(II)
2.5 μM Zn(II)
5 μM Zn(II)
10 μM Zn(II)
40 μM Zn(II)
Relative Growth (%)
MIC
BZI-178 (μM)
E
- Cu(II)
1.25 μM Cu(II)
2.5 μM Cu(II)
5 μM Cu(II)
10 μM Cu(II)
20 μM Cu(II)
40 μM Cu(II)
50 μM Cu(II)
Relative Growth (%)
MIC
BZI-250 (μM)
F
- Zn(II)
0.31 μM Zn(II)
0.62 μM Zn(II)
1.25 μM Zn(II)
2.5 μM Zn(II)
5 μM Zn(II)
10 μM Zn(II)
20 μM Zn(II)
Relative Growth (%)
MIC
BZI-250 (μM)
G
- Cu(II)
0.62 μM Cu(II)
1.25 μM Cu(II)
2.5 μM Cu(II)
5 μM Cu(II)
10 μM Cu(II)
20 μM Cu(II)
40 μM Cu(II)
Relative Growth (%)
MIC
BZI-613 (μM)
H
- Zn(II)
0.31 μM Zn(II)
0.62 μM Zn(II)
1.25 μM Zn(II)
2.5 μM Zn(II)
5 μM Zn(II)
10 μM Zn(II)
20 μM Zn(II)
Relative Growth (%)
MIC
BZI-613 (μM)

Figure 6 Minimal metal requirements of benzimidazoles with copper and zinc dependency.
Copper dose matrices of BZI-458 (A), BZI-178 (C), BZI-250 (E), and BZI-613 (G) and zinc dose matrices of BZI-458 (B), BZI-178 (D), BZI-250 (F), and BZI-613 (H) were performed against *S. aureus* Newman. Growth was measured after 20 hours of incubation at 37°C using A_{600} measurements. Growth was normalized as a percentage of the untreated control for each dose matrix. Data represents a single biological replicate.

Meanwhile, the two BZIs without Cu dependency, BZI-142 and BZI-486, greatly differ the amount of Zn required to cause antibacterial activation (Figure 7). BZI-142 only required 0.62 µM Zn for activation and was fully active (MIC = 0.31 µM) with just 10 µM Zn (Table 2). In contrast, BZI-486 needed at least 20 µM Zn for activation and at a 32-fold higher MIC than when incubated with 50 µM Zn, as in the challenge assays. BZI-142 and BZI-486 are identical molecules except for the ring structures incorporated in the R1-group. BZI-142 incorporates a phenyl group, while BZI-486 includes an oxazole ring structure. Intriguingly, oxazoles are known Zn-binding motifs [28, 29], yet the dose matrix of BZI-486 and Zn suggests lower Zn affinity compared to BZIs without an oxazole structure. Given this, we hypothesize this phenomenon could be due a change in Zn coordination geometry compared to compound-Zn complexes with the other BZIs in our panel, though further binding studies and complex structures will need to be determined to fully conclude this. In any case, the simple change in ring structure drastically altered the Zn requirements between two otherwise identical compounds, confirming metal requirements can be modulated across multiple compound classes.

Figure 7

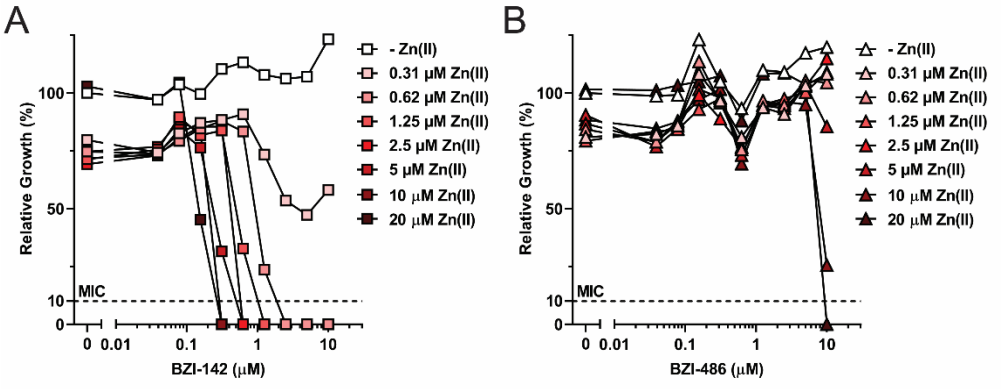

Figure 7 Minimal zinc requirements of benzimidazoles without copper dependency. BZI-142 (A) and BZI-486 (B) were serially titrated against serial titrations of Zn(II). *S. aureus* Newman was treated with each condition for 20 hours at 37°C. Relative growth was determined by measuring the A_{600} of each condition, and background subtracted values were normalized as a percentage of the untreated control for each compound. Data represents one biological replicate.

Analog	$MIC_{Cu(II)}$ (μM)	[Cu(II)] (μM)	$MIC_{Zn(II)}$ (μM)	[Zn(II)] (μM)
BZI-458	1.25	50	0.08	10
BZI-142	-	-	0.31	10
BZI-486	-	-	10	20
BZI-178	1.25	50	0.31	40
BZI-250	5	40	1.25	10
BZI-613	2.5	40	0.62	10

Table 2 Metal requirements for benzimidazole potency against *S. aureus* Newman. This table represents the most potent minimal inhibitory concentration (MIC) of each benzimidazole derivative with copper and with zinc based on the copper and zinc dose matrices in Figure 6 and Figure 7. The metal concentrations listed are the lowest metal concentration required to reach the listed MIC. Values are of a single biological replicate.

DISCUSSION

By performing two targeted SARs, we have demonstrated metallo-antibiotics have the potential for rational design. Though AVB is not a strong candidate for optimization using combinatorial chemistry, two different classes of privileged structures with metal-dependent anti-staphylococcal activity, 8HQs and BZIs, can be modulated and optimized for specific desired features. Derivatives of both the 8HQs and BZIs display differential metal dependency that are specific to a given R-group, such that halogenated 8HQ derivatives abolish Cu-dependent inhibition of *S. aureus* and instead display Zn-dependency. Similarly, R-group modifications can shift the metal specificities of certain BZIs. We also find R-group modifications of either class modify the quantity of metal required for inhibition. Of greatest import, the 8HQs and BZIs can be structurally modified to exclude a specific metal activity, a feature that will be necessary for future metal-antibiotic development.

It is promising that simple modifications to the 8HQ and BZI backbone result in noticeable differences in metal specificity. Halogens in particular appear to be beneficial for antibacterial Zn activation, though the reason for this is unclear. Previous reports indicate that halogens can form halogen bonds with target biomolecules in a similar manner to hydrogen bonding and that these follow an order of bonding likelihood defined by their polarizability [30]. Iodine forms the strongest interaction and is of similar strength to a hydrogen bond. Iodine is followed by bromine then chlorine and finally fluorine [30], with fluorine bonds being possible [31] though comparably rare [30]. The consequence of this binding is increased target affinity [32], and as such, halogen bonding is feature considered in rational drug design [33, 34]. The halogenated 8HQ

follow the pattern of halogen bonding strength, where CIQ, the only 8HQ tested with an iodine atom, and the di-brominated BXA and BQ have the strongest Zn-activated antibacterial action compared CQ. Interestingly, we also note the fluorinated BZI derivative, BZI-250, is the least potent of the BZIs that display Cu and Zn activation. Given the improved potency of the halogenated 8HQ derivatives, this may suggest Zn-activated 8HQs inhibit *S. aureus* by binding to a single target. However, this in contrast to reports showing CIQ [35, 36] and PBT2 [37-40], another 8HQ derivative, are metal ionophores. PBT2 was recently shown to inhibit *S. aureus*, Group A *Streptococcus*, and *Enterococcus* by inducing Zn intoxication [39, 41]. Mechanistic studies will therefore be required to determine the mechanism of action of the Zn-activated halogenated 8HQs in our experimental system.

The primary limitation of this study is that it is preliminary. We utilize two miniaturized SARs, which have allowed us to begin hypothesizing as to which modification will result in a given activity, but a larger, targeted SAR focused on hypothesis-driven modifications will be required to address this particular question. This SAR should also be expanded to include a wider array of desirable features for a metallo-antibiotic to better illustrate the consequences of structural modifications. These features could include reduced toxicity to eukaryotic cells, inhibition of multiple bacterial species, improved cell permeability, and induction inhibition with a single transition metal. Despite these limitations, this study lays the groundwork for systematic optimization of metallo-antibiotics furthers metallo-antibiotic development.

ACKNOWLEDGEMENTS

Parts of this work were funded by R01AI121364 (OK, SHB). RMA was by the AMC21 Scholarship from the UAB School of Medicine. We would like to thank Drs. Cameron L. Crawford, Alex G. Dalecki, Alexandra Duverger, and Ashley Landuyt and Frederic Wagner (UAB) for their scientific training, advice, and endless encouragement.

REFERENCES

1. Lee AS, de Lencastre H, Garau J *et al.* Methicillin-resistant Staphylococcus aureus. *Nature Reviews Disease Primers* 2018;**4**(1):18033. doi: 10.1038/nrdp.2018.33

2. Antibiotic resistance threats in the United States, 2019. 2019

3. Global antimicrobial resistance and use surveillance system (GLASS) report. *Geneva: World Health Orgnaization* 2021

4. Lewis K. Platforms for antibiotic discovery. *Nature Reviews Drug Discovery* 2013;**12**(5):371-87. doi: 10.1038/nrd3975

5. Cook MA, Wright GD. The past, present, and future of antibiotics. *Science Translational Medicine* 2022;**14**(657):eabo7793. doi: 10.1126/scitranslmed.abo7793

6. Bush K. Antibacterial drug discovery in the 21st century. *Clinical Microbiology and Infection* 2004;**10**:10-7. doi: https://doi.org/10.1111/j.1465-0691.2004.1005.x

7. Nathan C. Antibiotics at the crossroads. *Nature* 2004;**431**(7011):899-902. doi: 10.1038/431899a

8. Projan SJ. Why is big Pharma getting out of antibacterial drug discovery? *Current Opinion in Microbiology* 2003;**6**(5):427-30. doi: https://doi.org/10.1016/j.mib.2003.08.003

9. Nichols D, Cahoon N, Trakhtenberg EM *et al.* Use of Ichip for High-Throughput In Situ Cultivation of "Uncultivable" Microbial Species. *Applied and Environmental Microbiology* 2010;**76**(8):2445-50. doi: 10.1128/AEM.01754-09

10. Ling LL, Schneider T, Peoples AJ *et al.* A new antibiotic kills pathogens without detectable resistance. *Nature* 2015;**517**(7535):455-9. doi: 10.1038/nature14098

11. Shukla R, Lavore F, Maity S *et al.* Teixobactin kills bacteria by a two-pronged attack on the cell envelope. *Nature* 2022;**608**(7922):390-6. doi: 10.1038/s41586-022-05019-y

12. Lee N-Y, Ko W-C, Hsueh P-R. Nanoparticles in the Treatment of Infections Caused by Multidrug-Resistant Organisms. *Frontiers in Pharmacology* 2019;**10**

13. Brives C, Pourraz J. Phage therapy as a potential solution in the fight against AMR: obstacles and possible futures. *Palgrave Communications* 2020;**6**(1):100. doi: 10.1057/s41599-020-0478-4

14. Dalecki AG, Crawford CL, Wolschendorf F. Chapter Six - Copper and Antibiotics: Discovery, Modes of Action, and Opportunities for Medicinal Applications. In: Poole RKs (ed). *Advances in Microbial Physiology*: Academic Press, 2017, 193-260

15. Djoko Karrera Y, Goytia Maira M, Donnelly Paul S *et al.* Copper(II)-Bis(Thiosemicarbazonato) Complexes as Antibacterial Agents: Insights into Their Mode of Action and Potential as Therapeutics. *Antimicrobial Agents and Chemotherapy* 2015;**59**(10):6444-53. doi: 10.1128/AAC.01289-15

16. Djoko KY, Paterson BM, Donnelly PS *et al.* Antimicrobial effects of copper(ii) bis(thiosemicarbazonato) complexes provide new insight into their biochemical mode of action†. *Metallomics* 2014;**6**(4):854-63. doi: 10.1039/c3mt00348e

17. Delpe-Acharige A, Zhang M, Eschliman K *et al.* Pyrazolyl Thioureas and Carbothioamides with an NNSN Motif against MSSA and MRSA. *ACS Omega* 2021;**6**(9):6088-99. doi: 10.1021/acsomega.0c04513

18. Crawford CL, Dalecki AG, Narmore WT *et al.* Pyrazolopyrimidinones, a novel class of copper-dependent bactericidal antibiotics against multi-drug resistant S. aureus†. *Metallomics* 2019;**11**(4):784-98. doi: 10.1039/c8mt00316e

19. Shah S, Dalecki Alex G, Malalasekera Aruni P *et al.* 8-Hydroxyquinolines Are Boosting Agents of Copper-Related Toxicity in Mycobacterium tuberculosis. *Antimicrobial Agents and Chemotherapy* 2016;**60**(10):5765-76. doi: 10.1128/AAC.00325-16

20. Festa Richard A, Helsel Marian E, Franz Katherine J *et al.* Exploiting Innate Immune Cell Activation of a Copper-Dependent Antimicrobial Agent during Infection. *Chemistry & Biology* 2014;**21**(8):977-87. doi: https://doi.org/10.1016/j.chembiol.2014.06.009

21. Gonzalez H, Tarras-Wahlberg N, Strömdahl B *et al.* Photostability of commercial sunscreens upon sun exposure and irradiation by ultraviolet lamps. *BMC Dermatology* 2007;**7**(1):1. doi: 10.1186/1471-5945-7-1

22. Crawford CL, Dalecki AG, Perez MD *et al.* A copper-dependent compound restores ampicillin sensitivity in multidrug-resistant Staphylococcus aureus. *Scientific Reports* 2020;**10**(1):8955. doi: 10.1038/s41598-020-65978-y

23. Song Yn, Xu H, Chen W *et al.* 8-Hydroxyquinoline: a privileged structure with a broad-ranging pharmacological potential. *MedChemComm* 2015;**6**(1):61-74. doi: 10.1039/C4MD00284A

24. Dalecki AG, Malalasekera AP, Schaaf K *et al.* Combinatorial phenotypic screen uncovers unrecognized family of extended thiourea inhibitors with copper-dependent anti-staphylococcal activity. *Metallomics* 2016;**8**(4):412-21. doi: 10.1039/c6mt00003g

25. Horton DA, Bourne GT, Smythe ML. The Combinatorial Synthesis of Bicyclic Privileged Structures or Privileged Substructures. *Chemical Reviews* 2003;**103**(3):893-930. doi: 10.1021/cr020033s

26. Lane TJ, Quinlan KP. Metal Binding of the Benzimidazoles1. *Journal of the American Chemical Society* 1960;**82**(12):2994-7

27. Irving H, Williams RJP. 637. The stability of transition-metal complexes. *Journal of the Chemical Society (Resumed)* 1953(0):3192-210. doi: 10.1039/JR9530003192

28. Lemire JA, Harrison JJ, Turner RJ. Antimicrobial activity of metals: mechanisms, molecular targets and applications. *Nature Reviews Microbiology* 2013;**11**(6):371-84. doi: 10.1038/nrmicro3028

29. Duff EJ, Hughes MN. Oxazole complexes. Part I. N-Bonded complexes of benzoxazole with cobalt(II), nickel(II), copper(II), and zinc(II). *Journal of the Chemical Society A: Inorganic, Physical, Theoretical* 1968(0):2144-6. doi: 10.1039/J19680002144

30. Metrangolo P, Neukirch H, Pilati T *et al.* Halogen Bonding Based Recognition Processes: A World Parallel to Hydrogen Bonding. *Accounts of Chemical Research* 2005;**38**(5):386-95. doi: 10.1021/ar0400995

31. Metrangolo P, Murray JS, Pilati T *et al.* Fluorine-Centered Halogen Bonding: A Factor in Recognition Phenomena and Reactivity. *Crystal Growth & Design* 2011;**11**(9):4238-46. doi: 10.1021/cg200888n

32. Parisini E, Metrangolo P, Pilati T *et al.* Halogen bonding in halocarbon–protein complexes: a structural survey. *Chemical Society Reviews* 2011;**40**(5):2267-78. doi: 10.1039/C0CS00177E

33. Lu Y, Shi T, Wang Y *et al.* Halogen Bonding—A Novel Interaction for Rational Drug Design? *Journal of Medicinal Chemistry* 2009;**52**(9):2854-62. doi: 10.1021/jm9000133

34. Heidrich J, Sperl LE, Boeckler FM. Embracing the Diversity of Halogen Bonding Motifs in Fragment-Based Drug Discovery—Construction of a Diversity-Optimized Halogen-Enriched Fragment Library. *Frontiers in Chemistry* 2019;**7**

35. Andersson DA, Gentry C, Moss S *et al.* Clioquinol and pyrithione activate TRPA1 by increasing intracellular Zn2+. *Proceedings of the National Academy of Sciences* 2009;**106**(20):8374-9. doi: 10.1073/pnas.0812675106

36. Park M-H, Lee S-J, Byun H-r *et al.* Clioquinol induces autophagy in cultured astrocytes and neurons by acting as a zinc ionophore. *Neurobiology of Disease* 2011;**42**(3):242-51. doi: https://doi.org/10.1016/j.nbd.2011.01.009

37. Safety, tolerability, and efficacy of PBT2 in Huntington's disease: a phase 2, randomised, double-blind, placebo-controlled trial. *The Lancet Neurology* 2015;**14**(1):39-47. doi: https://doi.org/10.1016/S1474-4422(14)70262-5

38. Lannfelt L, Blennow K, Zetterberg H *et al.* Safety, efficacy, and biomarker findings of PBT2 in targeting Aβ as a modifying therapy for Alzheimer's disease: a phase

IIa, double-blind, randomised, placebo-controlled trial. *The Lancet Neurology* 2008;**7**(9):779-86. doi: https://doi.org/10.1016/S1474-4422(08)70167-4

39. Bohlmann L, De Oliveira David MP, El-Deeb Ibrahim M *et al.* Chemical Synergy between Ionophore PBT2 and Zinc Reverses Antibiotic Resistance. *mBio* 2018;**9**(6):e02391-18. doi: 10.1128/mBio.02391-18

40. Crouch PJ, Savva MS, Hung LW *et al.* The Alzheimer's therapeutic PBT2 promotes amyloid-β degradation and GSK3 phosphorylation via a metal chaperone activity. *Journal of Neurochemistry* 2011;**119**(1):220-30. doi: https://doi.org/10.1111/j.1471-4159.2011.07402.x

41. Harbison-Price N, Ferguson Scott A, Heikal A *et al.* Multiple Bactericidal Mechanisms of the Zinc Ionophore PBT2. *mSphere* 2020;**5**(2):e00157-20. doi: 10.1128/mSphere.00157-20

CONCLUSIONS

Summary of findings

Prior studies have predominantly focused on copper (Cu) as the activating metal that contributes to the inhibitory actions of metallo-antibiotics. These Cu-driven efforts laid the foundation for estimating potential classes of metallo-antibiotics from structural motifs [217, 218, 262] and describing mechanisms of action of antibacterial Cu-dependent inhibitors (CDIs) [214, 220, 263, 264], yet the sole focus on Cu underestimates the full breadth of possible metallo-antibiotics. In the studies described here, we demonstrate zinc (Zn) is an effective activator of antibacterial activity against Staphylococcus aureus with minimal toxicity against eukaryotic cells. By developing a simple and readily adaptable Zn-dependent antibiotic screening, we find Zn, rather than Cu, is a more efficient antibacterial activator among bioactive molecules and greatly improves the rate of hit identification of an antibiotic screen. This method also enabled the repurposing of avobenzone (AVB), a UV-A filter used in sunscreens, as a Zn-activated antibiotic against multi-drug resistant S. aureus. We also demonstrate antibacterial Zn activation is a more consistent feature of classes of privileged structures with documented metal-dependent bioactivities compared to Cu. Our structure activity relationship (SAR) study of these privileged classes reveals structural modifications to metallo-antibiotics can subsequently alter the metal specificity of a compound such that metallo-antibiotics could be designed for a single metal-specific action. In total, this work shows consideration of Zn broadens the metallo-antibiotic field and offers new

opportunities for metallo-antibiotic development at a time when novel antibiotics are sorely needed.

Preponderance of Zn-activated antimicrobials

A previous study estimated the total number of organic molecules in potential chemical space is 10^{63}. This number assumes all molecules follow Lipinski's Rule of Five and are only composed of carbon, nitrogen, oxygen, sulfur, and hydrogen [265]. Naturally, this number does not represent all molecules in available chemical space (i.e., synthesized molecules), nor does it consider halogens, which are commonly incorporated into drugs. The amount of known drug space, the available molecules with druggable features, is considerably smaller. Virtual screening suggests less than 0.1% of all possible small molecules have ever been synthesized [266], and a database of unknown chemical space, GDB-17, was developed in 2012 to represent chemical space composed of organic molecules of 17 atoms or less, contains 166.4 billion compounds [267]. In comparison, 112,407,039 compounds and 298,306,350 substances representing 301,290,840 bioactivities have been deposited in PubChem, an online chemical database hosted by the National Institute of Health (NIH) [268], at the time of writing. Some of these molecules, especially antibiotics that do not follow Lipinski's Rule of Five [130], expand upon the 10^{63} molecule estimate of chemical space.

Despite the sheer volume of molecules available for testing and the establishment of HTS, antibiotic discovery continues to languish. Our small-scale Zn-dependent screen indicates that, despite the lack of novel antibiotics, chemical space can be further mined for antibiotics by adapting available screening methods to include Zn. Generally, a

standard HTS effort can expect, at maximum, a hit rate of 2% [269]. In contrast, our metal-dependent screen boasts a hit rate of over 8%. The hit rate is likely inflated because of screening a library of known bioactive molecules. However, by assuming a similar ratio of independent hits to Zn hits with the independent hits representing a more conservative 1% of the total library, we can extrapolate these results to a larger number of compounds. For a library comprising 100,000 compounds, a standard screen would identify 1,000 compounds as hits based on a 1% hit rate. A Zn-dependent screen, however, would identify an additional 628 compounds, boosting the hit rate to 1.63% and increasing the pool of molecules that could be developed as lead compounds. If we speculate further to unknown chemical space, specifically the estimates from the GDB-17 database, with these same assumptions, approximately 1 billion molecules with druggable features could have antibacterial Zn-dependency. While this is a simple estimate with multiple assumptions, our proof-of-concept screen demonstrates Zn-dependent screening has the potential identify activities otherwise lost by the predominate antibiotic screening approach currently in use. Additionally, our screen identified Zn-activated metallo-antibiotics from characterized chemical space, not just known chemical space. Zn-activated metallo-antibiotics are present within the current pool of drugs. Therefore, drug repurposing efforts focused on antibiotics with Zn-dependency should be performed to streamline metallo-antibiotic development and potentially expedite FDA approval due to reduced risks of toxicity.

Interestingly, a previous Cu-dependent screen of a 10,000-compound library against MRSA identified 59 Cu-related hits out of a total 129 hits [216]. The total hit rate from this screen was 1.29%, while the Cu-related hit rate was only 0.59%, substantially

lower than the Zn and Cu hit rates from our proof-of-concept screen. Potentially, this suggests metallo-antibiotics targeting MRSA are more prevalent among bioactive molecules compared to a broader array of chemical space, though screening of a greater diversity of molecules will be required to confirm this. Additionally, the studies described here indicate anti-staphylococcal Zn-dependency is more ubiquitous than Cu-dependency. Our screen identified 49 Zn hits compared to just 37 hits with Cu, and both the 8HQs and BZIs were more consistently and potently activated with Zn rather than Cu. Despite the wealth of studies focused on Cu-dependent inhibitors, Zn may be a more potent activator of antibiotic activity compared to Cu. Given this, we propose Zn-activated metallo-antibiotics should be considered an included area of study within the field of metallo-antibiotics.

Lastly, consideration of physiological metals earlier in the development process can also eliminate unwanted compounds prior to downstream applications and thereby reduce unnecessary development costs. For instance, our pilot screen identified Cu and Zn inverse hits, molecules which become inactive in the presence of Cu or Zn respectively. Zn is distributed throughout all the major body systems [270], and studies of nutritional immunity demonstrate Zn localization and concentration will fluctuate throughout the course of an infection [147, 148, 183, 251-253, 271]. By identifying a compound that could become inactive at the site of an infection, lead development can be focused on compounds with consistent activation regardless of a metal.

Mechanisms of Zn-activated antimicrobials

Though the studies herein demonstrate the surprisingly abundant number of Zn-activated antibiotics, antibiotics that use Zn for their antibacterial activity are not new. The first evidence of antibacterial Zn activation was identified in 1971 by Stone *et. al.* by demonstrating the antibiotic bacitracin requires Zn to bind to undecaprenol pyrophosphate [259]. To our knowledge, only two other Zn-dependent antibiotics have been described. The first is Zn-pyrithione (Zn-PT), an antifungal drug most commonly used as the active ingredient anti-dandruff shampoos [261] and as an anti-fouling agent for waste water [261, 272]. The second is an 8HQ analog called PBT2. Previously a treatment for neurodegenerative diseases [211, 273], PBT2 has since been repurposed as a Zn antibiotic that reverses drug resistance in bacteria [274]. Here we will discuss the known mechanisms of Zn-activated antibiotics and potential mechanisms for the Zn-activated antibiotics by our studies.

Bacitracin was first identified in 1945 and is cyclic polypeptide antibiotic produced by *Bacillus subtilis* [257]. Previously, bacitracin-Zn was used locally and intravenously for the control of infectious diseases, but the nephrotoxicity of bacitracin-Zn [260] has limited its use in the current day as an ingredient in first-aid ointments. Bacitracin-Zn is a broad-spectrum, single-target antibiotic that inhibits peptidoglycan synthesis by binding to and preventing the dephosphorylation of undecaprenyl pyrophosphate (UPP) to undecaprenyl phosphate (UP) [259, 275]. UP is an intermediate lipid carrier for cell wall subunits. Preventing its formation thus presents these subunits from interacting with the inner leaflet of the bacterial cell membrane, resulting in reduced cell wall deposition [276]. Resistance to bacitracin-Zn has been documented since its

introduction and primarily occurs through increased polypeptide antibiotic export [277-280] or expression of a phosphatase that restores the pool of UP by dephosphorylating UPP [281-283]. Both resistance mechanisms can be found in *S. aureus* in a strain-dependent manner.

As previously discussed, Zn-activated AVB (AVB-Zn) is unlikely to act through the same mechanism of action as bacitracin-Zn. Clinical multi-drug resistant MRSA isolates we challenged with bacitracin-Zn were, to varying degrees, resistant to bacitracin-Zn but were still susceptible AVB-Zn. To inhibit these strains, AVB-Zn would need to bypass the resistance mechanisms encoded by the tested isolates. While AVB-Zn could have higher affinity for UPP than bacitracin-Zn or directly inhibit the phosphatase that converts UPP to UP, we find this possibility unlikely. The more probable possibility is that AVB-Zn has a separate target from bacitracin-Zn. Future studies will need to define this mechanism.

The second two Zn-dependent inhibitors, Zn-PT and PBT2, are considered ionophores that damage target organisms by disrupting intracellular metal homeostasis [261, 284]. While Zn-pyrithione is sold as Zn salt, it is unclear whether the precomplexed Zn ion plays a role its inhibitory action. Zn-PT increases intracellular Zn concentrations in mammalian cells [285-287] as would be expected of a Zn ionophore, but a mechanism separate from Zn has been described in microbes. Zn-PT synergizes with Cu to inhibit certain marine species [272, 288], and a 2011 study of the fungi *Saccharomyces cerevisiae* and *Malassezia globus* demonstrated Zn-PT degrades iron-sulfur clusters by increasing Cu uptake, not Zn [261]. Therefore, the classification of Zn-PT as a Zn-dependent antibiotic may be inappropriate.

There is greater evidence for PBT2 and other 8HQ analogs as Zn ionophores. Clioquinol (CIQ), another 8HQ analog that we included in our 8HQ panel, causes Zn influx in the neurons of mice [287], and PBT2 shunts extracellular Zn into neuroblastoma cells. This prevents the formation of protease-resistant amyloid-β aggregates seen in Alzheimer's disease [273]. PBT2 has since entered into clinical phase II trials as a treatment for Alzheimer's disease and Huntington's disease based on its Zn ionophore activity [211, 213]. In 2018, PBT2 gained attention as Zn-dependent antibiotic and for its ability to reverse antibiotic resistance across multiple pathogenic bacteria [274]. Treatment with PBT2 and Zn results in increased in total intracellular Zn concentration, regardless of species [274, 289, 290]. Since the 2018 study, PBT2 with Zn has been shown to reverse antibiotic resistance in Group A *Streptococcus, S. aureus*, *Enterococci* [274], *Klebsiella pneumoniae*, *E. coli*, *Acinetobacter baumanii*, *Pseudomonas aeruginosa* [289, 291], *Neisseria gonorrhoeae* [292-294], and *S. pneumoniae* [295]. Because of this, PBT2 is an established broad-spectrum Zn ionophore for which resistance has not developed [289]. Thus, PBT2 is an important molecule that demonstrates the potential of Zn-activated antibiotics.

Given the structural similarity of PBT2 and the 8HQ analogs included in our panel, the Zn-activated 8HQs we tested are likely Zn ionophores. This could explain why the 8HQs we tested were more consistently activated by Zn rather Cu. The question that remains is why some 8HQs were Zn specific and others were Cu-dependent. What factors determine the shift from one metal dependency to another when the compounds only differ by halogenation? A broader structure activity relationship (SAR) study will be necessary in order to answer this question.

Future directions

Clearly not all Zn-dependent antibiotics act in the same manner. The first step of future studies will be to determine the spectrum of possible mechanisms of action of Zn-activated antibiotics. Studies of bacitracin and PBT2 demonstrate inhibition of cell wall synthesis [259] and disruption of intracellular Zn homeostasis [274] are possibilities. Elucidating the range of Zn-dependent antibiotic modes of action will establish the targeted pathways as targets for future antibiotic development. First, future studies will need to compare the transcriptomic profiles of S. aureus cells treated with bacitracin-Zn, PBT2-Zn, major antibiotics, or the Zn-activated antibiotic of interest to see if similar pathways are upregulated due to treatment. If similar patterns of differential regulation are seen between two conditions, this would suggest they act on similar pathways, if not on identical targets. For instance, AVB-Zn and bacitracin-Zn share similar transcriptomic profiles, AVB-Zn like inhibits a step of peptidoglycan synthesis.

Second, Zn-activated metallo-antibiotics should be analyzed for Zn ionophore activity using inductively coupled plasma mass spectrometry (ICP-MS). This sensitive method measures total metal content in parts per million and is the standard method for measuring alterations metal levels in response to ionophore treatment. However, this method cannot detect labile metal content, an important aspect when considering Zn toxicity is hypothesized to be due to mis-metalation [246]. While total Zn content may increase in response to treatment, it is important to remember this increase may not be outside of the buffering concentration of the cell as defined by its metal-binding transcriptional regulators [296]. For instance, Bohlmann *et. al.* claim PBT2 acts as a Zn ionophore against vancomycin-resistant *Enterococci* based on a small but statistically

significant increase in total Zn content compared to an untreated control, supporting the claim through transcriptomic profiling [274], but such a small shift may be of little biological consequence. Monitoring labile metal concentrations would answer solve this issue.

Fluorescent chelators may provide a solution. Multiple fluorescent chelators with varying dissociation constants for different transition metals have been developed in recent years, and protocols have been developed for indirectly measuring intracellular metal concentrations in live cells [297-300]. Many of these fluorescent chelators are commercially available, and the fluorophores vary between chelators. This allows for simultaneous surveillance of several metals at once using flow cytometry or a plate reader for higher throughput operations. If transcriptomics profiles, total metal content, and labile content all indicate altered metal homeostasis due to treatment, the compound of interest is likely an ionophore.

A secondary condition to consider when studying potential ionophores is the nonspecific nature of their action. Though PBT2 is proven and safe Zn ionophore in humans [211, 213], PBT2 as an antibiotic will need to be considered for its off-target neural effects. The same is true for other ionophores. As multiple classes of metallo-antibiotics are metal ionophores, metallo-antibiotics, regardless of metal specificity, should be thoroughly evaluated for eukaryotic toxicity and safety in an animal model. Yet this same nonspecific action may also be beneficial from a development standpoint. Metal homeostasis is essential for all organisms [246]. Disruption of this would then be applicable to many different bacterial species. Metal ionophore antibiotics should then be evaluated for broad spectrum activity as well.

Lastly, larger Zn-dependent screens are required to begin building a database of structural classes associated with Zn-dependency. To potentially increase the initial hit discovery, it may be beneficial to bias the screen for antibiotic and chelator discovery. Antibiotics break Lipinski's Rule of Five [130]. Screening a library dedicated to breaking these rules, such as a macrocycle library, may increase the number of independent antibiotic hits from the screen, while screening a library of compounds with a preponderance of metal-binding motifs is more likely to identify metal-activated antibiotics. Hits from these screens should be clustered using strategies previously described [216] to cluster hit compounds by structural motif. The clusters can then be expanded using a SAR-by-catalog approach. These results can in turn be used to inform a hypothesis-driven SAR to define how metal specificity can shifted across a class of molecules.

New antibiotics are essential to continue treating infectious diseases as antibiotic resistance grows. Metallo-antibiotics are one such option. Our studies here show metallo-antibiotics are more ubiquitous than previously understood, even within characterized chemical space and that Zn-activated antibiotics are yet another type of metallo-antibiotics to further explore. Our initial characterization of AVB-Zn suggests the mechanisms of Zn-activation are also broader than simply inhibition of cell wall synthesis or disruption of Zn homeostasis. Finally, Zn-activated metallo-antibiotics provide an opportunity for rational design of antibiotics with particular metal specificities and improved potency using available methods. Zn-dependent antibiotics are then a rich source for antibiotic drug development.

LIST OF REFERENCES

1. Daum RS. Skin and Soft-Tissue Infections Caused by Methicillin-Resistant Staphylococcus aureus. New England Journal of Medicine 2007;357(4):380-90. doi: 10.1056/NEJMcp070747

2. Lam JC, Gregson DB, Robinson S et al. Epidemiology and Outcome Determinants of Staphylococcus aureus Bacteremia Revisited: A Population-Based Study. Infection 2019;47(6):961-71. doi: 10.1007/s15010-019-01330-5

3. Lee AS, de Lencastre H, Garau J et al. Methicillin-resistant Staphylococcus aureus. Nature Reviews Disease Primers 2018;4(1):18033. doi: 10.1038/nrdp.2018.33

4. Turner NA, Sharma-Kuinkel BK, Maskarinec SA et al. Methicillin-resistant Staphylococcus aureus: an overview of basic and clinical research. Nature Reviews Microbiology 2019;17(4):203-18. doi: 10.1038/s41579-018-0147-4

5. Lowy FD. Staphylococcus aureus Infections. New England Journal of Medicine 1998;339(8):520-32. doi: 10.1056/NEJM199808203390806

6. Vanhommerig E, Moons P, Pirici D et al. Comparison of Biofilm Formation between Major Clonal Lineages of Methicillin Resistant Staphylococcus aureus. PLOS ONE 2014;9(8):e104561. doi: 10.1371/journal.pone.0104561

7. Eleftheriadou I, Tentolouris N, Argiana V et al. Methicillin-Resistant Staphylococcus aureus in Diabetic Foot Infections. Drugs 2010;70(14):1785-97. doi: 10.2165/11538070-000000000-00000

8. Boucher HW, Corey GR. Epidemiology of Methicillin-Resistant Staphylococcus aureus. Clinical Infectious Diseases 2008;46(Supplement_5):S344-S9. doi: 10.1086/533590

9. Antibiotic resistance threats in the United States, 2019. 2019

10. Global antimicrobial resistance and use surveillance system (GLASS) report. Geneva: World Health Orgnaization 2021

11. Brown NM, Goodman AL, Horner C et al. Treatment of methicillin-resistant Staphylococcus aureus (MRSA): updated guidelines from the UK. JAC-Antimicrobial Resistance 2021;3(1):dlaa114. doi: 10.1093/jacamr/dlaa114

12. Park JT, Strominger JL. Mode of Action of Penicillin. Science 1957;125(3238):99-101. doi: 10.1126/science.125.3238.99

13. Waxman DJ, Strominger JL. PENICILLIN-BINDING PROTEINS AND THE MECHANISM OF ACTION OF BETA-LACTAM ANTIBIOTICS. Annual Review of Biochemistry 1983;52(1):825-69. doi: 10.1146/annurev.bi.52.070183.004141

14. Jevons MP. “Celbenin” - resistant Staphylococci. British Medical Journal 1961(0007-1447 (Print))

15. Larsen J, Raisen CL, Ba X et al. Emergence of methicillin resistance predates the clinical use of antibiotics. Nature 2022;602(7895):135-41. doi: 10.1038/s41586-021-04265-w

16. Givney R, Vickery A, Holliday A et al. Evolution of an endemic methicillin-resistant Staphylococcus aureus population in an Australian hospital from 1967 to 1996. J Clin Microbiol 1998;36(2):552-6. doi: 10.1128/jcm.36.2.552-556.1998

17. Barrett FF, McGehee RF, Finland M. Methicillin-Resistant Staphylococcus aureus at Boston City Hospital. New England Journal of Medicine 1968;279(9):441-8. doi: 10.1056/NEJM196808292790901

18. David Michael Z, Daum Robert S. Community-Associated Methicillin-Resistant Staphylococcus aureus: Epidemiology and Clinical Consequences of an Emerging Epidemic. Clinical Microbiology Reviews 2010;23(3):616-87. doi: 10.1128/CMR.00081-09

19. Calfee DP, Durbin LJ, Germanson TP et al. Spread of Methicillin-Resistant Staphylococcus aureus (MRSA) Among Household Contacts of Individuals With Nosocomially Acquired MRSA. Infection Control & Hospital Epidemiology 2003;24(6):422-6. doi: 10.1086/502225

20. Naimi TS, LeDell KH, Como-Sabetti K et al. Comparison of Community- and Health Care–Associated Methicillin-Resistant Staphylococcus aureus Infection. JAMA 2003;290(22):2976-84. doi: 10.1001/jama.290.22.2976

21. Charlebois ED, Perdreau-Remington F, Kreiswirth B et al. Origins of Community Strains of Methicillin-Resistant Staphylococcus aureus. Clinical Infectious Diseases 2004;39(1):47-54. doi: 10.1086/421090

22. Herold BC, Immergluck LC, Maranan MC et al. Community-Acquired Methicillin-Resistant Staphylococcus aureus in Children With No Identified Predisposing Risk. JAMA 1998;279(8):593-8. doi: 10.1001/jama.279.8.593

23. Pan ES, Diep BA, Carleton HA et al. Increasing Prevalence of Methicillin-Resistant Staphylococcus aureus Infection in California Jails. Clinical Infectious Diseases 2003;37(10):1384-8. doi: 10.1086/379019

24. Kazakova SV, Hageman JC, Matava M et al. A Clone of Methicillin-Resistant Staphylococcus aureus among Professional Football Players. New England Journal of Medicine 2005;352(5):468-75. doi: 10.1056/NEJMoa042859

25. Services USDoHaH. National Action Plan to Prevent Health-Care Associated Infections: Road Map to Elimination. 2008

26. Antibiotic resistance threats in the United States, 2013. 2013

27. Shorr AF. Epidemiology and Economic Impact of Meticillin-Resistant Staphylococcus aureus. PharmacoEconomics 2007;25(9):751-68. doi: 10.2165/00019053-200725090-00004

28. Cosgrove SE, Sakoulas G, Perencevich EN et al. Comparison of Mortality Associated with Methicillin-Resistant and Methicillin-Susceptible Staphylococcus aureus Bacteremia: A Meta-analysis. Clinical Infectious Diseases 2003;36(1):53-9. doi: 10.1086/345476

29. French GL. Clinical impact and relevance of antibiotic resistance. Advanced Drug Delivery Reviews 2005;57(10):1514-27. doi: https://doi.org/10.1016/j.addr.2005.04.005

30. Helms M, Vastrup P, Gerner-Smidt P et al. Excess mortality associated with antimicrobial drug-resistant Salmonella typhimurium. Emerg Infect Dis 2002;8(5):490-5. doi: 10.3201/eid0805.010267

31. Friedman ND, Temkin E, Carmeli Y. The negative impact of antibiotic resistance. Clinical Microbiology and Infection 2016;22(5):416-22. doi: https://doi.org/10.1016/j.cmi.2015.12.002

32. Tong SY, Davis JS, Eichenberger E et al. Staphylococcus aureus infections: epidemiology, pathophysiology, clinical manifestations, and management. Clin Microbiol Rev 2015;28(3):603-61. doi: 10.1128/cmr.00134-14

33. Malachowa N, DeLeo FR. Mobile genetic elements of Staphylococcus aureus. Cell Mol Life Sci 2010;67(18):3057-71. doi: 10.1007/s00018-010-0389-4

34. Haaber J, Penadés JR, Ingmer H. Transfer of Antibiotic Resistance in Staphylococcus aureus. Trends in Microbiology 2017;25(11):893-905. doi: 10.1016/j.tim.2017.05.011

35. Xia G, Wolz C. Phages of Staphylococcus aureus and their impact on host evolution. Infection, Genetics and Evolution 2014;21:593-601. doi: https://doi.org/10.1016/j.meegid.2013.04.022

36. Ingmer H, Gerlach D, Wolz C. Temperate Phages of Staphylococcus aureus. Microbiology Spectrum 2019;7(5):7.5.1. doi: 10.1128/microbiolspec.GPP3-0058-2018

37. Hatoum-Aslan A. The phages of staphylococci: critical catalysts in health and disease. Trends in Microbiology 2021;29(12):1117-29. doi: https://doi.org/10.1016/j.tim.2021.04.008

38. Chen J, Novick RP. Phage-Mediated Intergeneric Transfer of Toxin Genes. Science 2009;323(5910):139-41. doi: 10.1126/science.1164783

39. Cohen S, Sweeney Helen M. Transduction of Methicillin Resistance in Staphylococcus aureus Dependent on an Unusual Specificity of the Recipient Strain. Journal of Bacteriology 1970;104(3):1158-67. doi: 10.1128/jb.104.3.1158-1167.1970

40. Xia G, Corrigan Rebecca M, Winstel V et al. Wall Teichoic Acid-Dependent Adsorption of Staphylococcal Siphovirus and Myovirus. Journal of Bacteriology 2011;193(15):4006-9. doi: 10.1128/JB.01412-10

41. Koç C, Xia G, Kühner P et al. Structure of the host-recognition device of Staphylococcus aureus phage ϕ11. Scientific Reports 2016;6(1):27581. doi: 10.1038/srep27581

42. Goerke C, Pantucek R, Holtfreter S et al. Diversity of Prophages in Dominant Staphylococcus aureus Clonal Lineages. Journal of Bacteriology 2009;191(11):3462-8. doi: 10.1128/JB.01804-08

43. Kaneko J, Kimura T, Narita S et al. Complete nucleotide sequence and molecular characterization of the temperate staphylococcal bacteriophage φPVL carrying Panton–Valentine leukocidin genes. Gene 1998;215(1):57-67. doi: https://doi.org/10.1016/S0378-1119(98)00278-9

44. Choorit W, Kaneko J, Muramoto K et al. Existence of a new protein component with the same function as the LukF component of leukocidin or γ-hemolysin and its gene in Staphylococcus aureus P83. FEBS Letters 1995;357(3):260-4. doi: https://doi.org/10.1016/0014-5793(94)01372-8

45. Prévost G, Cribier B, Couppié P et al. Panton-Valentine leucocidin and gamma-hemolysin from Staphylococcus aureus ATCC 49775 are encoded by distinct genetic loci and have different biological activities. Infection and Immunity 1995;63(10):4121-9. doi: 10.1128/iai.63.10.4121-4129.1995

46. Löffler B, Hussain M, Grundmeier M et al. Staphylococcus aureus Panton-Valentine Leukocidin Is a Very Potent Cytotoxic Factor for Human Neutrophils. PLOS Pathogens 2010;6(1):e1000715. doi: 10.1371/journal.ppat.1000715

47. Otter JA, Kearns AM, French GL et al. Panton–Valentine leukocidin-encoding bacteriophage and gene sequence variation in community-associated methicillin-resistant Staphylococcus aureus. Clinical Microbiology and Infection 2010;16(1):68-73. doi: https://doi.org/10.1111/j.1469-0691.2009.02925.x

48. Labandeira-Rey M, Couzon F, Boisset S et al. Staphylococcus aureus Panton-Valentine Leukocidin Causes Necrotizing Pneumonia. Science 2007;315(5815):1130-3. doi: 10.1126/science.1137165

49. Gillet Y, Issartel B, Vanhems P et al. Association between Staphylococcus aureus strains carrying gene for Panton-Valentine leukocidin and highly lethal necrotising pneumonia in young immunocompetent patients. The Lancet 2002;359(9308):753-9. doi: https://doi.org/10.1016/S0140-6736(02)07877-7

50. Yamaguchi T, Hayashi T, Takami H et al. Phage conversion of exfoliative toxin A production in Staphylococcus aureus. Molecular Microbiology 2000;38(4):694-705. doi: https://doi.org/10.1046/j.1365-2958.2000.02169.x

51. Yoshizawa Y, Sakurada J, Sakurai S et al. An Exfoliative Toxin A-Converting Phage Isolated from Staphylococcus aureus Strain ZM. Microbiology and Immunology 2000;44(3):189-91. doi: https://doi.org/10.1111/j.1348-0421.2000.tb02481.x

52. Monday SR, Vath GM, Ferens WA et al. Unique Superantigen Activity of Staphylococcal Exfoliative Toxins1. The Journal of Immunology 1999;162(8):4550-9. doi: 10.4049/jimmunol.162.8.4550

53. Ladhani S. Understanding the mechanism of action of the exfoliative toxins of Staphylococcus aureus. FEMS Immunology & Medical Microbiology 2003;39(2):181-9. doi: 10.1016/S0928-8244(03)00225-6

54. Verkaik NJ, Benard M, Boelens HA et al. Immune evasion cluster-positive bacteriophages are highly prevalent among human Staphylococcus aureus strains, but they are not essential in the first stages of nasal colonization. Clinical Microbiology and Infection 2011;17(3):343-8. doi: https://doi.org/10.1111/j.1469-0691.2010.03227.x

55. de Jong Nienke WM, van Kessel Kok PM, van Strijp Jos AG. Immune Evasion by Staphylococcus aureus. Microbiology Spectrum 2019;7(2):7.2.20. doi: 10.1128/microbiolspec.GPP3-0061-2019

56. van Wamel Willem JB, Rooijakkers Suzan HM, Ruyken M et al. The Innate Immune Modulators Staphylococcal Complement Inhibitor and Chemotaxis Inhibitory Protein of Staphylococcus aureus Are Located on β-Hemolysin-Converting Bacteriophages. Journal of Bacteriology 2006;188(4):1310-5. doi: 10.1128/JB.188.4.1310-1315.2006

57. Postma B, Poppelier MJ, van Galen JC et al. Chemotaxis Inhibitory Protein of Staphylococcus aureus Binds Specifically to the C5a and Formylated Peptide Receptor. The Journal of Immunology 2004;172(11):6994-7001. doi: 10.4049/jimmunol.172.11.6994

58. de Haas CJ, Veldkamp KE, Peschel A et al. Chemotaxis inhibitory protein of Staphylococcus aureus, a bacterial antiinflammatory agent. J Exp Med 2004;199(5):687-95. doi: 10.1084/jem.20031636

59. Collen D. Staphylokinase: a potent, uniquely fibrin-selective thrombolytic agent. Nature Medicine 1998;4(3):279-84. doi: 10.1038/nm0398-279

60. Lijnen HR, Van Hoef B, De Cock F et al. On the mechanism of fibrin-specific plasminogen activation by staphylokinase. Journal of Biological Chemistry 1991;266(18):11826-32. doi: https://doi.org/10.1016/S0021-9258(18)99031-9

61. Rooijakkers SHM, van Wamel WJB, Ruyken M et al. Anti-opsonic properties of staphylokinase. Microbes and Infection 2005;7(3):476-84. doi: https://doi.org/10.1016/j.micinf.2004.12.014

62. Kwiecinski J, Jacobsson G, Karlsson M et al. Staphylokinase Promotes the Establishment of Staphylococcus aureus Skin Infections While Decreasing Disease Severity. The Journal of Infectious Diseases 2013;208(6):990-9. doi: 10.1093/infdis/jit288

63. Doery HM, Magnusson BJ, Cheyne IM et al. A Phospholipase in Staphylococcal Toxin which hydrolyses Sphingomyelin. Nature 1963;198(4885):1091-2. doi: 10.1038/1981091a0

64. Katayama Y, Baba T, Sekine M et al. Beta-Hemolysin Promotes Skin Colonization by Staphylococcus aureus. Journal of Bacteriology 2013;195(6):1194-203. doi: 10.1128/JB.01786-12

65. Rooijakkers SHM, Ruyken M, Roos A et al. Immune evasion by a staphylococcal complement inhibitor that acts on C3 convertases. Nature Immunology 2005;6(9):920-7. doi: 10.1038/ni1235

66. Weidenmaier C, Goerke C, Wolz C. Staphylococcus aureus determinants for nasal colonization. Trends in Microbiology 2012;20(5):243-50. doi: https://doi.org/10.1016/j.tim.2012.03.004

67. Humphrey S, Fillol-Salom A, Quiles-Puchalt N et al. Bacterial chromosomal mobility via lateral transduction exceeds that of classical mobile genetic elements. Nature Communications 2021;12(1):6509. doi: 10.1038/s41467-021-26004-5

68. Ubelaker MH, Rosenblum ED. Transduction of plasmid determinants in Staphylococcus aureus and Escherichia coli. Journal of Bacteriology 1978;133(2):699-707. doi: 10.1128/jb.133.2.699-707.1978

69. Haaber J, Leisner JJ, Cohn MT et al. Bacterial viruses enable their host to acquire antibiotic resistance genes from neighbouring cells. Nature Communications 2016;7(1):13333. doi: 10.1038/ncomms13333

70. Fillol-Salom A, Alsaadi A, Sousa JAMd et al. Bacteriophages benefit from generalized transduction. PLOS Pathogens 2019;15(7):e1007888. doi: 10.1371/journal.ppat.1007888

71. Varga M, Kuntová L, Pantůček R et al. Efficient transfer of antibiotic resistance plasmids by transduction within methicillin-resistant Staphylococcus aureus USA300 clone. FEMS Microbiology Letters 2012;332(2):146-52. doi: 10.1111/j.1574-6968.2012.02589.x

72. Stewart GC, Rosenblum ED. Transduction of methicillin resistance in Staphylococcus aureus: recipient effectiveness and beta-lactamase production.

Antimicrobial Agents and Chemotherapy 1980;18(3):424-32. doi: 10.1128/AAC.18.3.424

73. Hiramatsu K, Suzuki E, Takayama H et al. Role of penicillinase plasmids in the stability of the mecA gene in methicillin-resistant Staphylococcus aureus. Antimicrobial Agents and Chemotherapy 1990;34(4):600-4. doi: 10.1128/AAC.34.4.600

74. Scharn CR, Tenover FC, Goering RV. Transduction of staphylococcal cassette chromosome mec elements between strains of Staphylococcus aureus. Antimicrob Agents Chemother 2013;57(11):5233-8. doi: 10.1128/aac.01058-13

75. Hackbarth CJ, Chambers HF. blaI and blaR1 regulate beta-lactamase and PBP 2a production in methicillin-resistant Staphylococcus aureus. Antimicrob Agents Chemother 1993;37(5):1144-9. doi: 10.1128/aac.37.5.1144

76. Chen J, Quiles-Puchalt N, Chiang YN et al. Genome hypermobility by lateral transduction. Science 2018;362(6411):207-12. doi: 10.1126/science.aat5867

77. Novick RP, Christie GE, Penadés JR. The phage-related chromosomal islands of Gram-positive bacteria. Nature Reviews Microbiology 2010;8(8):541-51. doi: 10.1038/nrmicro2393

78. Lindsay JA, Ruzin A, Ross HF et al. The gene for toxic shock toxin is carried by a family of mobile pathogenicity islands in Staphylococcus aureus. Molecular Microbiology 1998;29(2):527-43. doi: https://doi.org/10.1046/j.1365-2958.1998.00947.x

79. Boyd EF, Davis BM, Hochhut B. Bacteriophage–bacteriophage interactions in the evolution of pathogenic bacteria. Trends in Microbiology 2001;9(3):137-44. doi: https://doi.org/10.1016/S0966-842X(01)01960-6

80. Kwong SM, Ramsay JP, Jensen SO et al. Replication of Staphylococcal Resistance Plasmids. Frontiers in Microbiology 2017;8. doi: 10.3389/fmicb.2017.02279

81. Khan SA, Novick RP. Complete nucleotide sequence of pT181, a tetracycline-resistance plasmid from Staphylococcus aureus. Plasmid 1983;10(3):251-9. doi: 10.1016/0147-619x(83)90039-2

82. Mojumdar M, Khan SA. Characterization of the tetracycline resistance gene of plasmid pT181 of Staphylococcus aureus. Journal of Bacteriology 1988;170(12):5522-8. doi: 10.1128/jb.170.12.5522-5528.1988

83. Shaw WV, Brenner DG, LeGrice SFJ et al. Chloramphenicol acetyltransferase gene of staphylococcal plasmid pC221. FEBS Letters 1985;179(1):101-6. doi: https://doi.org/10.1016/0014-5793(85)80200-3

84. Maciag IE, Viret J-F, Alonso JC. Replication and incompatibility properties of plasmid pUB110 in Bacillus subtilis. Molecular and General Genetics MGG 1988;212(2):232-40. doi: 10.1007/BF00334690

85. Rouch DA, Byrne ME, Kong YC et al. The aacA-aphD gentamicin and kanamycin resistance determinant of Tn4001 from Staphylococcus aureus: expression and nucleotide sequence analysis. J Gen Microbiol 1987;133(11):3039-52. doi: 10.1099/00221287-133-11-3039

86. Shaw KJ, Rather PN, Hare RS et al. Molecular genetics of aminoglycoside resistance genes and familial relationships of the aminoglycoside-modifying enzymes. Microbiol Rev 1993;57(1):138-63. doi: 10.1128/mr.57.1.138-163.1993

87. Berg T, Firth N, Apisiridej S et al. Complete Nucleotide Sequence of pSK41: Evolution of Staphylococcal Conjugative Multiresistance Plasmids. Journal of Bacteriology 1998;180(17):4350-9. doi: 10.1128/JB.180.17.4350-4359.1998

88. Liu MA, Kwong SM, Jensen SO et al. Biology of the staphylococcal conjugative multiresistance plasmid pSK41. Plasmid 2013;70(1):42-51. doi: https://doi.org/10.1016/j.plasmid.2013.02.001

89. Heir E, Sundheim G, Holck AL. Resistance to quaternary ammonium compounds in Staphylococcus spp. isolated from the food industry and nucleotide sequence of the resistance plasmid pST827. J Appl Bacteriol 1995;79(2):149-56. doi: 10.1111/j.1365-2672.1995.tb00928.x

90. O'Brien FG, Ramsay JP, Monecke S et al. Staphylococcus aureus plasmids without mobilization genes are mobilized by a novel conjugative plasmid from community isolates. Journal of Antimicrobial Chemotherapy 2015;70(3):649-52. doi: 10.1093/jac/dku454

91. O'Brien FG, Yui Eto K, Murphy Riley JT et al. Origin-of-transfer sequences facilitate mobilisation of non-conjugative antimicrobial-resistance plasmids in Staphylococcus aureus. Nucleic Acids Research 2015;43(16):7971-83. doi: 10.1093/nar/gkv755

92. Liu J, Chen D, Peters BM et al. Staphylococcal chromosomal cassettes mec (SCCmec): A mobile genetic element in methicillin-resistant Staphylococcus aureus. Microbial Pathogenesis 2016;101:56-67. doi: https://doi.org/10.1016/j.micpath.2016.10.028

93. Beck WD, Berger-Bächi B, Kayser FH. Additional DNA in methicillin-resistant Staphylococcus aureus and molecular cloning of mec-specific DNA. Journal of Bacteriology 1986;165(2):373-8. doi: 10.1128/jb.165.2.373-378.1986

94. Matsuhashi M, Song MD, Ishino F et al. Molecular cloning of the gene of a penicillin-binding protein supposed to cause high resistance to beta-lactam antibiotics in Staphylococcus aureus. Journal of Bacteriology 1986;167(3):975-80. doi: 10.1128/jb.167.3.975-980.1986

95. Song MD, Wachi M, Doi M et al. Evolution of an inducible penicillin-target protein in methicillin-resistant Staphylococcus aureus by gene fusion. FEBS Letters 1987;221(1):167-71. doi: https://doi.org/10.1016/0014-5793(87)80373-3

96. Urushibara N, Aung MS, Kawaguchiya M et al. Novel staphylococcal cassette chromosome mec (SCCmec) type XIV (5A) and a truncated SCCmec element in SCC composite islands carrying speG in ST5 MRSA in Japan. Journal of Antimicrobial Chemotherapy 2020;75(1):46-50. doi: 10.1093/jac/dkz406

97. Classification of Staphylococcal Cassette Chromosome mec (SCCmec): Guidelines for Reporting Novel SCCmec Elements. Antimicrobial Agents and Chemotherapy 2009;53(12):4961-7. doi: 10.1128/AAC.00579-09

98. Wang L, Archer GL. Roles of CcrA and CcrB in excision and integration of staphylococcal cassette chromosome mec, a Staphylococcus aureus genomic island. J Bacteriol 2010;192(12):3204-12. doi: 10.1128/jb.01520-09

99. Shore Anna C, Deasy Emily C, Slickers P et al. Detection of Staphylococcal Cassette Chromosome mec Type XI Carrying Highly Divergent mecA, mecI, mecR1, blaZ, and ccr Genes in Human Clinical Isolates of Clonal Complex 130 Methicillin-Resistant Staphylococcus aureus. Antimicrobial Agents and Chemotherapy 2011;55(8):3765-73. doi: 10.1128/AAC.00187-11

100. Tsubakishita S, Kuwahara-Arai K, Baba T et al. Staphylococcal Cassette Chromosome mec-Like Element in Macrococcus caseolyticus. Antimicrobial Agents and Chemotherapy 2010;54(4):1469-75. doi: 10.1128/AAC.00575-09

101. Hiramatsu K, Asada K, Suzuki E et al. Molecular cloning and nucleotide sequence determination of the regulator region of mecA gene in methicillin-resistant Staphylococcus aureus (MRSA). FEBS Letters 1992;298(2-3):133-6. doi: https://doi.org/10.1016/0014-5793(92)80039-J

102. Belluzo BS, Abriata LA, Giannini E et al. An experiment-informed signal transduction model for the role of the Staphylococcus aureus MecR1 protein in β-lactam resistance. Scientific Reports 2019;9(1):19558. doi: 10.1038/s41598-019-55923-z

103. Seybold U, Kourbatova EV, Johnson JG et al. Emergence of Community-Associated Methicillin-Resistant Staphylococcus aureus USA300 Genotype as a Major Cause of Health Care—Associated Blood Stream Infections. Clinical Infectious Diseases 2006;42(5):647-56. doi: 10.1086/499815

104. Moran GJ, Krishnadasan A, Gorwitz RJ et al. Methicillin-Resistant S. aureus Infections among Patients in the Emergency Department. New England Journal of Medicine 2006;355(7):666-74. doi: 10.1056/NEJMoa055356

105. Talan DA, Krishnadasan A, Gorwitz RJ et al. Comparison of Staphylococcus aureus From Skin and Soft-Tissue Infections in US Emergency Department Patients, 2004 and 2008. Clinical Infectious Diseases 2011;53(2):144-9. doi: 10.1093/cid/cir308

106. Diep BA, Gill SR, Chang RF et al. Complete genome sequence of USA300, an epidemic clone of community-acquired meticillin-resistant Staphylococcus aureus. The Lancet 2006;367(9512):731-9. doi: 10.1016/S0140-6736(06)68231-7

107. Shore AC, Rossney AS, Brennan OM et al. Characterization of a novel arginine catabolic mobile element (ACME) and staphylococcal chromosomal cassette mec composite island with significant homology to Staphylococcus epidermidis ACME type II in methicillin-resistant Staphylococcus aureus genotype ST22-MRSA-IV. Antimicrob Agents Chemother 2011;55(5):1896-905. doi: 10.1128/aac.01756-10

108. Diep BA, Stone GG, Basuino L et al. The Arginine Catabolic Mobile Element and Staphylococcal Chromosomal Cassette mec Linkage: Convergence of Virulence and Resistance in the USA300 Clone of Methicillin-Resistant Staphylococcus aureus. The Journal of Infectious Diseases 2008;197(11):1523-30. doi: 10.1086/587907

109. Diep BA, Otto M. The role of virulence determinants in community-associated MRSA pathogenesis. Trends in Microbiology 2008;16(8):361-9. doi: https://doi.org/10.1016/j.tim.2008.05.002

110. Thurlow Lance R, Joshi Gauri S, Clark Justin R et al. Functional Modularity of the Arginine Catabolic Mobile Element Contributes to the Success of USA300 Methicillin-Resistant Staphylococcus aureus. Cell Host & Microbe 2013;13(1):100-7. doi: https://doi.org/10.1016/j.chom.2012.11.012

111. Planet Paul J, LaRussa Samuel J, Dana A et al. Emergence of the Epidemic Methicillin-Resistant Staphylococcus aureus Strain USA300 Coincides with Horizontal Transfer of the Arginine Catabolic Mobile Element and speG-mediated Adaptations for Survival on Skin. mBio 2013;4(6):e00889-13. doi: 10.1128/mBio.00889-13

112. Maiques E, Úbeda C, Campoy S et al. β-Lactam Antibiotics Induce the SOS Response and Horizontal Transfer of Virulence Factors in Staphylococcus aureus. Journal of Bacteriology 2006;188(7):2726-9. doi: 10.1128/JB.188.7.2726-2729.2006

113. Meessen-Pinard M, Sekulovic O, Fortier L-C. Evidence of In Vivo Prophage Induction during Clostridium difficile Infection. Applied and Environmental Microbiology 2012;78(21):7662-70. doi: 10.1128/AEM.02275-12

114. Zhang X, McDaniel AD, Wolf LE et al. Quinolone Antibiotics Induce Shiga Toxin-Encoding Bacteriophages, Toxin Production, and Death in Mice. The Journal of Infectious Diseases 2000;181(2):664-70. doi: 10.1086/315239

115. Modi SR, Lee HH, Spina CS et al. Antibiotic treatment expands the resistance reservoir and ecological network of the phage metagenome. Nature 2013;499(7457):219-22. doi: 10.1038/nature12212

116. Resch A, Fehrenbacher B, Eisele K et al. Phage release from biofilm and planktonic Staphylococcus aureus cells. FEMS Microbiology Letters 2005;252(1):89-96. doi: https://doi.org/10.1016/j.femsle.2005.08.048

117. Savage VJ, Chopra I, O'Neill AJ. Staphylococcus aureus biofilms promote horizontal transfer of antibiotic resistance. Antimicrob Agents Chemother 2013;57(4):1968-70. doi: 10.1128/aac.02008-12

118. Clark NC, Weigel LM, Patel JB et al. Comparison of Tn1546-like elements in vancomycin-resistant Staphylococcus aureus isolates from Michigan and Pennsylvania. Antimicrob Agents Chemother 2005;49(1):470-2. doi: 10.1128/aac.49.1.470-472.2005

119. Aminov R. History of antimicrobial drug discovery: Major classes and health impact. Biochemical Pharmacology 2017;133:4-19. doi: https://doi.org/10.1016/j.bcp.2016.10.001

120. Aminov RI. A brief history of the antibiotic era: lessons learned and challenges for the future. Front Microbiol 2010;1:134. doi: 10.3389/fmicb.2010.00134

121. Fleming A. On the Antibacterial Action of Cultures of a Penicillium, with Special Reference to their Use in the Isolation of B. influenzæ. British Journal of Experimental Pathology 1929;10(0007-1021 (Print)):226-36

122. Lewis K. Platforms for antibiotic discovery. Nature Reviews Drug Discovery 2013;12(5):371-87. doi: 10.1038/nrd3975

123. Schatz A, Waksman SA. Effect of Streptomycin and Other Antibiotic Substances upon Mycobacterium tuberculosis and Related Organisms. Proceedings of the Society for Experimental Biology and Medicine 1944;57(2):244-8. doi: 10.3181/00379727-57-14769

124. Lewis K. The Science of Antibiotic Discovery. Cell 2020;181(1):29-45. doi: 10.1016/j.cell.2020.02.056

125. Payne DJ, Gwynn MN, Holmes DJ et al. Drugs for bad bugs: confronting the challenges of antibacterial discovery. Nature Reviews Drug Discovery 2007;6(1):29-40. doi: 10.1038/nrd2201

126. Hayden MK, Rezai K, Hayes RA et al. Development of Daptomycin Resistance In Vivo in Methicillin-Resistant Staphylococcus aureus. Journal of Clinical Microbiology 2005;43(10):5285-7. doi: 10.1128/JCM.43.10.5285-5287.2005

127. Hartkoorn Ruben C, Uplekar S, Cole Stewart T. Cross-Resistance between Clofazimine and Bedaquiline through Upregulation of MmpL5 in Mycobacterium tuberculosis. Antimicrobial Agents and Chemotherapy 2014;58(5):2979-81. doi: 10.1128/AAC.00037-14

128. Projan SJ. Why is big Pharma getting out of antibacterial drug discovery? Current Opinion in Microbiology 2003;6(5):427-30. doi: https://doi.org/10.1016/j.mib.2003.08.003

129. Bush K. Antibacterial drug discovery in the 21st century. Clinical Microbiology and Infection 2004;10:10-7. doi: https://doi.org/10.1111/j.1465-0691.2004.1005.x

130. Clardy J, Walsh C. Lessons from natural molecules. Nature 2004;432(7019):829-37. doi: 10.1038/nature03194

131. Nathan C. Antibiotics at the crossroads. Nature 2004;431(7011):899-902. doi: 10.1038/431899a

132. Lipinski CA, Lombardo F, Dominy BW et al. Experimental and computational approaches to estimate solubility and permeability in drug discovery and development settings1PII of original article: S0169-409X(96)00423-1. The article was originally published in Advanced Drug Delivery Reviews 23 (1997) 3–25.1. Advanced Drug Delivery Reviews 2001;46(1):3-26. doi: https://doi.org/10.1016/S0169-409X(00)00129-0

133. Lam KS. New aspects of natural products in drug discovery. Trends in Microbiology 2007;15(6):279-89. doi: https://doi.org/10.1016/j.tim.2007.04.001

134. Nichols D, Cahoon N, Trakhtenberg EM et al. Use of Ichip for High-Throughput In Situ Cultivation of "Uncultivable" Microbial Species. Applied and Environmental Microbiology 2010;76(8):2445-50. doi: 10.1128/AEM.01754-09

135. Ling LL, Schneider T, Peoples AJ et al. A new antibiotic kills pathogens without detectable resistance. Nature 2015;517(7535):455-9. doi: 10.1038/nature14098

136. Rybniker J, Chen Jeffrey M, Sala C et al. Anticytolytic Screen Identifies Inhibitors of Mycobacterial Virulence Protein Secretion. Cell Host & Microbe 2014;16(4):538-48. doi: https://doi.org/10.1016/j.chom.2014.09.008

137. Rasmussen Thomas B, Bjarnsholt T, Skindersoe Mette E et al. Screening for Quorum-Sensing Inhibitors (QSI) by Use of a Novel Genetic System, the QSI Selector. Journal of Bacteriology 2005;187(5):1799-814. doi: 10.1128/JB.187.5.1799-1814.2005

138. Müh U, Schuster M, Heim R et al. Novel Pseudomonas aeruginosa Quorum-Sensing Inhibitors Identified in an Ultra-High-Throughput Screen. Antimicrobial Agents and Chemotherapy 2006;50(11):3674-9. doi: 10.1128/AAC.00665-06

139. Rasmussen TB, Givskov M. Quorum sensing inhibitors: a bargain of effects. Microbiology 2006;152(4):895-904. doi: https://doi.org/10.1099/mic.0.28601-0

140. Park J, Jagasia R, Kaufmann GF et al. Infection Control by Antibody Disruption of Bacterial Quorum Sensing Signaling. Chemistry & Biology 2007;14(10):1119-27. doi: https://doi.org/10.1016/j.chembiol.2007.08.013

141. Borregaard N, Sørensen OE, Theilgaard-Mönch K. Neutrophil granules: a library of innate immunity proteins. Trends in Immunology 2007;28(8):340-5. doi: https://doi.org/10.1016/j.it.2007.06.002

142. Ragland SA, Criss AK. From bacterial killing to immune modulation: Recent insights into the functions of lysozyme. PLOS Pathogens 2017;13(9):e1006512. doi: 10.1371/journal.ppat.1006512

143. Houghton AM, Hartzell WO, Robbins CS et al. Macrophage elastase kills bacteria within murine macrophages. Nature 2009;460(7255):637-41. doi: 10.1038/nature08181

144. Di A, Brown ME, Deriy LV et al. CFTR regulates phagosome acidification in macrophages and alters bactericidal activity. Nature Cell Biology 2006;8(9):933-44. doi: 10.1038/ncb1456

145. Amulic B, Cazalet C, Hayes GL et al. Neutrophil Function: From Mechanisms to Disease. Annual Review of Immunology 2012;30(1):459-89. doi: 10.1146/annurev-immunol-020711-074942

146. Winterbourn CC, Kettle AJ, Hampton MB. Reactive Oxygen Species and Neutrophil Function. Annual Review of Biochemistry 2016;85(1):765-92. doi: 10.1146/annurev-biochem-060815-014442

147. Djoko KY, Ong C-lY, Walker MJ et al. The Role of Copper and Zinc Toxicity in Innate Immune Defense against Bacterial Pathogens *. Journal of Biological Chemistry 2015;290(31):18954-61. doi: 10.1074/jbc.R115.647099

148. Hood MI, Skaar EP. Nutritional immunity: transition metals at the pathogen–host interface. Nature Reviews Microbiology 2012;10(8):525-37. doi: 10.1038/nrmicro2836

149. Skaar EP, Raffatellu M. Metals in infectious diseases and nutritional immunity. Metallomics 2015;7(6):926-8. doi: 10.1039/c5mt90021b

150. Ganz T, Nemeth E. Iron homeostasis in host defence and inflammation. Nature Reviews Immunology 2015;15(8):500-10. doi: 10.1038/nri3863

151. Crichton RR, Pierre JL. Old iron, young copper: from Mars to Venus. Biometals 2001;14(2):99-112. doi: 10.1023/a:1016710810701

152. Andrews NC. Disorders of Iron Metabolism. New England Journal of Medicine 1999;341(26):1986-95. doi: 10.1056/NEJM199912233412607

153. Morgan WT, Smith A, Koskelo P. The interaction of human serum albumin and hemopexin with porphyrins. Biochimica et Biophysica Acta (BBA) - Protein Structure 1980;624(1):271-85. doi: https://doi.org/10.1016/0005-2795(80)90246-9

154. Otto BR, Verweij-van Vught AMJJ, Maclaren DM. Transferrins and Heme-Compounds as Iron Sources for Pathogenic Bacteria. Critical Reviews in Microbiology 1992;18(3):217-33. doi: 10.3109/10408419209114559

155. Takahashi N, Takahashi Y, Putnam FW. Complete amino acid sequence of human hemopexin, the heme-binding protein of serum. Proceedings of the National Academy of Sciences 1985;82(1):73-7. doi: 10.1073/pnas.82.1.73

156. Legrand D, Elass E, Carpentier M et al. Lactoferrin. Cellular and Molecular Life Sciences 2005;62(22):2549. doi: 10.1007/s00018-005-5370-2

157. Macara IG, Hoy TG, Harrison PM. The formation of ferritin from apoferritin. Kinetics and mechanism of iron uptake. Biochemical Journal 1972;126(1):151-62. doi: 10.1042/bj1260151

158. Harrison PM. Ferritin and haemosiderin. In: Gross Fs (ed). Iron Metabolism: An International Symposium. Berlin, Heidelberg: Springer Berlin Heidelberg, 1964, 40-59

159. Oppenheimer SJ. Iron and Its Relation to Immunity and Infectious Disease. The Journal of Nutrition 2001;131(2):616S-35S. doi: 10.1093/jn/131.2.616S

160. Hider RC, Kong X. Chemistry and biology of siderophores. Natural Product Reports 2010;27(5):637-57. doi: 10.1039/B906679A

161. Sia AK, Allred BE, Raymond KN. Siderocalins: Siderophore binding proteins evolved for primary pathogen host defense. Current Opinion in Chemical Biology 2013;17(2):150-7. doi: https://doi.org/10.1016/j.cbpa.2012.11.014

162. Clifton MC, Corrent C, Strong RK. Siderocalins: siderophore-binding proteins of the innate immune system. BioMetals 2009;22(4):557-64. doi: 10.1007/s10534-009-9207-6

163. Abergel RJ, Wilson MK, Arceneaux JEL et al. Anthrax pathogen evades the mammalian immune system through stealth siderophore production. Proceedings of the National Academy of Sciences 2006;103(49):18499-503. doi: 10.1073/pnas.0607055103

164. Fischbach MA, Lin H, Liu DR et al. How pathogenic bacteria evade mammalian sabotage in the battle for iron. Nature Chemical Biology 2006;2(3):132-8. doi: 10.1038/nchembio771

165. Wiseman GM. The hemolysins of Staphylococcus aureus. Bacteriol Rev 1975;39(4):317-44. doi: 10.1128/br.39.4.317-344.1975

166. Bobrov AG, Kirillina O, Fetherston JD et al. The Yersinia pestis siderophore, yersiniabactin, and the ZnuABC system both contribute to zinc acquisition and the development of lethal septicaemic plague in mice. Molecular Microbiology 2014;93(4):759-75. doi: https://doi.org/10.1111/mmi.12693

167. Mastropasqua MC, D'Orazio M, Cerasi M et al. Growth of Pseudomonas aeruginosa in zinc poor environments is promoted by a nicotianamine-related metallophore. Molecular Microbiology 2017;106(4):543-61. doi: https://doi.org/10.1111/mmi.13834

168. Mehdiratta K, Singh S, Sharma S et al. Kupyaphores are zinc homeostatic metallophores required for colonization of Mycobacterium tuberculosis. Proceedings of the National Academy of Sciences 2022;119(8):e2110293119. doi: 10.1073/pnas.2110293119

169. Ammendola S, Secli V, Pacello F et al. Zinc-binding metallophores protect Pseudomonas aeruginosa from calprotectin-mediated metal starvation. FEMS Microbiology Letters 2022;369(1):fnac071. doi: 10.1093/femsle/fnac071

170. Lhospice S, Gomez NO, Ouerdane L et al. Pseudomonas aeruginosa zinc uptake in chelating environment is primarily mediated by the metallophore pseudopaline. Scientific Reports 2017;7(1):17132. doi: 10.1038/s41598-017-16765-9

171. Ghssein G, Brutesco C, Ouerdane L et al. Biosynthesis of a broad-spectrum nicotianamine-like metallophore in Staphylococcus aureus. Science 2016;352(6289):1105-9. doi: 10.1126/science.aaf1018

172. Song L, Zhang Y, Chen W et al. Mechanistic insights into staphylopine-mediated metal acquisition. Proceedings of the National Academy of Sciences 2018;115(15):3942-7. doi: 10.1073/pnas.1718382115

173. Patzer SI, Hantke K. The ZnuABC high-affinity zinc uptake system and its regulator Zur in Escherichia coli. Molecular Microbiology 1998;28(6):1199-210. doi: https://doi.org/10.1046/j.1365-2958.1998.00883.x

174. Grass G, Wong Marco D, Rosen Barry P et al. ZupT Is a Zn(II) Uptake System in Escherichia coli. Journal of Bacteriology 2002;184(3):864-6. doi: 10.1128/JB.184.3.864-866.2002

175. Pederick VG, Eijkelkamp BA, Begg SL et al. ZnuA and zinc homeostasis in Pseudomonas aeruginosa. Scientific Reports 2015;5(1):13139. doi: 10.1038/srep13139

176. Maunders Eve A, Ganio K, Hayes Andrew J et al. The Role of ZntA in Klebsiella pneumoniae Zinc Homeostasis. Microbiology Spectrum 2022;10(1):e01773-21. doi: 10.1128/spectrum.01773-21

177. Campoy S, Jara M, Busquets N et al. Role of the High-Affinity Zinc Uptake znuABC System in Salmonella enterica Serovar Typhimurium Virulence. Infection and Immunity 2002;70(8):4721-5. doi: 10.1128/IAI.70.8.4721-4725.2002

178. Ammendola S, Pasquali P, Pistoia C et al. High-Affinity Zn2+ Uptake System ZnuABC Is Required for Bacterial Zinc Homeostasis in Intracellular Environments and Contributes to the Virulence of Salmonella enterica. Infection and Immunity 2007;75(12):5867-76. doi: 10.1128/IAI.00559-07

179. Hesse Laura E, Lonergan Zachery R, Beavers William N et al. The Acinetobacter baumannii Znu System Overcomes Host-Imposed Nutrient Zinc Limitation. Infection and Immunity 2019;87(12):e00746-19. doi: 10.1128/IAI.00746-19

180. Dintilhac A, Alloing G, Granadel C et al. Competence and virulence of Streptococcus pneumoniae: Adc and PsaA mutants exhibit a requirement for Zn and Mn resulting from inactivation of putative ABC metal permeases. Molecular Microbiology 1997;25(4):727-39. doi: https://doi.org/10.1046/j.1365-2958.1997.5111879.x

181. Grim Kyle P, San Francisco B, Radin Jana N et al. The Metallophore Staphylopine Enables Staphylococcus aureus To Compete with the Host for Zinc and Overcome Nutritional Immunity. mBio 2017;8(5):e01281-17. doi: 10.1128/mBio.01281-17

182. Kehl-Fie Thomas E, Chitayat S, Hood MI et al. Nutrient Metal Sequestration by Calprotectin Inhibits Bacterial Superoxide Defense, Enhancing Neutrophil Killing of Staphylococcus aureus. Cell Host & Microbe 2011;10(2):158-64. doi: https://doi.org/10.1016/j.chom.2011.07.004

183. Liu Janet Z, Jellbauer S, Poe AJ et al. Zinc Sequestration by the Neutrophil Protein Calprotectin Enhances Salmonella Growth in the Inflamed Gut. Cell Host & Microbe 2012;11(3):227-39. doi: https://doi.org/10.1016/j.chom.2012.01.017

184. Zackular JP, Chazin WJ, Skaar EP. Nutritional Immunity: S100 Proteins at the Host-Pathogen Interface*. Journal of Biological Chemistry 2015;290(31):18991-8. doi: https://doi.org/10.1074/jbc.R115.645085

185. Steinbakk M, Naess-Andresen CF, Fagerhol MK et al. Antimicrobial actions of calcium binding leucocyte L1 protein, calprotectin. The Lancet 1990;336(8718):763-5. doi: https://doi.org/10.1016/0140-6736(90)93237-J

186. Damo SM, Kehl-Fie TE, Sugitani N et al. Molecular basis for manganese sequestration by calprotectin and roles in the innate immune response to invading bacterial pathogens. Proceedings of the National Academy of Sciences 2013;110(10):3841-6. doi: 10.1073/pnas.1220341110

187. Gaddy JA, Radin JN, Loh JT et al. The host protein calprotectin modulates the Helicobacter pylori cag type IV secretion system via zinc sequestration. PLoS Pathog 2014;10(10):e1004450. doi: 10.1371/journal.ppat.1004450

188. Hayden JA, Brophy MB, Cunden LS et al. High-Affinity Manganese Coordination by Human Calprotectin Is Calcium-Dependent and Requires the Histidine-Rich Site Formed at the Dimer Interface. Journal of the American Chemical Society 2013;135(2):775-87. doi: 10.1021/ja3096416

189. Brophy MB, Hayden JA, Nolan EM. Calcium Ion Gradients Modulate the Zinc Affinity and Antibacterial Activity of Human Calprotectin. Journal of the American Chemical Society 2012;134(43):18089-100. doi: 10.1021/ja307974e

190. Corbin BD, Seeley EH, Raab A et al. Metal Chelation and Inhibition of Bacterial Growth in Tissue Abscesses. Science 2008;319(5865):962-5. doi: 10.1126/science.1152449

191. White C, Lee J, Kambe T et al. A Role for the ATP7A Copper-transporting ATPase in Macrophage Bactericidal Activity *. Journal of Biological Chemistry 2009;284(49):33949-56. doi: 10.1074/jbc.M109.070201

192. Dalecki AG, Crawford CL, Wolschendorf F. Chapter Six - Copper and Antibiotics: Discovery, Modes of Action, and Opportunities for Medicinal Applications. In: Poole RKs (ed). Advances in Microbial Physiology: Academic Press, 2017, 193-260

193. Tan G, Yang J, Li T et al. Anaerobic Copper Toxicity and Iron-Sulfur Cluster Biogenesis in Escherichia coli. Applied and Environmental Microbiology 2017;83(16):e00867-17. doi: 10.1128/AEM.00867-17

194. Macomber L, Imlay JA. The iron-sulfur clusters of dehydratases are primary intracellular targets of copper toxicity. Proceedings of the National Academy of Sciences 2009;106(20):8344-9. doi: 10.1073/pnas.0812808106

195. Chillappagari S, Seubert A, Trip H et al. Copper Stress Affects Iron Homeostasis by Destabilizing Iron-Sulfur Cluster Formation in Bacillus subtilis. Journal of Bacteriology 2010;192(10):2512-24. doi: 10.1128/JB.00058-10

196. Fung Danny Ka C, Lau Wai Y, Chan Wing T et al. Copper Efflux Is Induced during Anaerobic Amino Acid Limitation in Escherichia coli To Protect Iron-Sulfur Cluster Enzymes and Biogenesis. Journal of Bacteriology 2013;195(20):4556-68. doi: 10.1128/JB.00543-13

197. Tan G, Cheng Z, Pang Y et al. Copper binding in IscA inhibits iron-sulphur cluster assembly in Escherichia coli. Molecular Microbiology 2014;93(4):629-44. doi: https://doi.org/10.1111/mmi.12676

198. Price EE, Boyd JM. Genetic Regulation of Metal Ion Homeostasis in Staphylococcus aureus. Trends in Microbiology 2020;28(10):821-31. doi: https://doi.org/10.1016/j.tim.2020.04.004

199. Baker J, Sengupta M, Jayaswal RK et al. The Staphylococcus aureus CsoR regulates both chromosomal and plasmid-encoded copper resistance mechanisms. Environmental Microbiology 2011;13(9):2495-507. doi: https://doi.org/10.1111/j.1462-2920.2011.02522.x

200. Sitthisak S, Knutsson L, Webb JW et al. Molecular characterization of the copper transport system in Staphylococcus aureus. Microbiology 2007;153(12):4274-83. doi: https://doi.org/10.1099/mic.0.2007/009860-0

201. Rosario-Cruz Z, Eletsky A, Daigham NS et al. The copBL operon protects Staphylococcus aureus from copper toxicity: CopL is an extracellular membrane–associated copper-binding protein. Journal of Biological Chemistry 2019;294(11):4027-44. doi: 10.1074/jbc.RA118.004723

202. Rowland Jennifer L, Niederweis M. A Multicopper Oxidase Is Required for Copper Resistance in Mycobacterium tuberculosis. Journal of Bacteriology 2013;195(16):3724-33. doi: 10.1128/JB.00546-13

203. Grass G, Rensing C. CueO Is a Multi-copper Oxidase That Confers Copper Tolerance in Escherichia coli. Biochemical and Biophysical Research Communications 2001;286(5):902-8. doi: https://doi.org/10.1006/bbrc.2001.5474

204. Alfonso-Prieto M, Biarnés X, Vidossich P et al. The Molecular Mechanism of the Catalase Reaction. Journal of the American Chemical Society 2009;131(33):11751-61. doi: 10.1021/ja9018572

205. Hinsa-Leasure SM, Nartey Q, Vaverka J et al. Copper alloy surfaces sustain terminal cleaning levels in a rural hospital. American Journal of Infection Control 2016;44(11):e195-e203. doi: 10.1016/j.ajic.2016.06.033

206. Ala A, Walker AP, Ashkan K et al. Wilson's disease. The Lancet 2007;369(9559):397-408. doi: https://doi.org/10.1016/S0140-6736(07)60196-2

207. Brewer GJ, Dick RD, Johnson VD et al. Treatment of Wilson's disease with zinc: XV long-term follow-up studies. Journal of Laboratory and Clinical Medicine 1998;132(4):264-78. doi: https://doi.org/10.1016/S0022-2143(98)90039-7

208. Denoyer D, Masaldan S, La Fontaine S et al. Targeting copper in cancer therapy: 'Copper That Cancer'. Metallomics 2015;7(11):1459-76. doi: 10.1039/c5mt00149h

209. Santini C, Pellei M, Gandin V et al. Advances in Copper Complexes as Anticancer Agents. Chemical Reviews 2014;114(1):815-62. doi: 10.1021/cr400135x

210. Cater MA, Pearson HB, Wolyniec K et al. Increasing Intracellular Bioavailable Copper Selectively Targets Prostate Cancer Cells. ACS Chemical Biology 2013;8(7):1621-31. doi: 10.1021/cb400198p

211. Safety, tolerability, and efficacy of PBT2 in Huntington's disease: a phase 2, randomised, double-blind, placebo-controlled trial. The Lancet Neurology 2015;14(1):39-47. doi: 10.1016/S1474-4422(14)70262-5

212. Nguyen T, Hamby A, Massa SM. Clioquinol down-regulates mutant huntingtin expression in vitro and mitigates pathology in a Huntington's disease mouse model. Proceedings of the National Academy of Sciences 2005;102(33):11840-5. doi: 10.1073/pnas.0502177102

213. Lannfelt L, Blennow K, Zetterberg H et al. Safety, efficacy, and biomarker findings of PBT2 in targeting Aβ as a modifying therapy for Alzheimer's disease: a phase IIa, double-blind, randomised, placebo-controlled trial. The Lancet Neurology 2008;7(9):779-86. doi: https://doi.org/10.1016/S1474-4422(08)70167-4

214. Crawford CL, Dalecki AG, Narmore WT et al. Pyrazolopyrimidinones, a novel class of copper-dependent bactericidal antibiotics against multi-drug resistant S. aureus†. Metallomics 2019;11(4):784-98. doi: 10.1039/c8mt00316e

215. Crawford CL, Dalecki AG, Perez MD et al. A copper-dependent compound restores ampicillin sensitivity in multidrug-resistant Staphylococcus aureus. Scientific Reports 2020;10(1):8955. doi: 10.1038/s41598-020-65978-y

216. Dalecki AG, Malalasekera AP, Schaaf K et al. Combinatorial phenotypic screen uncovers unrecognized family of extended thiourea inhibitors with copper-dependent anti-staphylococcal activity. Metallomics 2016;8(4):412-21. doi: 10.1039/c6mt00003g

217. Dalecki AG, Zorn KM, Clark AM et al. High-throughput screening and Bayesian machine learning for copper-dependent inhibitors of Staphylococcus aureus†. Metallomics 2019;11(3):696-706. doi: 10.1039/c8mt00342d

218. Delpe-Acharige A, Zhang M, Eschliman K et al. Pyrazolyl Thioureas and Carbothioamides with an NNSN Motif against MSSA and MRSA. ACS Omega 2021;6(9):6088-99. doi: 10.1021/acsomega.0c04513

219. Dalecki Alex G, Haeili M, Shah S et al. Disulfiram and Copper Ions Kill Mycobacterium tuberculosis in a Synergistic Manner. Antimicrobial Agents and Chemotherapy 2015;59(8):4835-44. doi: 10.1128/AAC.00692-15

220. Djoko Karrera Y, Goytia Maira M, Donnelly Paul S et al. Copper(II)-Bis(Thiosemicarbazonato) Complexes as Antibacterial Agents: Insights into Their Mode of Action and Potential as Therapeutics. Antimicrobial Agents and Chemotherapy 2015;59(10):6444-53. doi: 10.1128/AAC.01289-15

221. Shah S, Dalecki Alex G, Malalasekera Aruni P et al. 8-Hydroxyquinolines Are Boosting Agents of Copper-Related Toxicity in Mycobacterium tuberculosis. Antimicrobial Agents and Chemotherapy 2016;60(10):5765-76. doi: 10.1128/AAC.00325-16

222. Patteson JB, Putz AT, Tao L et al. Biosynthesis of fluopsin C, a copper-containing antibiotic from Pseudomonas aeruginosa. Science 2021;374(6570):1005-9. doi: 10.1126/science.abj6749

223. Navarro MOP, Simionato AS, Pérez JCB et al. Fluopsin C for Treating Multidrug-Resistant Infections: In vitro Activity Against Clinically Important Strains and in vivo Efficacy Against Carbapenemase-Producing Klebsiella pneumoniae. Frontiers in Microbiology 2019;10

224. Speer A, Shrestha Tej B, Bossmann Stefan H et al. Copper-Boosting Compounds: a Novel Concept for Antimycobacterial Drug Discovery. Antimicrobial Agents and Chemotherapy 2013;57(2):1089-91. doi: 10.1128/AAC.01781-12

225. Totten AH, Crawford CL, Dalecki AG et al. Differential Susceptibility of Mycoplasma and Ureaplasma Species to Compound-Enhanced Copper Toxicity. Frontiers in Microbiology 2019;10

226. Berg JM, Shi Y. The Galvanization of Biology: A Growing Appreciation for the Roles of Zinc. Science 1996;271(5252):1081-5. doi: 10.1126/science.271.5252.1081

227. McDevitt CA, Ogunniyi AD, Valkov E et al. A Molecular Mechanism for Bacterial Susceptibility to Zinc. PLOS Pathogens 2011;7(11):e1002357

228. Andreini C, Banci L, Bertini I et al. Zinc through the Three Domains of Life. Journal of Proteome Research 2006;5(11):3173-8. doi: 10.1021/pr0603699

229. Andreini C, Banci L, Bertini I et al. Counting the Zinc-Proteins Encoded in the Human Genome. Journal of Proteome Research 2006;5(1):196-201. doi: 10.1021/pr050361j

230. Andreini C, Bertini I, Cavallaro G et al. Metal ions in biological catalysis: from enzyme databases to general principles. JBIC Journal of Biological Inorganic Chemistry 2008;13(8):1205-18. doi: 10.1007/s00775-008-0404-5

231. Andreini C, Bertini I. A bioinformatics view of zinc enzymes. Journal of Inorganic Biochemistry 2012;111:150-6. doi: https://doi.org/10.1016/j.jinorgbio.2011.11.020

232. Weston J. Mode of Action of Bi- and Trinuclear Zinc Hydrolases and Their Synthetic Analogues. Chemical Reviews 2005;105(6):2151-74. doi: 10.1021/cr020057z

233. Bazzicalupi C, Bencini A, Bonaccini C et al. Tuning the Activity of Zn(II) Complexes in DNA Cleavage: Clues for Design of New Efficient Metallo-Hydrolases. Inorganic Chemistry 2008;47(12):5473-84. doi: 10.1021/ic800085n

234. Karsisiotis AI, Damblon CF, Roberts GCK. A variety of roles for versatile zinc in metallo-β-lactamases. Metallomics 2014;6(7):1181-97. doi: 10.1039/c4mt00066h

235. Tamilselvi A, Mugesh G. Zinc and antibiotic resistance: metallo-β-lactamases and their synthetic analogues. JBIC Journal of Biological Inorganic Chemistry 2008;13(7):1039-53. doi: 10.1007/s00775-008-0407-2

236. Cho Y, Gorina S, Jeffrey PD et al. Crystal Structure of a p53 Tumor Suppressor-DNA Complex: Understanding Tumorigenic Mutations. Science 1994;265(5170):346-55. doi: 10.1126/science.8023157

237. Giedroc DP, Coleman JE. Structural and functional differences between the two intrinsic zinc ions of Escherichia coli RNA polymerase. Biochemistry 1986;25(17):4969-78. doi: 10.1021/bi00365a037

238. Hu Y, Liu B. Roles of zinc-binding domain of bacterial RNA polymerase in transcription. Trends in Biochemical Sciences 2022;47(8):710-24. doi: 10.1016/j.tibs.2022.03.007

239. Solaiman D, Wu FY. Intrinsic zinc ion is essential for proper conformation of active Escherichia coli RNA polymerase. Biochemistry 1984;23(26):6369-77. doi: 10.1021/bi00321a013

240. Owen Gillian A, Pascoe B, Kallifidas D et al. Zinc-Responsive Regulation of Alternative Ribosomal Protein Genes in Streptomyces coelicolor Involves Zur and σR. Journal of Bacteriology 2007;189(11):4078-86. doi: 10.1128/JB.01901-06

241. Dow A, Prisic S. Alternative ribosomal proteins are required for growth and morphogenesis of Mycobacterium smegmatis under zinc limiting conditions. PLOS ONE 2018;13(4):e0196300. doi: 10.1371/journal.pone.0196300

242. Prisic S, Hwang H, Dow A et al. Zinc regulates a switch between primary and alternative S18 ribosomal proteins in Mycobacterium tuberculosis. Molecular Microbiology 2015;97(2):263-80. doi: https://doi.org/10.1111/mmi.13022

243. Panina EM, Mironov AA, Gelfand MS. Comparative genomics of bacterial zinc regulons: Enhanced ion transport, pathogenesis, and rearrangement of ribosomal proteins. Proceedings of the National Academy of Sciences 2003;100(17):9912-7. doi: 10.1073/pnas.1733691100

244. Gabriel Scott E, Helmann John D. Contributions of Zur-Controlled Ribosomal Proteins to Growth under Zinc Starvation Conditions. Journal of Bacteriology 2009;191(19):6116-22. doi: 10.1128/JB.00802-09

245. Somers W, Ultsch M, De Vos AM et al. The X-ray structure of a growth hormone–prolactin receptor complex. Nature 1994;372(6505):478-81. doi: 10.1038/372478a0

246. Lemire JA, Harrison JJ, Turner RJ. Antimicrobial activity of metals: mechanisms, molecular targets and applications. Nature Reviews Microbiology 2013;11(6):371-84. doi: 10.1038/nrmicro3028

247. Irving H, Williams RJP. 637. The stability of transition-metal complexes. Journal of the Chemical Society (Resumed) 1953(0):3192-210. doi: 10.1039/JR9530003192

248. Xu Fang F, Imlay James A. Silver(I), Mercury(II), Cadmium(II), and Zinc(II) Target Exposed Enzymic Iron-Sulfur Clusters when They Toxify Escherichia coli. Applied and Environmental Microbiology 2012;78(10):3614-21. doi: 10.1128/AEM.07368-11

249. Costello LC, Liu Y, Franklin RB et al. Zinc Inhibition of Mitochondrial Aconitase and Its Importance in Citrate Metabolism of Prostate Epithelial Cells *. Journal of Biological Chemistry 1997;272(46):28875-81. doi: 10.1074/jbc.272.46.28875

250. Li J, Ren X, Fan B et al. Zinc Toxicity and Iron-Sulfur Cluster Biogenesis in Escherichia coli. Applied and Environmental Microbiology 2019;85(9):e01967-18. doi: 10.1128/AEM.01967-18

251. Wagner D, Maser Jr, Lai B et al. Elemental Analysis of Mycobacterium avium-, Mycobacterium tuberculosis-, and Mycobacterium smegmatis-Containing Phagosomes Indicates Pathogen-Induced Microenvironments within the Host Cell's Endosomal System1. The Journal of Immunology 2005;174(3):1491-500. doi: 10.4049/jimmunol.174.3.1491

252. Botella H, Peyron P, Levillain F et al. Mycobacterial P1-Type ATPases Mediate Resistance to Zinc Poisoning in Human Macrophages. Cell Host & Microbe 2011;10(3):248-59. doi: https://doi.org/10.1016/j.chom.2011.08.006

253. Ong C-lY, Gillen CM, Barnett TC et al. An Antimicrobial Role for Zinc in Innate Immune Defense Against Group A Streptococcus. The Journal of Infectious Diseases 2014;209(10):1500-8. doi: 10.1093/infdis/jiu053

254. Hambidge M. Human Zinc Deficiency. The Journal of Nutrition 2000;130(5):1344S-9S. doi: 10.1093/jn/130.5.1344S

255. Prasad AS. Zinc deficiency. Bmj 2003;326(7386):409-10. doi: 10.1136/bmj.326.7386.409

256. Walker CF, Black RE. ZINC AND THE RISK FOR INFECTIOUS DISEASE. Annual Review of Nutrition 2004;24(1):255-75. doi: 10.1146/annurev.nutr.23.011702.073054

257. Johnson BA, Anker H, Meleney FL. Bacitracin: A New Antibiotic Produced by a Member of the B. subtilis Group. Science 1945;102(2650):376-7. doi: 10.1126/science.102.2650.376

258. Smith JL, Weinberg ED. Mechanisms of Antibacterial Action of Bacitracin. Microbiology 1962;28(3):559-69. doi: https://doi.org/10.1099/00221287-28-3-559

259. Stone KJ, Strominger JL. Mechanism of Action of Bacitracin: Complexation with Metal Ion and C55-Isoprenyl Pyrophosphate. Proceedings of the National Academy of Sciences 1971;68(12):3223-7. doi: 10.1073/pnas.68.12.3223

260. Miller JH, McDonald RK, Shock NW. The effect of bacitracin on renal function. The Journal of Clinical Investigation 1950;29(4):389-95

261. Reeder Nancy L, Kaplan J, Xu J et al. Zinc Pyrithione Inhibits Yeast Growth through Copper Influx and Inactivation of Iron-Sulfur Proteins. Antimicrobial Agents and Chemotherapy 2011;55(12):5753-60. doi: 10.1128/AAC.00724-11

262. Wolohan P, Yoo J, Welch MJ et al. QSAR Studies of Copper Azamacrocycles and Thiosemicarbazones: MM3 Parameter Development and Prediction of Biological Properties. Journal of Medicinal Chemistry 2005;48(17):5561-9. doi: 10.1021/jm0501376

263. Djoko KY, Paterson BM, Donnelly PS et al. Antimicrobial effects of copper(ii) bis(thiosemicarbazonato) complexes provide new insight into their biochemical mode of action†. Metallomics 2014;6(4):854-63. doi: 10.1039/c3mt00348e

264. Festa Richard A, Helsel Marian E, Franz Katherine J et al. Exploiting Innate Immune Cell Activation of a Copper-Dependent Antimicrobial Agent during Infection. Chemistry & Biology 2014;21(8):977-87. doi: https://doi.org/10.1016/j.chembiol.2014.06.009

265. Bohacek RS, McMartin C, Guida WC. The art and practice of structure-based drug design: A molecular modeling perspective. Medicinal Research Reviews 1996;16(1):3-50. doi: https://doi.org/10.1002/(SICI)1098-1128(199601)16:1<3::AID-MED1>3.0.CO;2-6

266. Reymond J-L, Awale M. Exploring Chemical Space for Drug Discovery Using the Chemical Universe Database. ACS Chemical Neuroscience 2012;3(9):649-57. doi: 10.1021/cn3000422

267. Ruddigkeit L, van Deursen R, Blum LC et al. Enumeration of 166 Billion Organic Small Molecules in the Chemical Universe Database GDB-17. Journal of Chemical Information and Modeling 2012;52(11):2864-75. doi: 10.1021/ci300415d

268. Kim S, Thiessen PA, Bolton EE et al. PubChem Substance and Compound databases. Nucleic Acids Res 2016;44(D1):D1202-13. doi: 10.1093/nar/gkv951

269. Iversen PW, Beck B, Chen Y-F et al. HTS Assay Validation. The Assay Guidance Manual 2012

270. Jackson MJ. Physiology of Zinc: General Aspects. In: Mills CFs (ed). Zinc in Human Biology. London: Springer London, 1989, 1-14

271. Lonergan ZR, Skaar EP. Nutrient Zinc at the Host–Pathogen Interface. Trends in Biochemical Sciences 2019;44(12):1041-56. doi: https://doi.org/10.1016/j.tibs.2019.06.010

272. Bao VWW, Leung KMY, Kwok KWH et al. Synergistic toxic effects of zinc pyrithione and copper to three marine species: Implications on setting appropriate water quality criteria. Marine Pollution Bulletin 2008;57(6):616-23. doi: https://doi.org/10.1016/j.marpolbul.2008.03.041

273. Crouch PJ, Savva MS, Hung LW et al. The Alzheimer's therapeutic PBT2 promotes amyloid-β degradation and GSK3 phosphorylation via a metal chaperone activity. Journal of Neurochemistry 2011;119(1):220-30. doi: https://doi.org/10.1111/j.1471-4159.2011.07402.x

274. Bohlmann L, De Oliveira David MP, El-Deeb Ibrahim M et al. Chemical Synergy between Ionophore PBT2 and Zinc Reverses Antibiotic Resistance. mBio 2018;9(6):e02391-18. doi: 10.1128/mBio.02391-18

275. Economou NJ, Cocklin S, Loll PJ. High-resolution crystal structure reveals molecular details of target recognition by bacitracin. Proceedings of the National Academy of Sciences 2013;110(35):14207-12. doi: 10.1073/pnas.1308268110

276. El Ghachi M, Howe N, Huang C-Y et al. Crystal structure of undecaprenyl-pyrophosphate phosphatase and its role in peptidoglycan biosynthesis. Nature Communications 2018;9(1):1078. doi: 10.1038/s41467-018-03477-5

277. Yoshida Y, Matsuo M, Oogai Y et al. Bacitracin sensing and resistance in Staphylococcus aureus. FEMS Microbiology Letters 2011;320(1):33-9. doi: 10.1111/j.1574-6968.2011.02291.x

278. Hiron A, Falord M, Valle J et al. Bacitracin and nisin resistance in Staphylococcus aureus: a novel pathway involving the BraS/BraR two-component system (SA2417/SA2418) and both the BraD/BraE and VraD/VraE ABC transporters. Molecular Microbiology 2011;81(3):602-22. doi: https://doi.org/10.1111/j.1365-2958.2011.07735.x

279. Ouyang J, Tian X-L, Versey J et al. The BceABRS Four-Component System Regulates the Bacitracin-Induced Cell Envelope Stress Response in Streptococcus mutans. Antimicrobial Agents and Chemotherapy 2010;54(9):3895-906. doi: 10.1128/AAC.01802-09

280. Bernard R, Guiseppi A, Chippaux M et al. Resistance to Bacitracin in Bacillus subtilis: Unexpected Requirement of the BceAB ABC Transporter in the Control of Expression of Its Own Structural Genes. Journal of Bacteriology 2007;189(23):8636-42. doi: 10.1128/JB.01132-07

281. Bernard R, El Ghachi M, Mengin-Lecreulx D et al. BcrC from Bacillus subtilis Acts as an Undecaprenyl Pyrophosphate Phosphatase in Bacitracin Resistance *. Journal of Biological Chemistry 2005;280(32):28852-7. doi: 10.1074/jbc.M413750200

282. Ghachi ME, Bouhss A, Blanot D et al. The bacA Gene of Escherichia coli Encodes an Undecaprenyl Pyrophosphate Phosphatase Activity *. Journal of Biological Chemistry 2004;279(29):30106-13. doi: 10.1074/jbc.M401701200

283. Shaaly A, Kalamorz F, Gebhard S et al. Undecaprenyl pyrophosphate phosphatase confers low-level resistance to bacitracin in Enterococcus faecalis. Journal of Antimicrobial Chemotherapy 2013;68(7):1583-93. doi: 10.1093/jac/dkt048

284. Harbison-Price N, Ferguson Scott A, Heikal A et al. Multiple Bactericidal Mechanisms of the Zinc Ionophore PBT2. mSphere 2020;5(2):e00157-20. doi: 10.1128/mSphere.00157-20

285. Magda D, Lecane P, Wang Z et al. Synthesis and anticancer properties of water-soluble zinc ionophores. Cancer Res 2008;68(13):5318-25. doi: 10.1158/0008-5472.Can-08-0601

286. Krenn BM, Gaudernak E, Holzer B et al. Antiviral Activity of the Zinc Ionophores Pyrithione and Hinokitiol against Picornavirus Infections. Journal of Virology 2009;83(1):58-64. doi: 10.1128/JVI.01543-08

287. Andersson DA, Gentry C, Moss S et al. Clioquinol and pyrithione activate TRPA1 by increasing intracellular Zn2+. Proceedings of the National Academy of Sciences 2009;106(20):8374-9. doi: 10.1073/pnas.0812675106

288. Bao VWW, Lui GCS, Leung KMY. Acute and chronic toxicities of zinc pyrithione alone and in combination with copper to the marine copepod Tigriopus japonicus. Aquatic Toxicology 2014;157:81-93. doi: https://doi.org/10.1016/j.aquatox.2014.09.013

289. De Oliveira DMP, Bohlmann L, Conroy T et al. Repurposing a neurodegenerative disease drug to treat Gram-negative antibiotic-resistant bacterial sepsis. Science Translational Medicine 2020;12(570):eabb3791. doi: 10.1126/scitranslmed.abb3791

290. Van Zuylen EM, Ferguson SA, Hughes A et al. Disruption of Metallostasis in the Anaerobic Human Pathogen Fusobacterium nucleatum by the Zinc Ionophore PBT2. ACS Infectious Diseases 2021;7(8):2285-98. doi: 10.1021/acsinfecdis.0c00887

291. De Oliveira David MP, Forde Brian M, Phan M-D et al. Rescuing Tetracycline Class Antibiotics for the Treatment of Multidrug-Resistant Acinetobacter baumannii Pulmonary Infection. mBio 2022;13(1):e03517-21. doi: 10.1128/mbio.03517-21

292. Jen FEC, Everest-Dass AV, El-Deeb IM et al. Neisseria gonorrhoeae Becomes Susceptible to Polymyxin B and Colistin in the Presence of PBT2. ACS Infectious Diseases 2020;6(1):50-5. doi: 10.1021/acsinfecdis.9b00307

293. Jen FEC, El-Deeb IM, Zalucki YM et al. A drug candidate for Alzheimer's and Huntington's disease, PBT2, can be repurposed to render Neisseria gonorrhoeae susceptible to natural cationic antimicrobial peptides. Journal of Antimicrobial Chemotherapy 2021;76(11):2850-3. doi: 10.1093/jac/dkab291

294. Jen Freda EC, Edwards Jennifer L, El-Deeb Ibrahim M et al. Repurposing the Ionophore, PBT2, for Treatment of Multidrug-Resistant Neisseria gonorrhoeae Infections. Antimicrobial Agents and Chemotherapy 2022;66(9):e02318-21. doi: 10.1128/aac.02318-21

295. Brazel EB, Tan A, Neville SL et al. Dysregulation of Streptococcus pneumoniae zinc homeostasis breaks ampicillin resistance in a pneumonia infection model. Cell Reports 2022;38(2):110202. doi: https://doi.org/10.1016/j.celrep.2021.110202

296. Reyes-Caballero H, Campanello GC, Giedroc DP. Metalloregulatory proteins: Metal selectivity and allosteric switching. Biophysical Chemistry 2011;156(2):103-14. doi: https://doi.org/10.1016/j.bpc.2011.03.010

297. Maret W. Analyzing free zinc(ii) ion concentrations in cell biology with fluorescent chelating molecules. Metallomics 2015;7(2):202-11. doi: 10.1039/c4mt00230j

298. Trusso Sfrazzetto G, Satriano C, Tomaselli GA et al. Synthetic fluorescent probes to map metallostasis and intracellular fate of zinc and copper. Coordination Chemistry Reviews 2016;311:125-67. doi: https://doi.org/10.1016/j.ccr.2015.11.012

299. Carter KP, Young AM, Palmer AE. Fluorescent Sensors for Measuring Metal Ions in Living Systems. Chemical Reviews 2014;114(8):4564-601. doi: 10.1021/cr400546e

300. Radford RJ, Lippard SJ. Chelators for investigating zinc metalloneurochemistry. Current Opinion in Chemical Biology 2013;17(2):129-36. doi: https://doi.org/10.1016/j.cbpa.2013.01.009